ELECTRONIC SUPPLEMENTARY MATERIAL

Clinical Pharmacokinetics

Development and Evaluation of a Virtual Population of Children with Obesity for Physiologically-Based Pharmacokinetic Modeling

Jacqueline G. Gerhart[1], Fernando O. Carreño[1], Andrea N. Edginton[2], Jaydeep Sinha[1], Eliana M. Perrin[3], Karan R. Kumar[4,5], Aruna Rikhi[4], Christoph P. Hornik[4,5], Vincent Harris[1], Samit Ganguly[1,6], Michael Cohen-Wolkowiez[4,5], and Daniel Gonzalez[1,*]; on behalf of the Best Pharmaceuticals for Children Act – Pediatric Trials Network Steering Committee

[1]Division of Pharmacotherapy and Experimental Therapeutics, UNC Eshelman School of Pharmacy, The University of North Carolina at Chapel Hill, Chapel Hill, NC, USA; [2]School of Pharmacy, University of Waterloo, Waterloo, ON, Canada; [3]Department of Pediatrics, School of Medicine and School of Nursing, Johns Hopkins University, Baltimore, MD, USA; [4]Duke Clinical Research Institute, Durham, NC, USA; [5]Department of Pediatrics, Duke University School of Medicine, Durham, NC, USA; [6]Regeneron Pharmaceuticals, Inc., Tarrytown, NY, USA.

Address correspondence to: Daniel Gonzalez, UNC Eshelman School of Pharmacy, The University of North Carolina at Chapel Hill, 301 Pharmacy Lane, Campus Box #7569, Chapel Hill, NC 27599-7569, USA. Tel: +1-919-966-9984; Fax: +1-919-962-0644; E-mail: daniel.gonzalez@unc.edu

TABLE OF CONTENTS

1 SUPPLEMENTARY METHODS 4

1.1 Comprehensive Literature Search 4

1.2 Virtual Population Data Analysis 4

1.3 Growth Curve Development and Validation 5

1.4 Calculations for Glomerular Filtration Rate (GFR) 6

1.5 Clinical Data for Clindamycin PBPK Modeling – External Data Study 8

1.6 Clindamycin Oral Absorption Model Development and Evaluation 9

2 SUPPLEMENTARY RESULTS 9

2.1 Virtual Population Demographics 9

2.2 Clindamycin Oral Absorption Model 10

2.3 Incorporating AAG Concentration into Fu for Clindamycin 10

3 SUPPLEMENTARY FIGURES 12

Supplementary Figure 1. Updated growth curves. 13

Supplementary Figure 2. Updated growth curves, validation. 15

Supplementary Figure 3. Hematocrit versus age. 16

Supplementary Figure 4. Albumin versus age. 17

Supplementary Figure 5. AAG versus age. 18

Supplementary Figure 6. Kidney and liver volume increases. 19

Supplementary Figure 7. Cardiac output versus age. 20

Supplementary Figure 8. CLIN obese population simulations, AAG-adjusted. 29

Supplementary Figure 9. TMP nonobese population simulations. 31

Supplementary Figure 10. SMX nonobese population simulations. 33

Supplementary Figure 11. TMP obese population simulations. 38

Supplementary Figure 12. TMP/SMX obese AFE. 40

Supplementary Figure 13. SMX obese population simulations. 45

Supplementary Figure 14. Weight-normalized PK parameter simulations, 6-12 years. 47

Supplementary Figure 15. Weight-normalized PK parameter simulations, 2-6 years. 49

Supplementary Figure 16. Absolute PK parameter simulations, 12-18 years. 51

Supplementary Figure 17. Absolute PK parameter simulations, 6-12 years. 53

Supplementary Figure 18. Absolute PK parameter simulations, 2-6 years. 55

Supplementary Figure 19. CLIN dosing simulations, nonobese versus obese. 56

Supplementary Figure 20. TMP/SMX dosing simulations, nonobese versus obese. 57
Supplementary Figure 21. SMX obese population simulations, increased NAT2 clearance. 62
Supplementary Figure 22. Height versus age. 63
Supplementary Figure 23. Weight versus age. 64
Supplementary Figure 24. CLIN adult PO population simulations. 66
Supplementary Figure 25. CLIN obese AFE. 67
Supplementary Figure 26. CLIN nonobese population simulations, AAG-adjusted. 70
Supplementary Figure 27. CLIN obese AFE, AAG-adjusted. 72
4 SUPPLEMENTARY TABLES 73
Supplementary Table 1. Summary of clinical studies. 73
Supplementary Table 2. CLIN nonobese subject demographics 74
Supplementary Table 3. CLIN obese subject demographics 76
Supplementary Table 4. TMP/SMX nonobese subject demographics 78
Supplementary Table 5. TMP/SMX obese subject demographics 79
Supplementary Table 6. CLIN PBPK model parameters 81
Supplementary Table 7. TMP/SMX PBPK model parameters 83
Supplementary Table 8. Virtual population demographics for dosing simulations 85
Supplementary Table 9. Hematocrit literature data 86
Supplementary Table 10. Albumin literature data 87
Supplementary Table 11. AAG literature data 89
Supplementary Table 12. Organ volume scaling factors 90
Supplementary Table 13. Kidney and liver volume increases in the literature 91
Supplementary Table 14. Cardiac output literature data 94
Supplementary Table 15. Literature search terms 96
Supplementary Table 16. CLIN adult PO subject demographics and AFE 99
5 REFERENCES 101

1 SUPPLEMENTARY METHODS

1.1 Comprehensive Literature Search

In order to leverage existing physiological data from children with obesity into our virtual population, a comprehensive literature search was conducted in PubMed. A detailed search plan was developed in collaboration with medical librarians at the University of North Carolina – Chapel Hill's Health Science Library that included each of 121 physiological terms relevant to PK modeling combined with keywords 'obese' and 'pediatric', as well as related MeSH (Medical Subject Headings) terms (**Supplementary Table 15**). Articles from all dates were included, and the Human Species filter was used to limit the results. The titles and abstracts from 26,369 resulting search hits were screened for relevance to the virtual population development work using Covidence (Veritas Health Innovation Ltd, Melbourne, Australia) systematic reviews production tool for title/abstract screening, full-text screening, data abstraction, and quality assessment. Each article's title and abstract was reviewed by two independent screeners, with two rejections required to exclude the article. The full-text of articles approved by one or both screeners was reviewed, and any relevant physiological data extracted to inform the virtual population development. Extracted data for several key physiological parameters relevant to pharmacokinetics are summarized in the **Supplementary Tables 9-11, 13-14** below.

1.2 Virtual Population Data Analysis

In combining data across multiple sources and studies, all units were converted to a single standard unit. When a range was reported for any particular parameter, the midpoint and standard deviation were used. For electronic health record data, recorded height and weight values significantly far above the 3rd and 97th percentile for 2 and 20 year-olds, respectively, were discarded as implausible outliers. All virtual population modeling and validation was performed

using PK-Sim® (version 9.0, Open Systems Pharmacology Suite, open-systems-pharmacology.com). Data analysis and growth curve development and validation were performed using the software R (version 3.5.3) and RStudio (version 1.1.463; RStudio, Boston, MA).

1.3 Growth Curve Development and Validation

While the current definition of obesity as defined by the 95th BMI percentile from the 2000 CDC growth charts was retained, the growth curves were updated with more recent demographic data to better represent the higher shift in BMI of today's children, such that a greater percent are above the obesity cutoff. Growth curves of BMI versus age were developed using pooled NHANES data from 1999 – 2016, then validated using demographic data from the PTN Data Repository. Growth curves were calculated using the same lambda-mu-sigma (LMS) estimation method that the U.S. Center for Disease Control and Prevention (CDC) used to develop the current growth curves [1]. Briefly, selected empirical percentiles of BMI for age are smoothed using locally estimated polynomial regression. Selected empirical percentiles included the 3rd, 5th, 10th, 25th, 50th, 75th, 85th, 90th, 95th, 97th, and 99th percentile BMI for age. Then, the smoothed curves for each percentile are approximated using LMS estimation method, resulting in final percentile curves closely matching the smoothed ones, thus allowing for computation of additional percentiles and z-scores using the LMS parameters. In the LMS estimation method, a Box-Cox transformation is first applied to make the BMI for age distribution approximately normal. Then, the LMS parameters are estimated using the following equations:

$$X = M(1 + LSZ)^{\frac{1}{L}}; L \neq 0 \quad (1)$$

$$X = Mexp(SZ); L = 0 \quad (2)$$

where X is the BMI value and Z is the z-score that corresponds to the percentile. LMS parameters were estimated simultaneously across the 11 percentiles at each age point as the best solution to the system of 11 equations by minimizing the sum of squared errors. Thus, the BMI percentile for a given age (X) can then be obtained from a normal distribution table from the z-score estimated using the LMS parameters. Separate growth curves were generated for male and female Asian Americans, Black Americans, Mexican Americans, and White Americans, as well as pooled males and females (ten curves total, **Figure 1**, **Supplementary Figure 1**).

BMI for age data for males and females for all three available racial groups included the PTN Data Repository (Asian American, Black American, and White American children, as well as pooled males and females) was used to validate the growth curves. To validate the updated growth curves, observed subjects' ages were rounded to the nearest month, then the observed BMI percentile was calculated at each age point for key percentiles (5^{th}, 50^{th}, 85^{th}, and 95^{th} percentiles). These points were overlaid on top of the updated growth curves described above, and fit to the observed PTN Data Repository points was determined visually (**Supplementary Figure 2**). Excel sheets with LMS parameters for calculating updated growth curves and BMI percentiles are provided as **Electronic Supplementary Files 2**.

1.4 Calculations for Glomerular Filtration Rate (GFR)

Simulated pediatric GFR is calculated in PK-Sim® as a function of adult GFR and kidney size using the equation:

$$GFR_{ped} = \frac{GFR_{adult} * F_{age}}{V_{standard\ kidney}} \quad (3)$$

Where $GFRp_{ed}$ is the simulated pediatric GFR (in mL/min/100g kidney), GFR_{adult} is the standard adult GFR value, F_{age} is a scaling factor to account for age in children, and $V_{standard\ kidney}$ is the volume of a standard adult kidney.

Simulated GFR values for virtual children with obesity were compared to observed values reported in the literature using a number of different GFR calculations [2]. The observed study calculated creatinine clearance (CrCl) through 24-hour urine collection and estimated GFR using the Zappitelli and Schwartz equations as follows:

$$GFR_{Zappitelli} = \frac{43.82e^{0.003*Height}}{CysC^{0.635}*SCr^{0.547}} \quad (4)$$

$$GFR_{Schwartz} = 39.1\left(\frac{Height}{SCr}\right)^{0.516}\left(\frac{1.8}{CysC}\right)^{0.294}\left(\frac{30}{BUN}\right)^{0.169}(1.099)^{Male}\left(\frac{Height}{1.4}\right)^{0.188} \quad (5)$$

where height is in meters, CysC is cystatin C in mg/L, SCr is serum creatinine in mg/dL [2-4], BUN is blood urea nitrogen in mg/dL, and Male is an indicator variable equal to one if male. Absolute GFR values were normalized to a number of different body size metrics, including total body weight, BMI, lean body mass (LBM) as calculated by the Peters equation, fat-free mass (FFM) as calculated by the Al-Sallami equation, and body surface area (BSA) as calculated by the Haycock equation using the following equations:

$$LBM = 3.8(0.0215 * Weight^{0.6469} * Height^{0.7236}) \quad (6)$$

$$FFM_{males} = \left[0.88 + \left(\frac{1-0.88}{1+\left(\frac{Age}{13.4}\right)^{-12.7}}\right)\right]\left[\frac{9270*Weight}{6680+(216*BMI)}\right] \quad (7a)$$

$$FFM_{females} = \left[1.11 + \left(\frac{1-1.11}{1+\left(\frac{Age}{7.1}\right)^{-1.1}}\right)\right]\left[\frac{9270*Weight}{8780+(244*BMI)}\right] \quad (7b)$$

$$BSA = Weight^{0.5378} * Height^{0.3964} * 0.024265 \quad (8)$$

where weight is in kg, height is in centimeters, age is in years, and BMI is in kg/m^2 [5-7]. Note that the observed study calculated FFM using the Schaeffer equation, but this was not applicable to the simulated population since it calculates FFM using bioimpedance [8]. The final GFR comparisons are shown in **Table 2**.

1.5 Clinical Data for Clindamycin PBPK Modeling – External Data Study

The External Data Study (ClinicalTrials.gov #NCT02475876) was a multicenter (n = 10), open-label, interventional PK and safety study that enrolled children aged 36 weeks postmenstrual age and 16 years of age receiving clindamycin per clinical care at the physician's discretion. Exclusion criteria included failure to obtain consent or assent, known pregnancy or breastfeeding, history of allergic reactions to study drugs, serum creatinine >2 mg/dL, alanine aminotransferase >250 U/L or aspartate transaminase >500 U/L, or on extracorporeal membrane oxygenation support. Protocol specified clindamycin dose was 9 mg/kg, 12 mg/kg, and 10 mg/kg every 8 hours for subjects between 1-5 months, >5 months – 6 years, and >6 years to 16 years of age, respectively. PK samples were collected at protocol specified times, which were after the 1^{st} and the $>6^{th}$ dose at between 0-10 min and 2-4 h after the dose and <30 minutes before the next dose. The plasma samples were quantified at a single central laboratory (OpAns, LLC, Durham, NC, USA) using a validated high-performance liquid chromatography-tandem mass spectrometry assay with a lower limit of quantitation of clindamycin of 50 ng/L as previously described [9]. The External Data Study protocol was approved by the institutional review board of participating instructions, and informed consent was obtained from the parent or guardian and assent from the subject when appropriate.

1.6 Clindamycin Oral Absorption Model Development and Evaluation

In this study, we also developed an oral clindamycin hydrochloride absorption model using available adult data from the literature in order simulate exposure for 15 observed children with obesity who received oral doses (**Supplementary Table 16**). Clindamycin hydrochloride dosing was adjusted using the salt factor (0.9151) and simulated as a clindamycin dose. Intestinal transcellular permeability and Weibull parameters were optimized using digitized data across seven adult oral clindamycin studies using the Levenberg-Marquardt algorithm [10]. Final clindamycin PBPK model parameters are shown in **Supplementary Table 6**. For five pediatric subjects who received both intravenous and oral doses (all of whom had samples taken after an oral dose), all doses were modeled as clindamycin doses adjusted using the salt factor.

2 SUPPLEMENTARY RESULTS

2.1 Virtual Population Demographics

Each virtual child's height in the virtual population is randomly selected from published distributions from the International Commission on Radiological Protection (ICRP) database depending on the child's age. Simulated height was reflective of the ICRP values and increased with age (**Supplementary Figure 22**).

Each virtual child's weight is determined as the sum of the 19 organ compartments modeled in PK-Sim®. Individual organ weights are selected from published ICRP distributions depending on the child's age, with additional scaling factors introduced for children with obesity. The remaining extra weight is added to both the adipose and skin organs to increase the virtual child's weight to a BMI within the obese range (e.g., $\geq 95^{th}$ percentile BMI for age and sex). Simulated height and weight were correlated, with a rightward shift in the height-weight curve

for children with versus without obesity observed, reflecting an increase in weight (**Supplementary Figure 23**).

2.2 Clindamycin Oral Absorption Model

The clindamycin oral absorption model was able to capture the majority of digitized adult data, with an overall AFE of 0.90 (mean [range] of 0.99 [0.50, 2.23] across seven studies of orally dosed clindamycin in healthy adult volunteers) (**Supplementary Table 16**, **Supplementary Figure 24**).

2.3 Incorporating AAG Concentration into Fu for Clindamycin

Expanding the previously developed pediatric clindamycin PBPK model to include children with obesity first resulted in 64% of observed concentrations falling within the 90% model prediction interval (with 26% above and 10% below), and an overall AFE of 0.76. Exploring model misspecification revealed a trend in increasing underestimation of observed concentrations with increasing AAG concentration (**Supplementary Figure 25**). Thus, the fraction unbound for each observed subject was adjusted based on their individual AAG concentration using the equation:

$$f_{u,ped} = \frac{1}{1+\left(\frac{AAG_{ped}}{AAG_{adult}}\right)\left(\frac{1-f_{u,adult}}{f_{u,adult}}\right)} \quad (9)$$

where $f_{u,ped}$ is the AAG-adjusted fraction unbound for the observed pediatric subject, AAG_{ped} is the reported AAG concentration for the observed pediatric subject, AAG_{adult} is the upper or lower bound reference healthy adult AAG concentration (0.77 and 1.46 mg/mL, respectively), and $f_{u,adult}$ is the reported adult fraction unbound [11-12]. After adjusting fraction unbound using the AAG concentration, the model captured observed concentrations from children without obesity well, with 74% of observed concentrations falling within the 90% model prediction interval (15% above and 11% below) and a revised AFE of 0.88 (**Supplementary Figure 26**).

Seventy-seven percent of concentrations from children with obesity fell within the 90% model prediction interval (7% above and 16% below) with an overall AFE of 1.09, following adjusting the fraction unbound (**Supplementary Figures 8, 27**). No further trends in model misspecification were identified by study, age, body size, or AAG concentration (**Supplementary Figure 27**).

3 SUPPLEMENTARY FIGURES

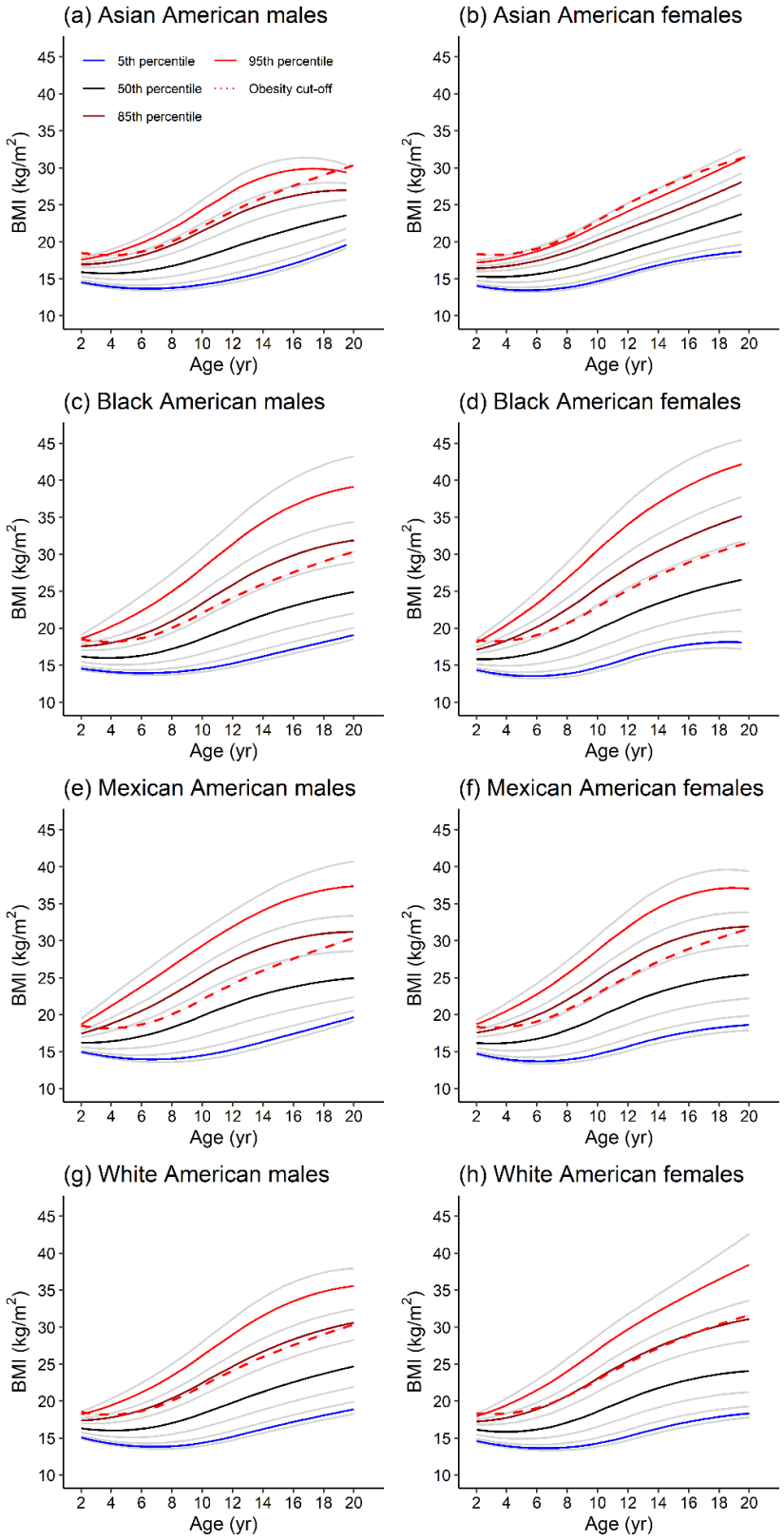

Supplementary Figure 1. Updated growth curves based on NHANES pooled data for male and female groups. Key BMI percentiles are highlighted in blue (5th percentile), black (50th percentile), dark red (85th percentile), and red (95th percentile). The BMI cutoff for obesity as defined by the CDC is represented by the bold, red dashed line, such that children with a BMI above that line for a given age are considered obese.

BMI, body mass index; CDC, Center for Disease Control and Prevention; NHANES, National Health and Nutrition Examination Survey

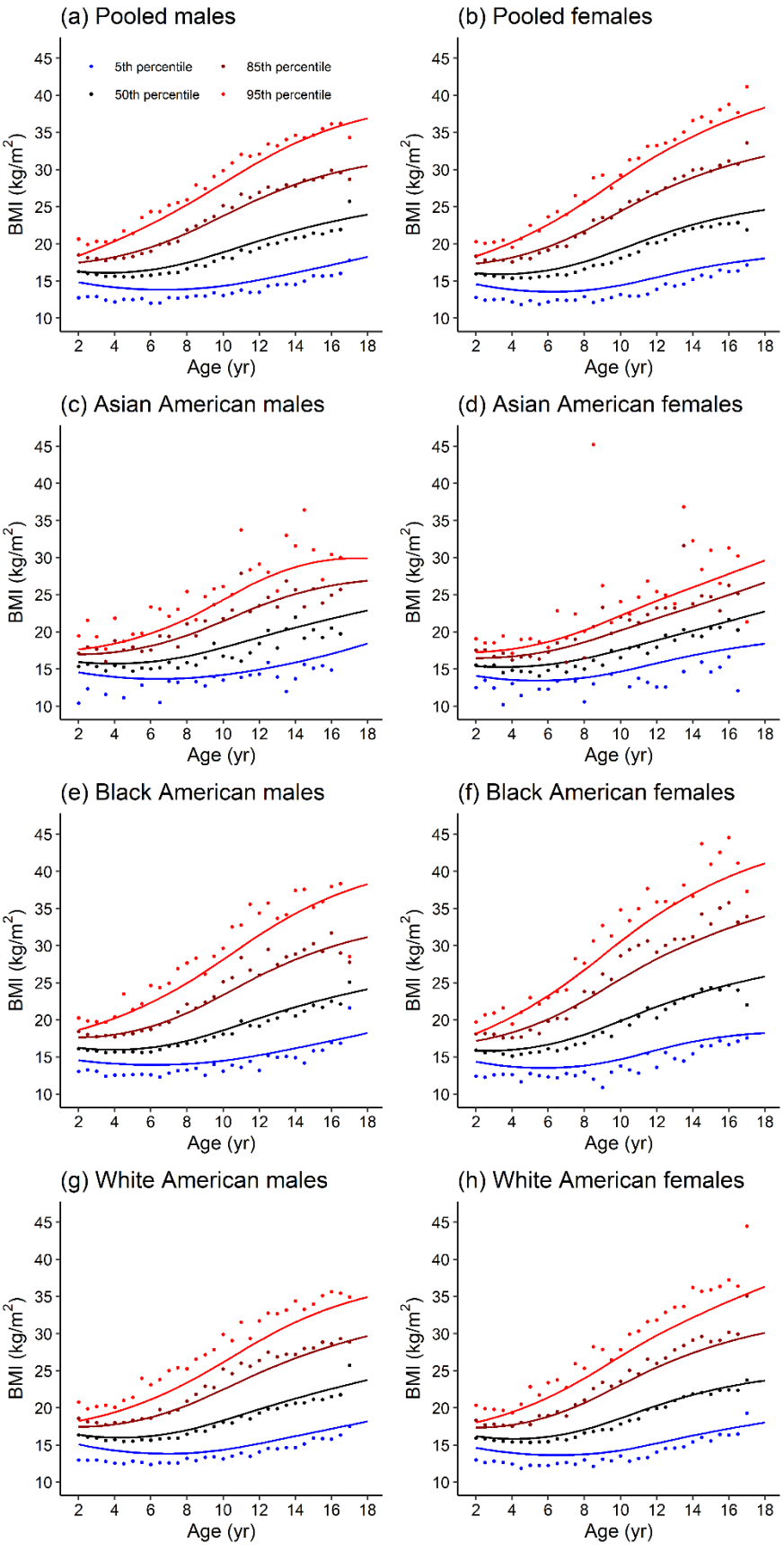
(a) Pooled males
5th percentile
85th percentile
50th percentile
95th percentile
BMI (kg/m2)
Age (yr)
(b) Pooled females
(c) Asian American males
(d) Asian American females
(e) Black American males
(f) Black American females
(g) White American males
(h) White American females

Supplementary Figure 2. Validation of updated growth curves for males and female groups. Key BMI percentiles are represented in blue (5^{th} percentile), black (50^{th} percentile), dark red (85^{th} percentile), and red (95^{th} percentile). Solid lines are the updated growth curves based on pooled NHANES data, and points represent the BMI for a given percentile for a given age bin based on demographic data obtained from the PTN Data Repository.

BMI, body mass index; NHANES, National Health and Nutrition Examination Survey; PTN, Pediatric Trials Network

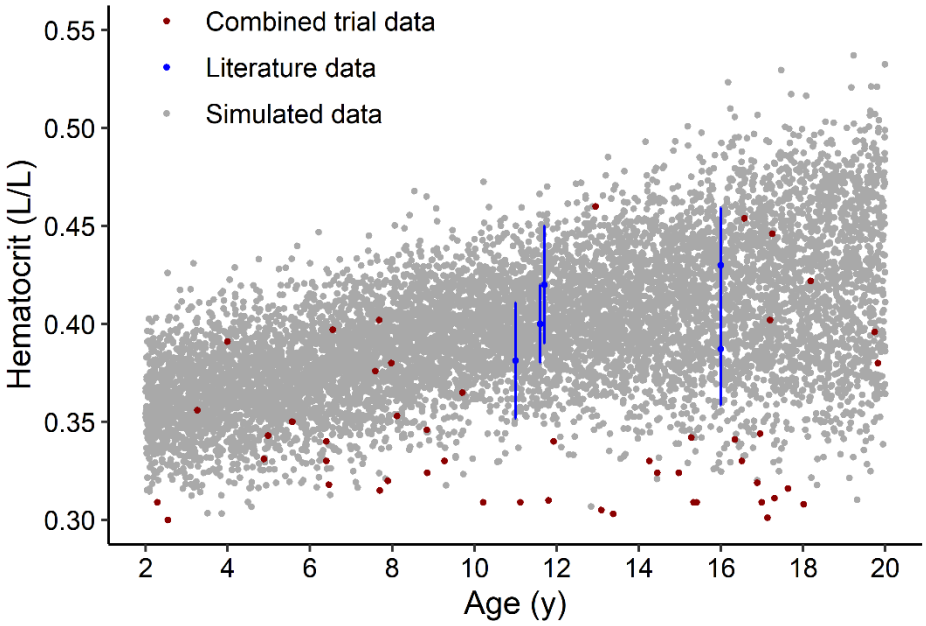

Supplementary Figure 3. Hematocrit versus age for virtual and real-world children with obesity. Simulated hematocrit values from virtual children with obesity (n = 10,000) generated from PK-Sim® are shown in gray, reported hematocrit values (mean ± standard deviation) found in the literature search from children with obesity are shown in blue, and individual observed hematocrit values from children (n = 136) with obesity in the clinical trial data are shown in red. See **Table 1** for combined trial data summary and **Supplementary Table 9** for literature hematocrit values.

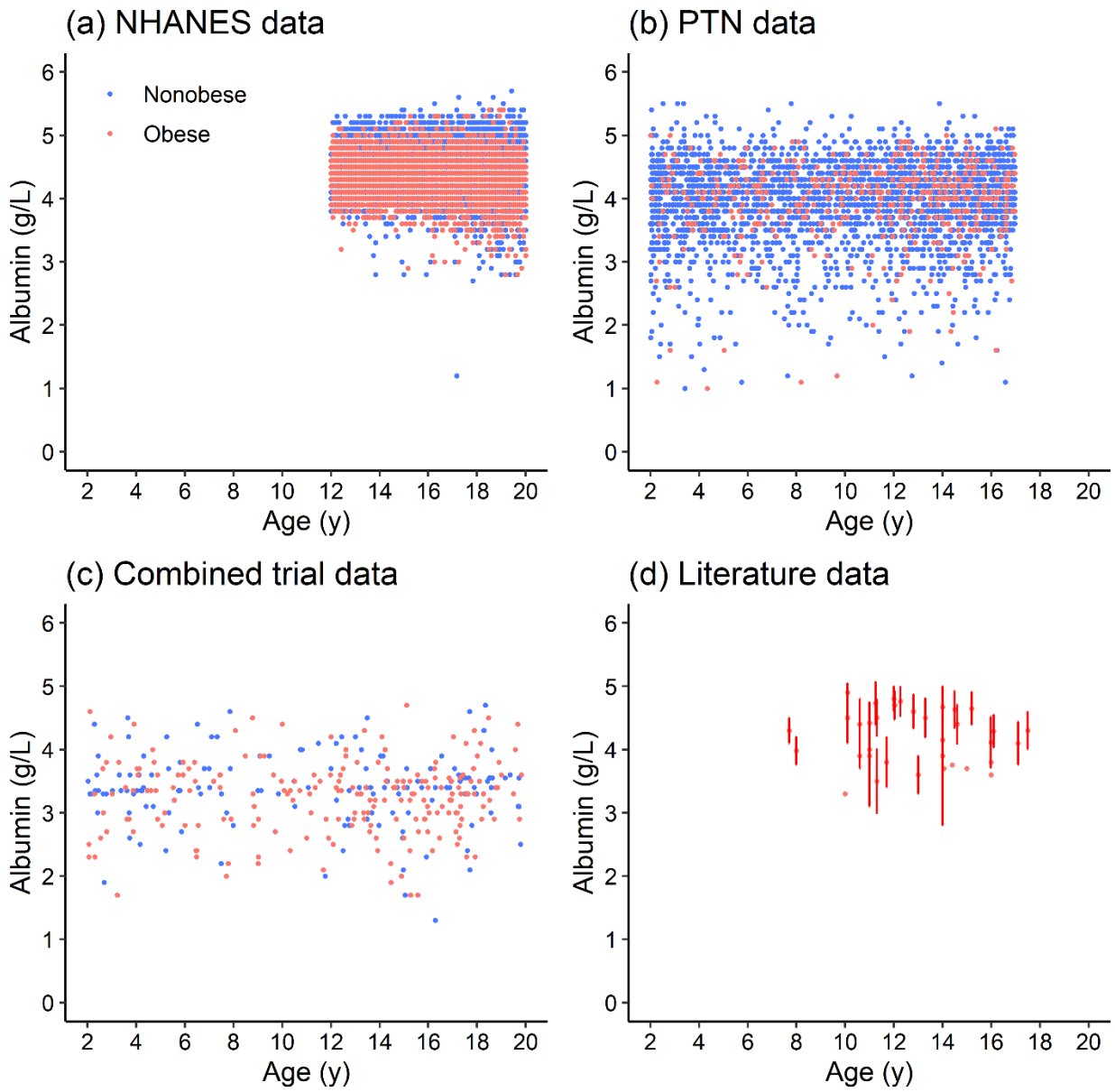

Supplementary Figure 4. Observed albumin concentration versus age for children without (blue) and with (red) obesity from four different data sources – individual values from NHANES survey (n = 14,293) (a), PTN data repository (n = 3,193) (b), and combined trial data (n = 393) (c), and mean values (mean ± standard deviation) found in the literature search (d). Data sources are shown in separate panels for better visualization. Note that albumin concentrations were only reported for children >12 years for NHANES.

NHANES, National Health and Nutrition Examination Survey; PTN, Pediatric Trials Network

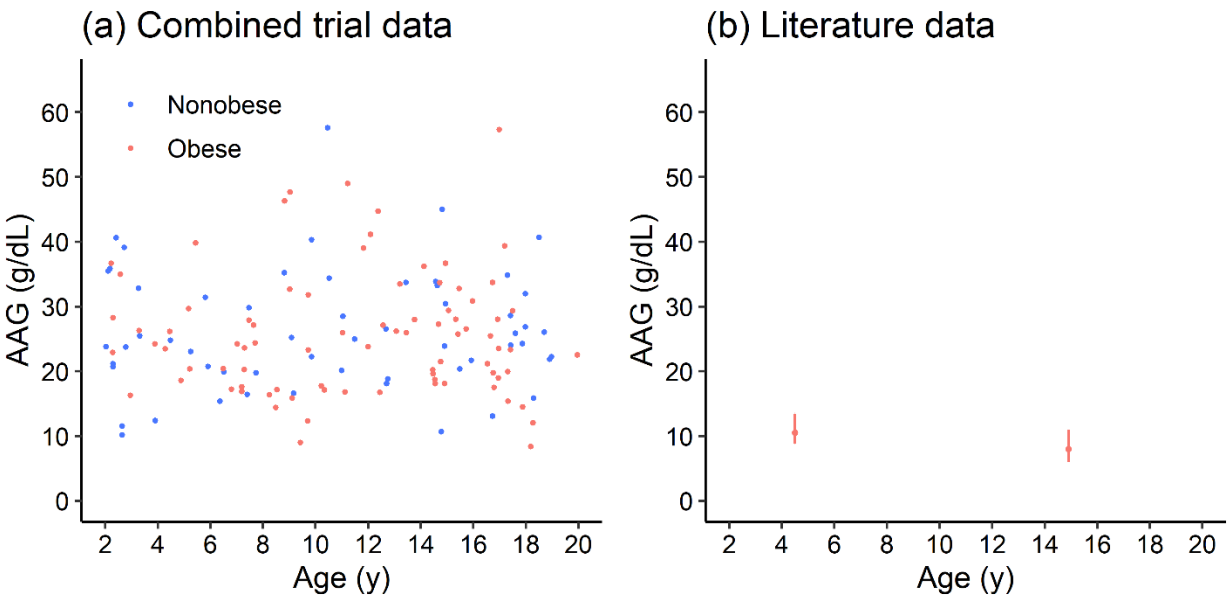

Supplementary Figure 5. AAG concentration versus age for children without (blue) and with (red) obesity, including observed values from the combined trial data (n = 60 and 88 for children without at with obesity, respectively) (a) and reported values (mean ± standard deviation) from the literature search (b) with corresponding standard deviation error bars. Data sources are shown in separate panels for better visualization.

AAG, α1-acid glycoprotein

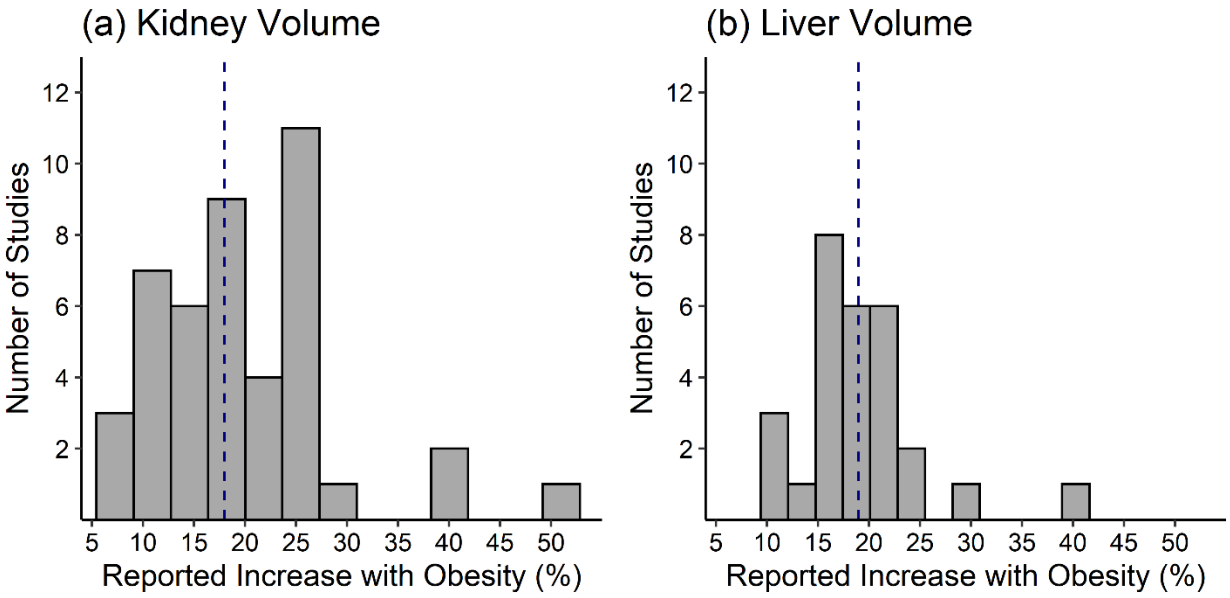

Supplementary Figure 6. Reported percent increase in children's kidney volume (a) and liver volume (b) with obesity for a number of studies found in the literature search. Dashed lines represent the median increase (18% and 19% for kidney and liver, respectively) across all of the studies for reference.

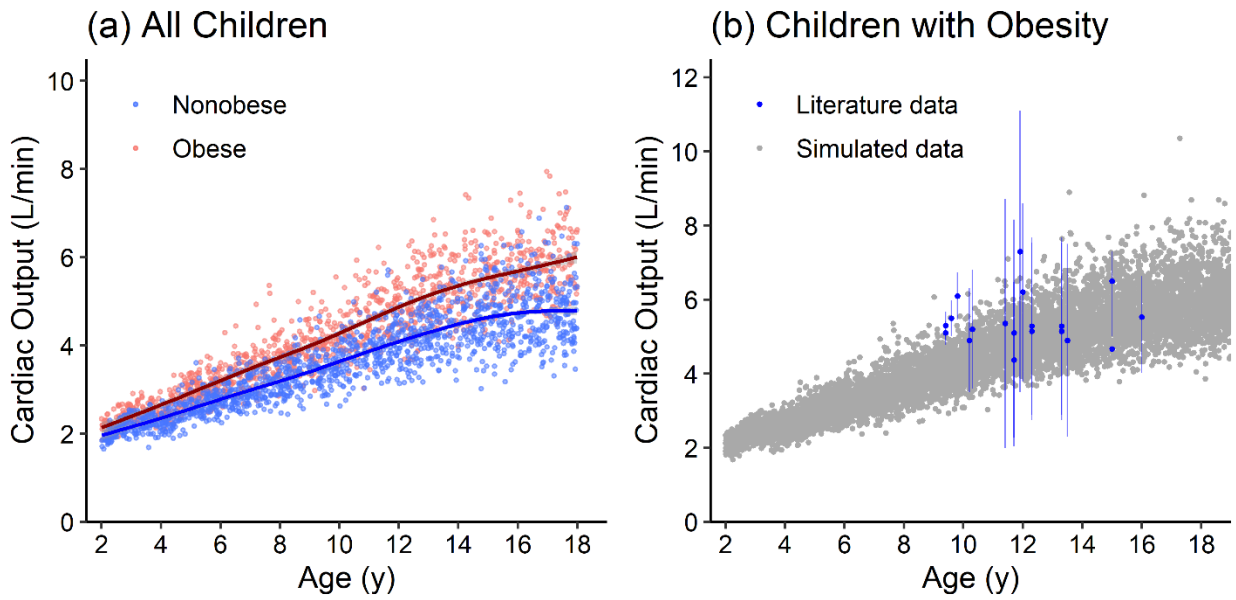

Supplementary Figure 7. Simulated cardiac output in virtual children. Panel (a) represents changes in cardiac output with age for 1,500 virtual children without (blue) and 1,500 virtual children with obesity (red). Solid lines represent the central tendency, which is the Loess line as calculated by the generalized additive model. Panel (b) represents simulated versus reported cardiac output values for children with obesity. Gray points represent simulated cardiac output for 10,000 virtual children, and blue points represented reported values with corresponding reported variation.

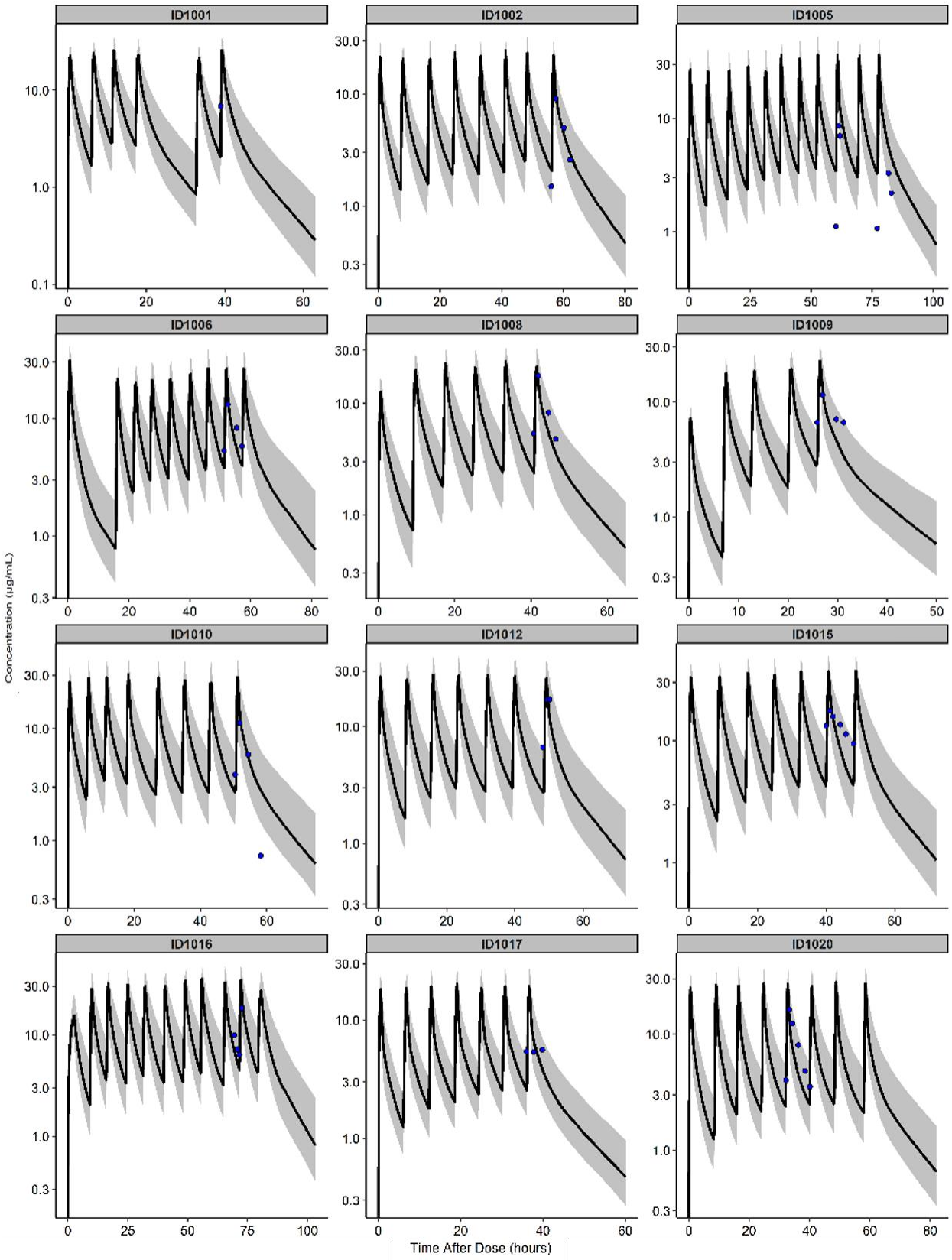
ID1001
ID1002
ID1005
ID1006
ID1008
ID1009
ID1010
ID1012
ID1015
ID1016
ID1017
ID1020
Concentration (µg/mL)
Time After Dose (hours)

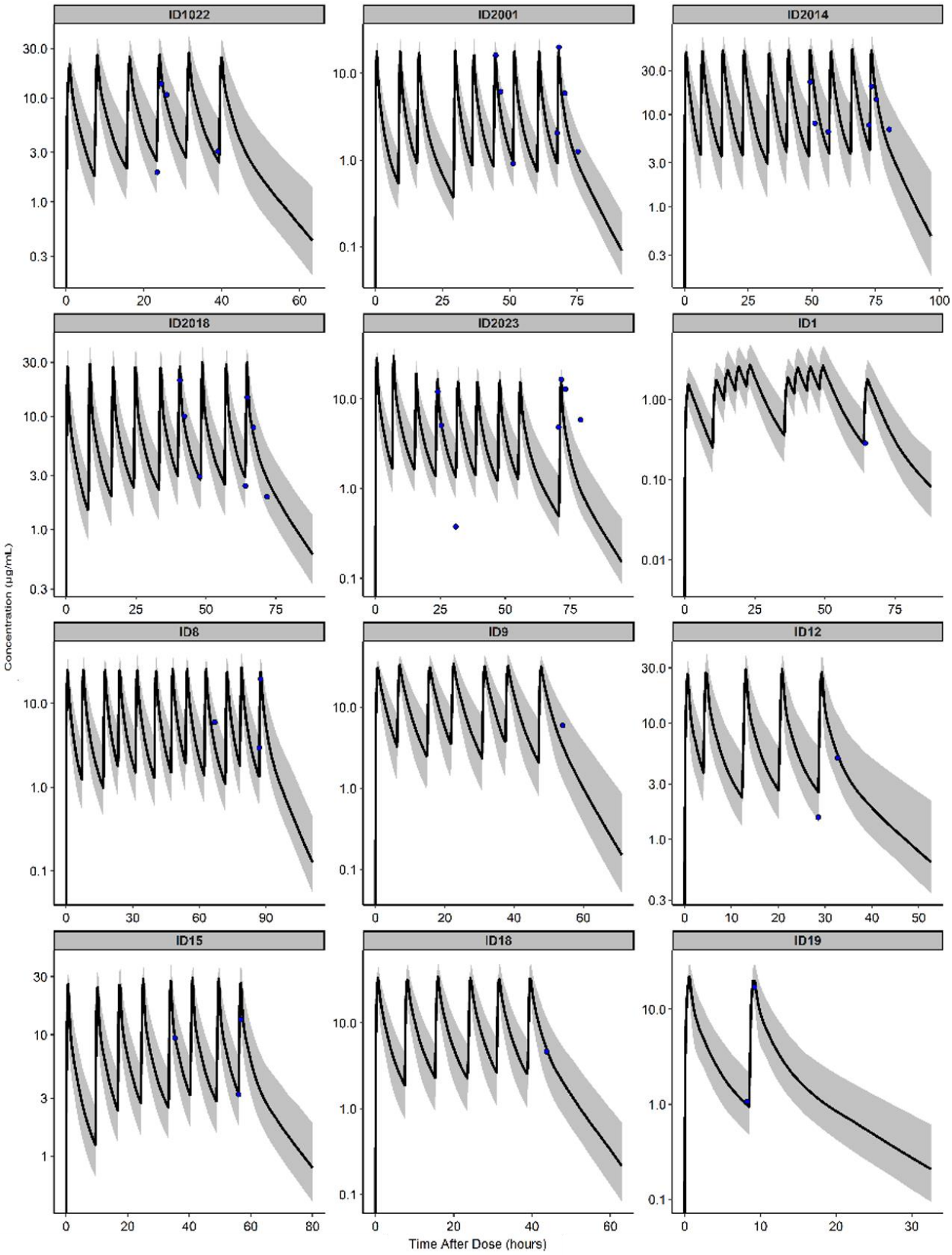
ID1022
ID2001
ID2014
ID2018
ID2023
ID1
ID8
ID9
ID12
ID15
ID18
ID19
Concentration (µg/mL)
Time After Dose (hours)

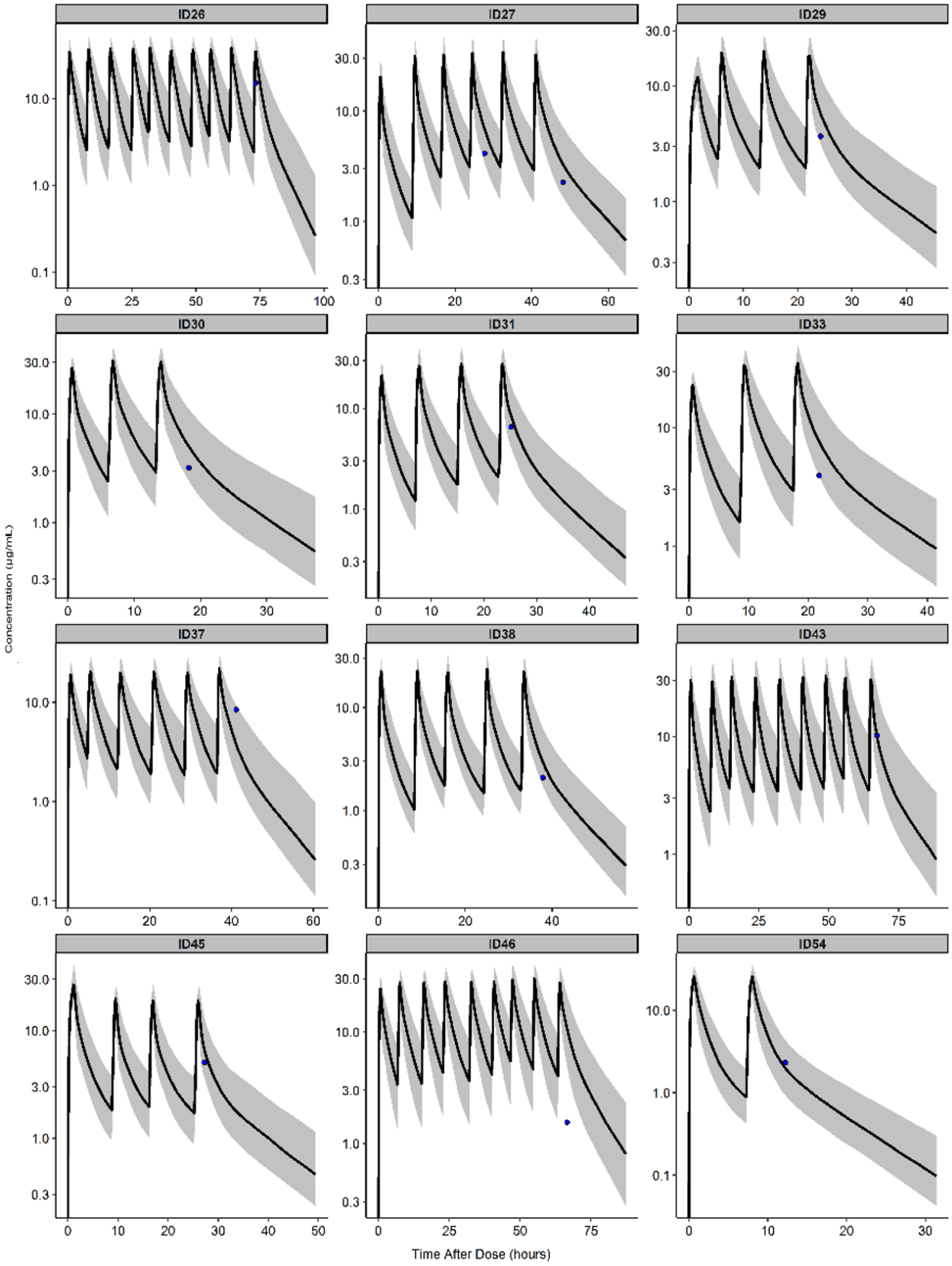
ID26
ID27
ID29
ID30
ID31
ID33
ID37
ID38
ID43
ID45
ID46
ID54
Concentration (µg/mL)
Time After Dose (hours)

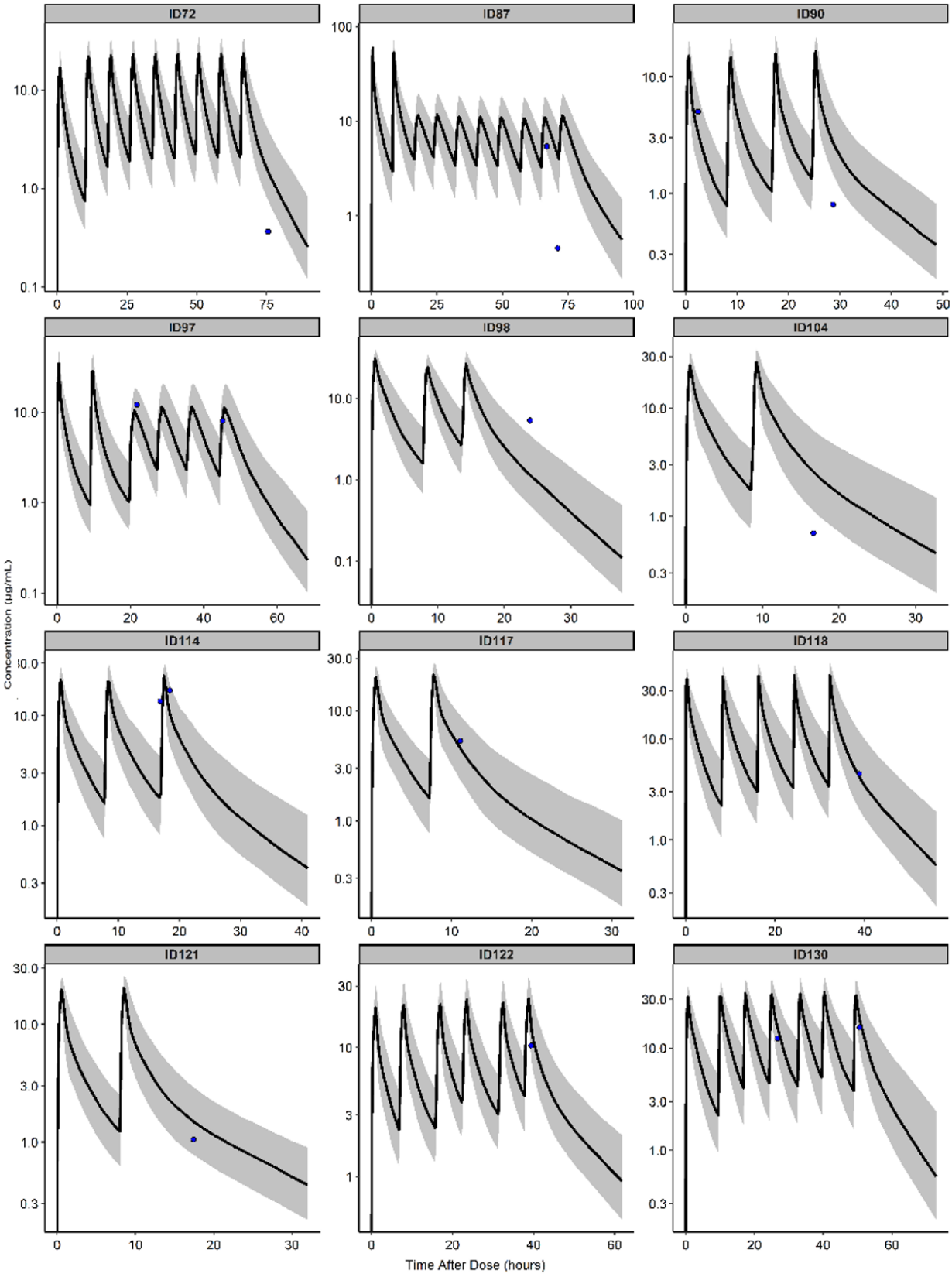
ID72
ID87
ID90
ID97
ID98
ID104
ID114
ID117
ID118
ID121
ID122
ID130
Concentration (µg/mL)
Time After Dose (hours)

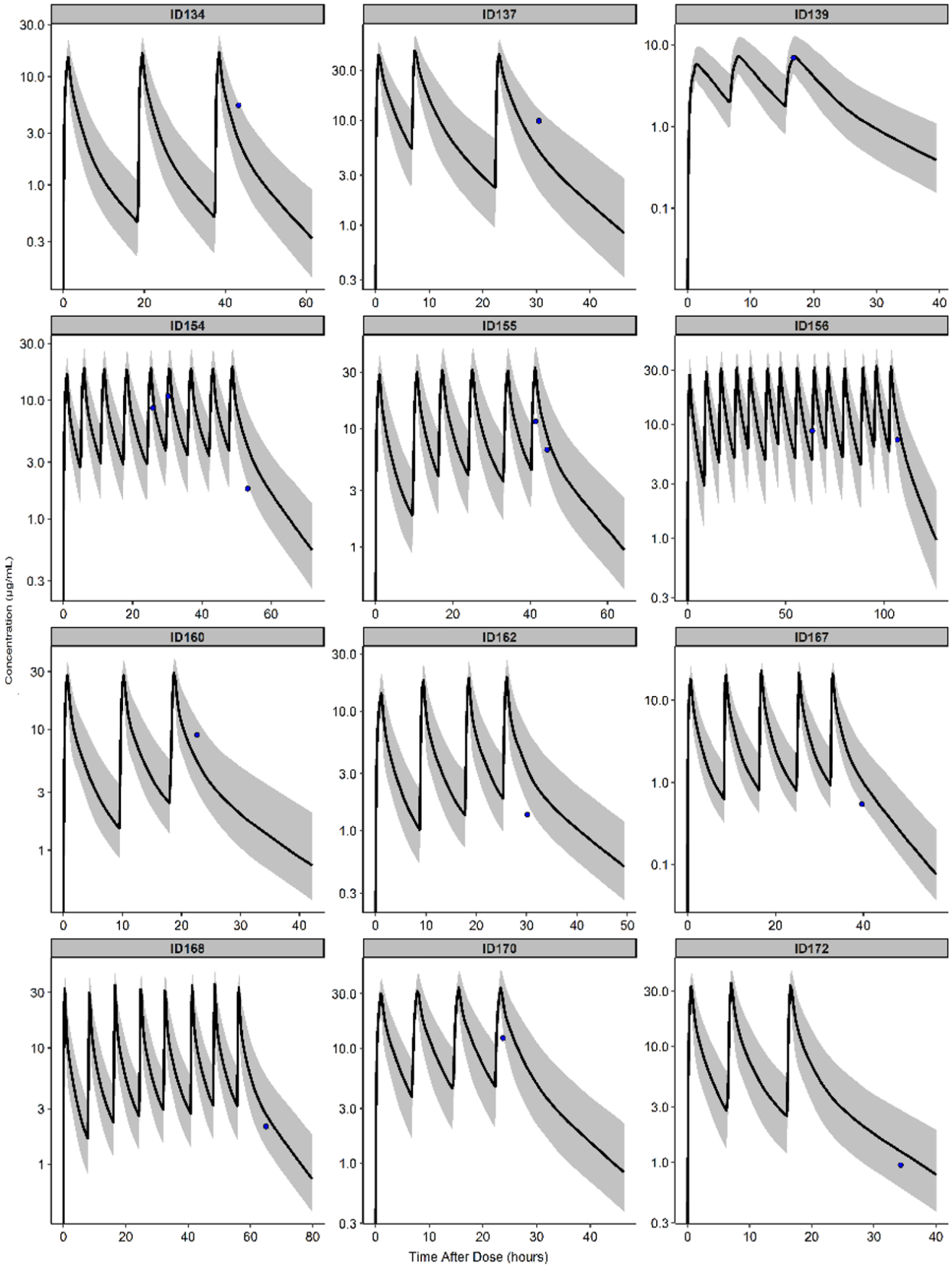
ID134
ID137
ID139
ID154
ID155
ID156
ID160
ID162
ID167
ID168
ID170
ID172
Concentration (ug/mL)
Time After Dose (hours)

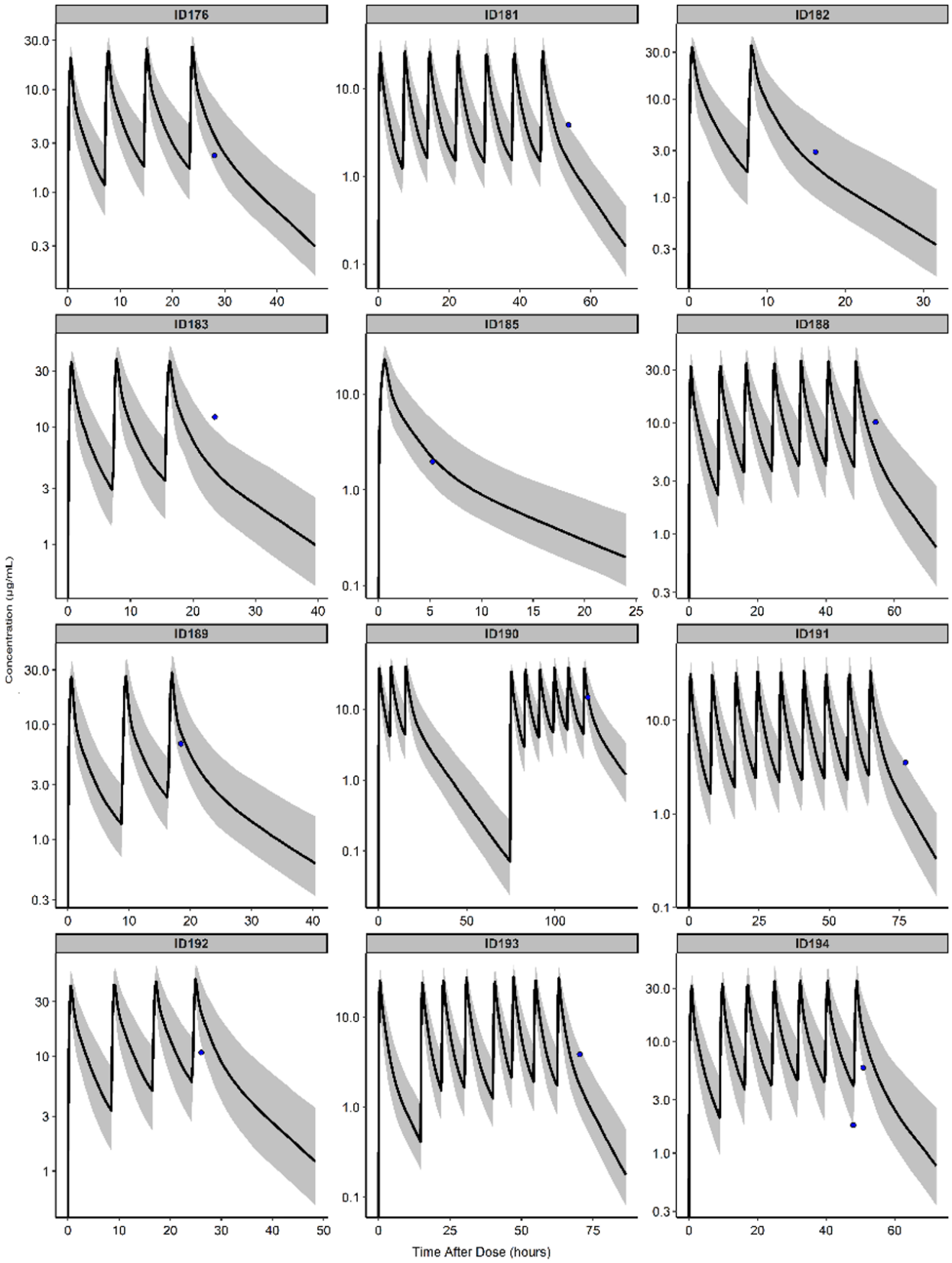
ID176
ID181
ID182
ID183
ID185
ID188
ID189
ID190
ID191
ID192
ID193
ID194
Concentration (µg/mL)
Time After Dose (hours)

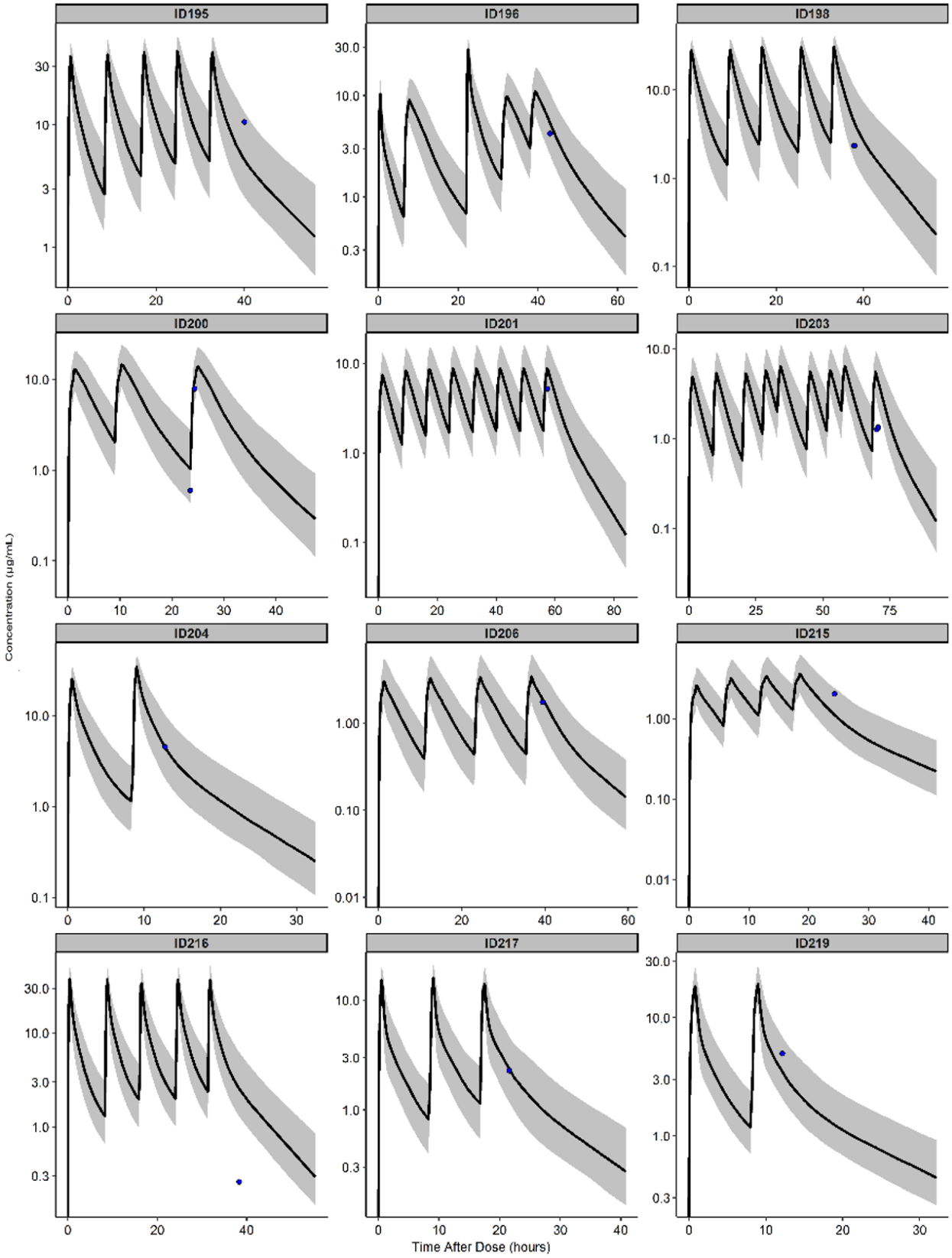
ID195
ID196
ID198
ID200
ID201
ID203
ID204
ID206
ID215
ID216
ID217
ID219
Concentration (µg/mL)
Time After Dose (hours)

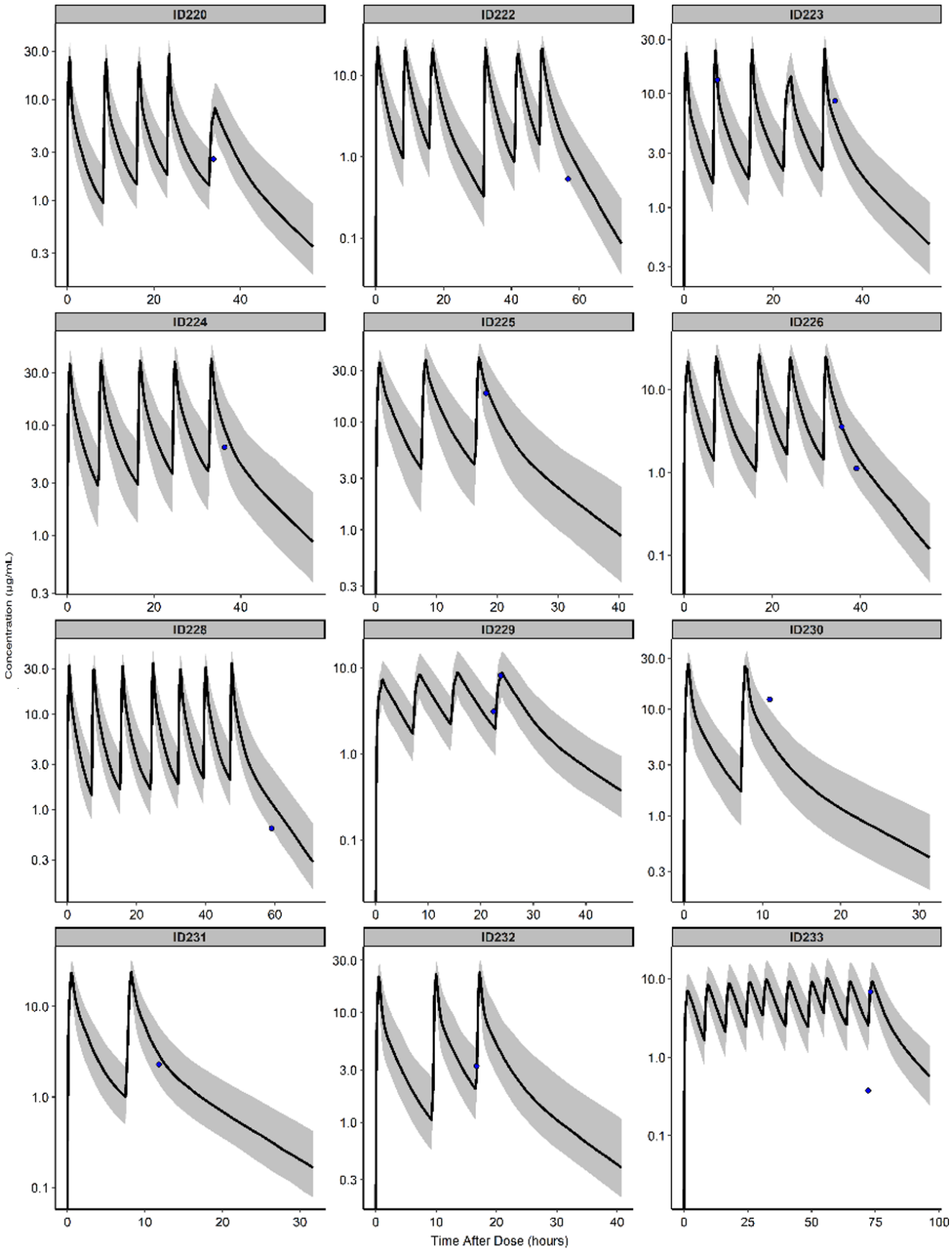
ID220
ID222
ID223
ID224
ID225
ID226
ID228
ID229
ID230
ID231
ID232
ID233
Concentration (ug/mL)
Time After Dose (hours)

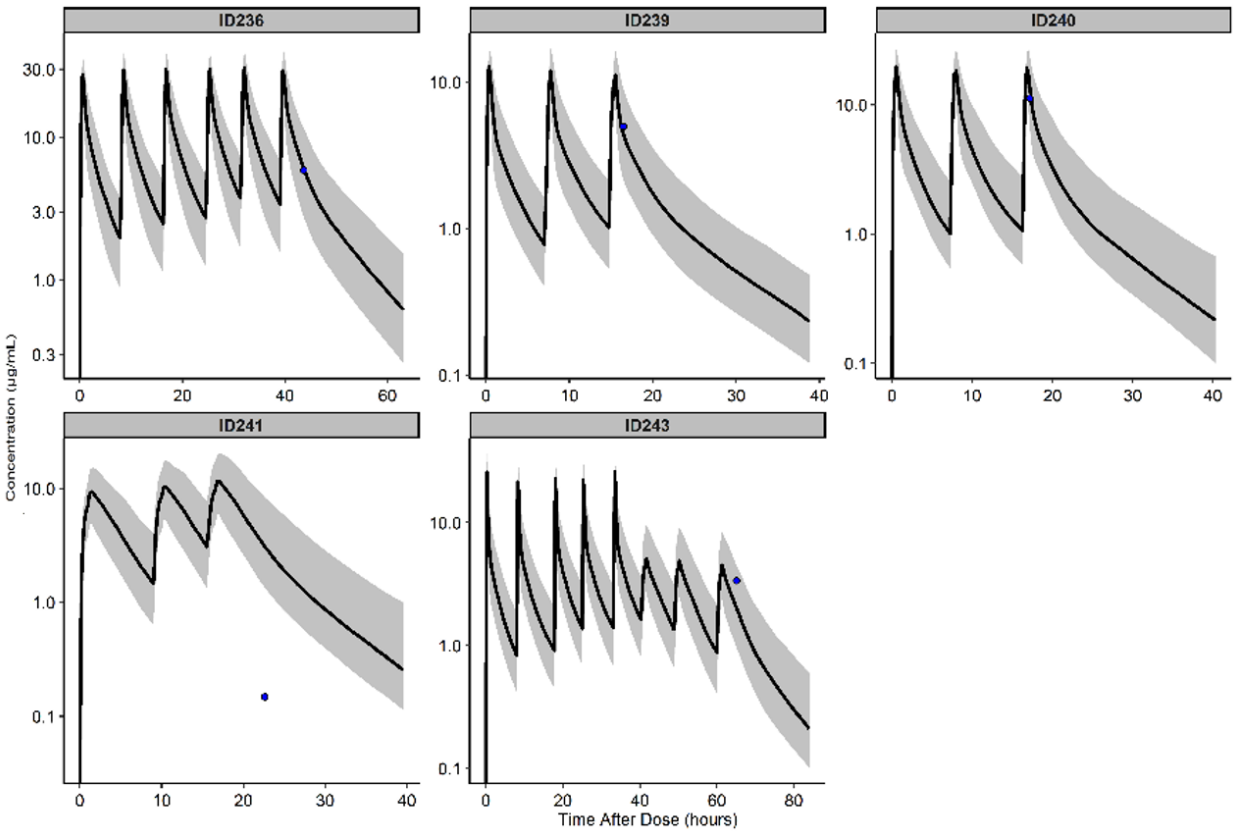

Supplementary Figure 8. Population simulations (n=250) of plasma clindamycin concentration after adjusting fraction unbound using reported AAG concentrations using "individualized populations" for each observed pediatric subject with obesity that are matched to that particular subject's demographics and dosing regimen. The shaded regions are the 90% model prediction interval, which are overlaid with points representing observed plasma concentrations from the POP01, CLIN01, and External Data Study.

AAG, α1-acid glycoprotein; CLIN01, Safety and Pharmacokinetics of Clindamycin in Pediatric Subjects with BMI ≥ 85th Percentile (ClinicalTrials.gov #NCT01744730) Study; POP01, Pharmacokinetics of Understudied Drugs Administered to Children Per Standard of Care (ClinicalTrials.gov #NCT01431326) Study

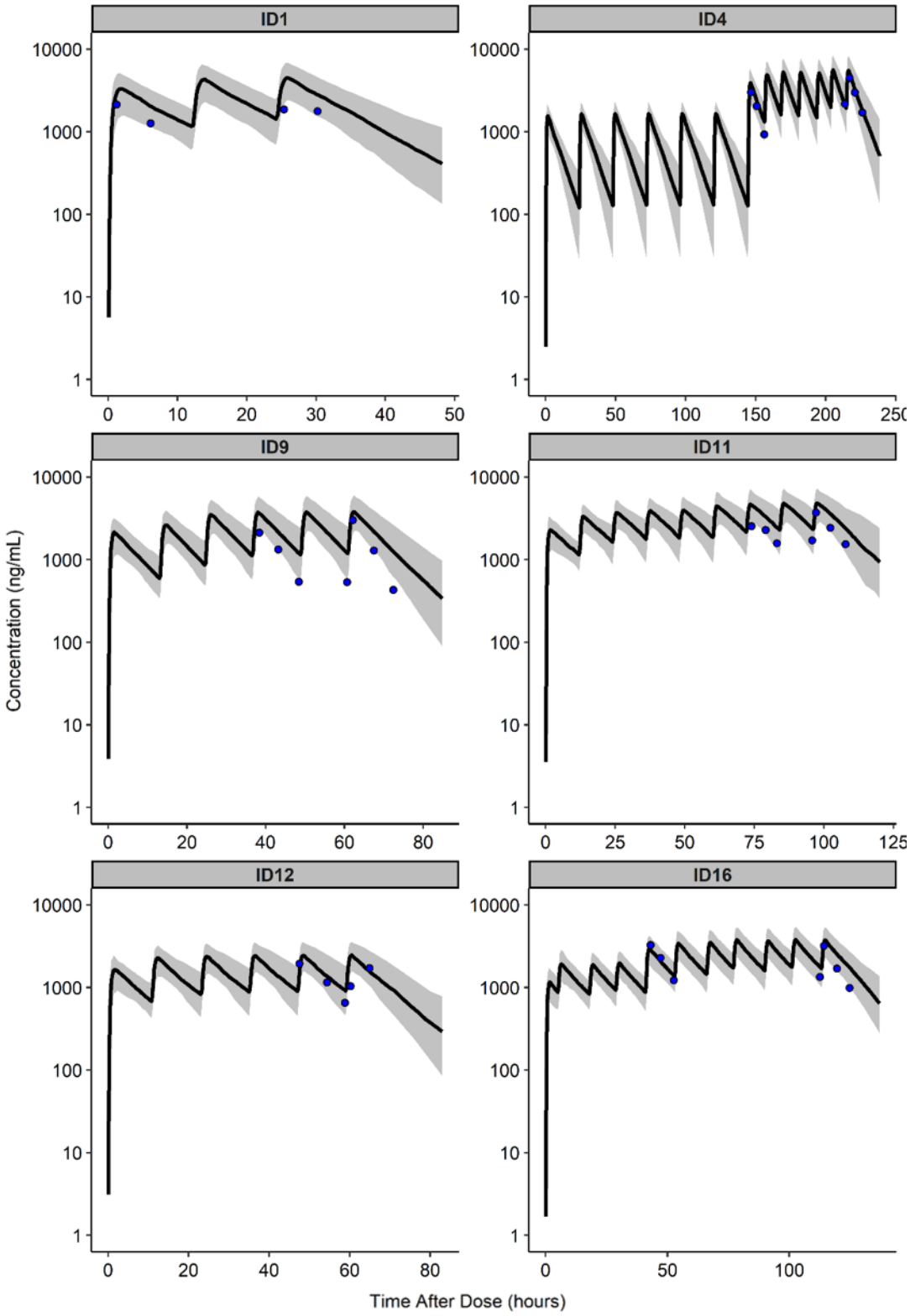
ID1
ID4
ID9
ID11
ID12
ID16
Concentration (ng/mL)
Time After Dose (hours)

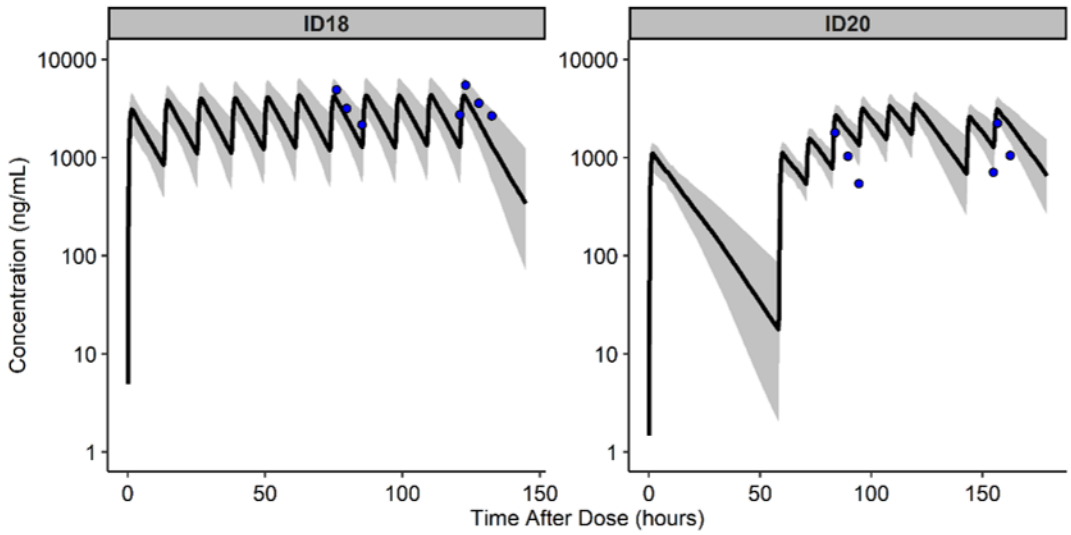

Supplementary Figure 9. Population simulations (n=250) of plasma trimethoprim concentration using "individualized populations" for each observed pediatric subject without obesity that are matched to that particular subject's demographics and dosing regimen. The shaded regions are the 90% model prediction interval, which are overlaid with points representing observed plasma concentrations from the External Data Study.

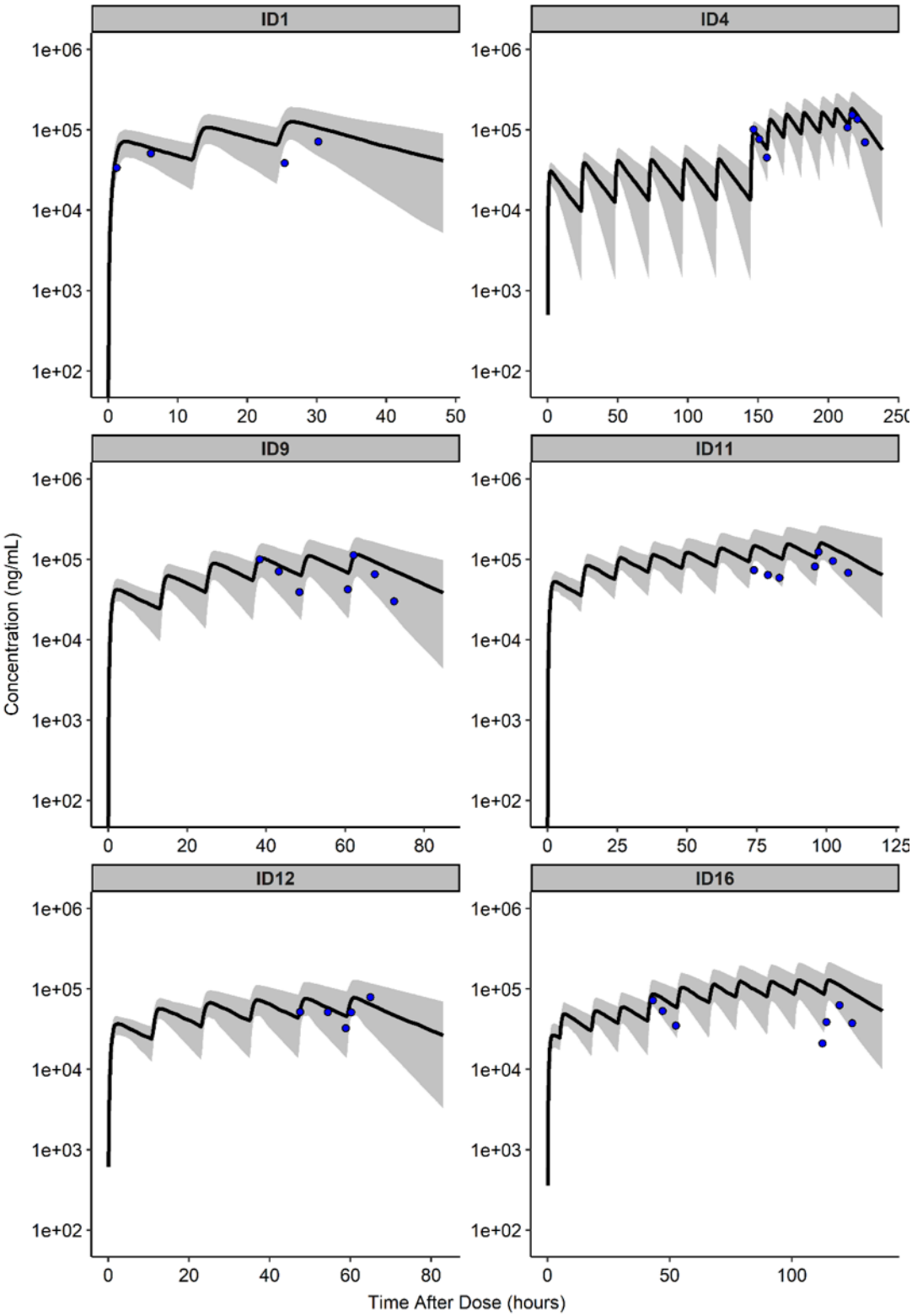
ID1
ID4
ID9
ID11
ID12
ID16
Concentration (ng/mL)
Time After Dose (hours)
1e+02
1e+03
1e+04
1e+05
1e+06

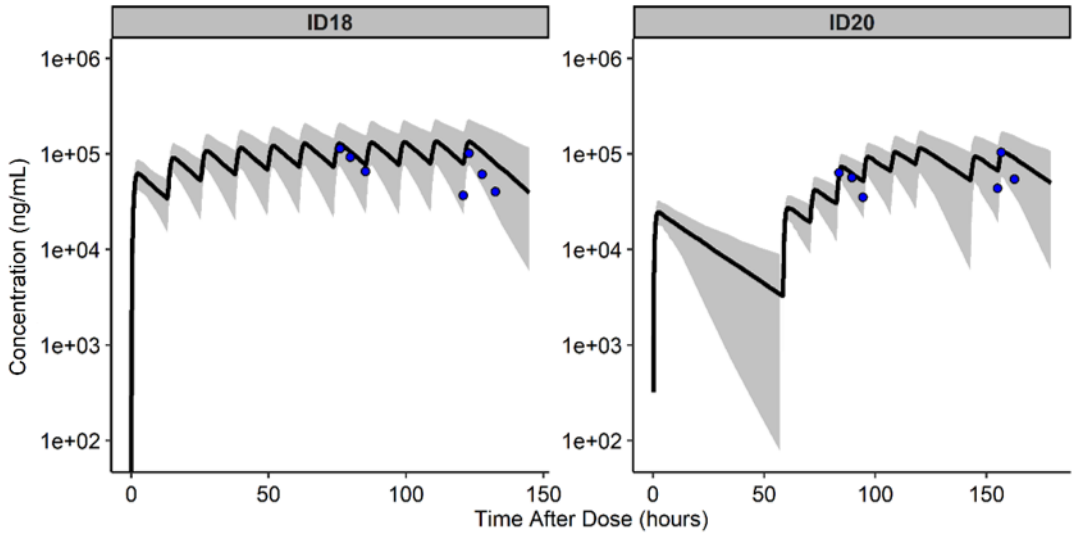

Supplementary Figure 10. Population simulations (n=250) of plasma sulfamethoxazole concentration using "individualized populations" for each observed pediatric subject without obesity that are matched to that particular subject's demographics and dosing regimen. The shaded regions are the 90% model prediction interval, which are overlaid with points representing observed plasma concentrations from the External Data Study.

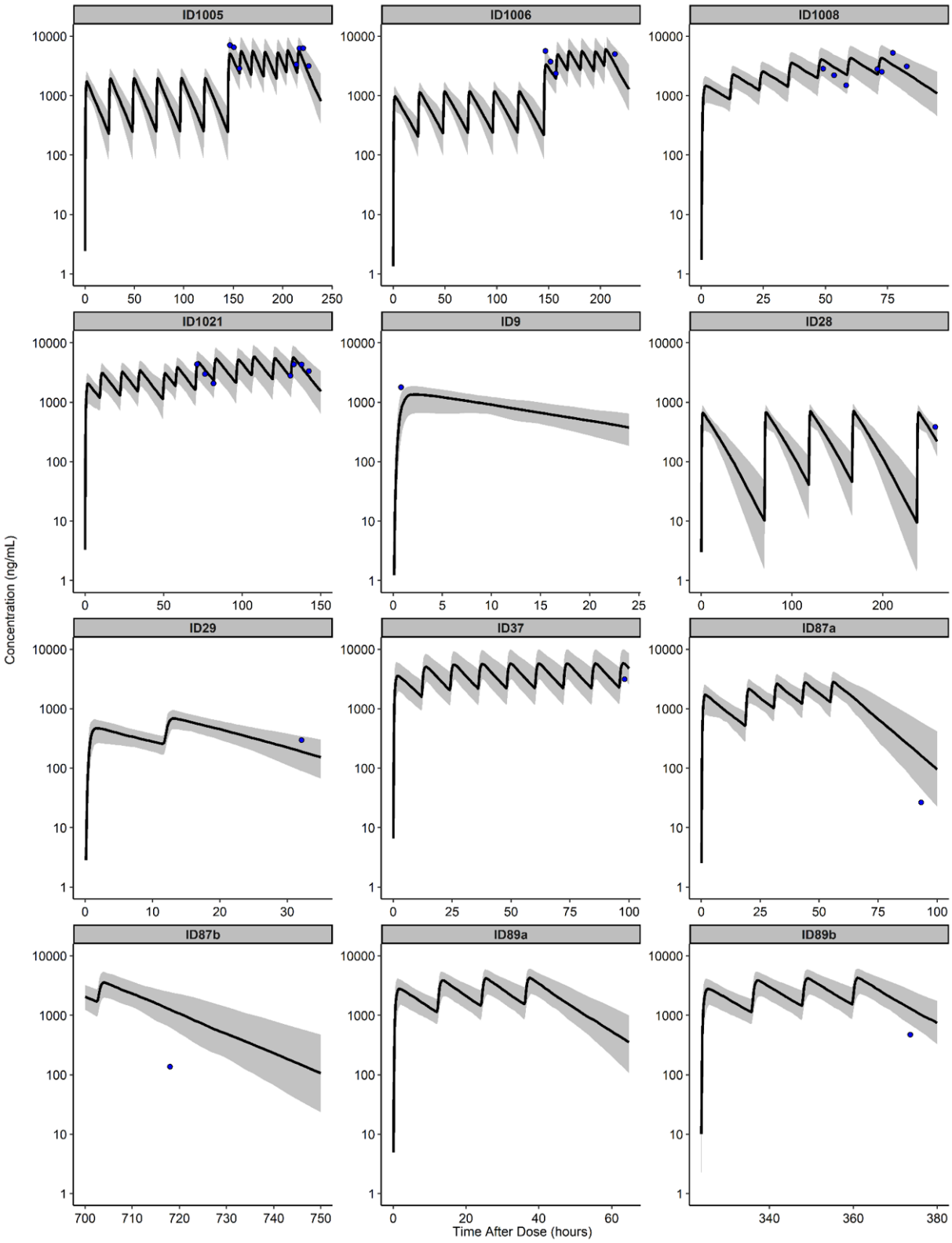
ID1005
ID1006
ID1008
ID1021
ID9
ID28
ID29
ID37
ID87a
ID87b
ID89a
ID89b
Concentration (ng/mL)
Time After Dose (hours)

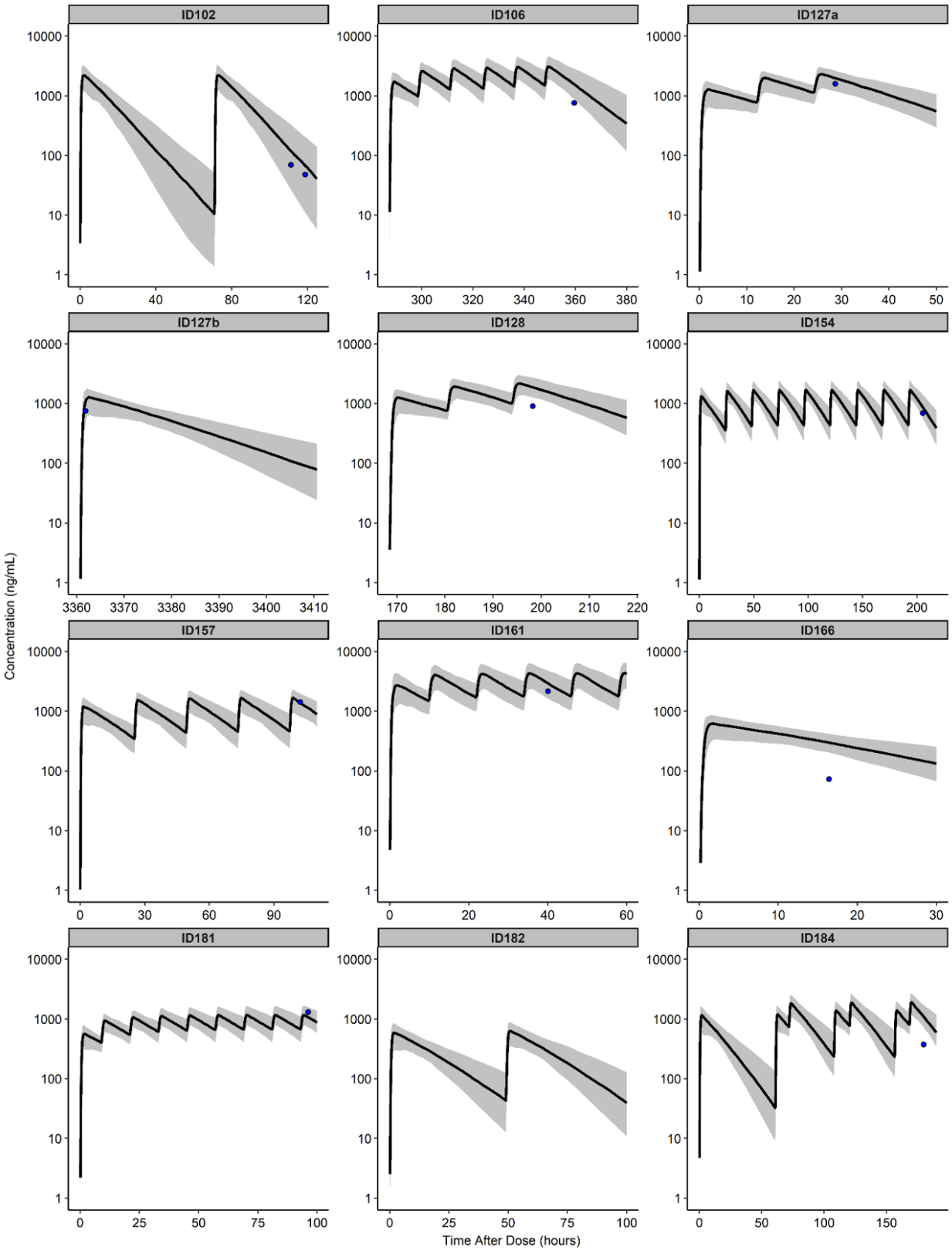
ID102
ID106
ID127a
ID127b
ID128
ID154
ID157
ID161
ID166
ID181
ID182
ID184
Concentration (ng/mL)
Time After Dose (hours)

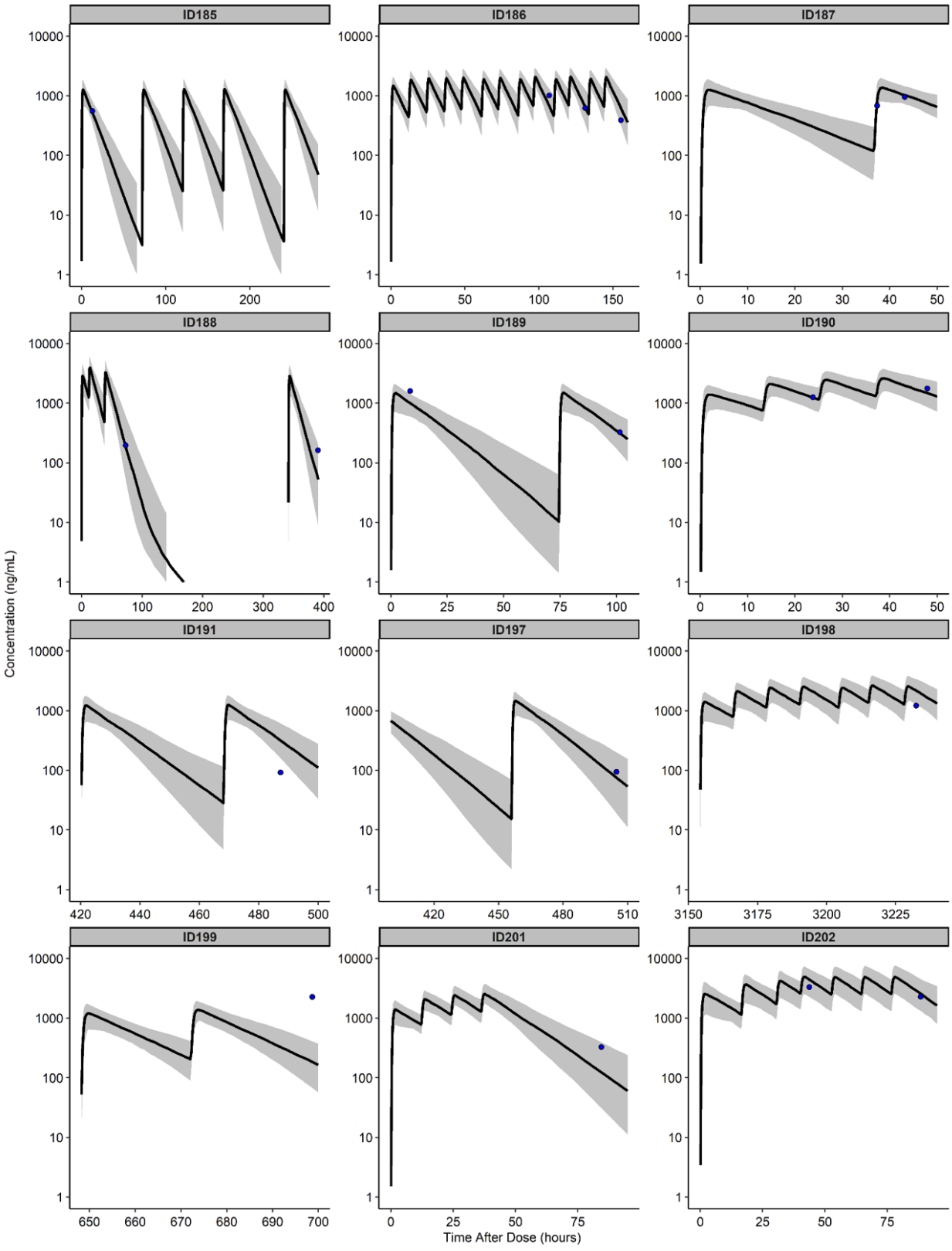
ID185
ID186
ID187
ID188
ID189
ID190
ID191
ID197
ID198
ID199
ID201
ID202
Concentration (ng/mL)
Time After Dose (hours)

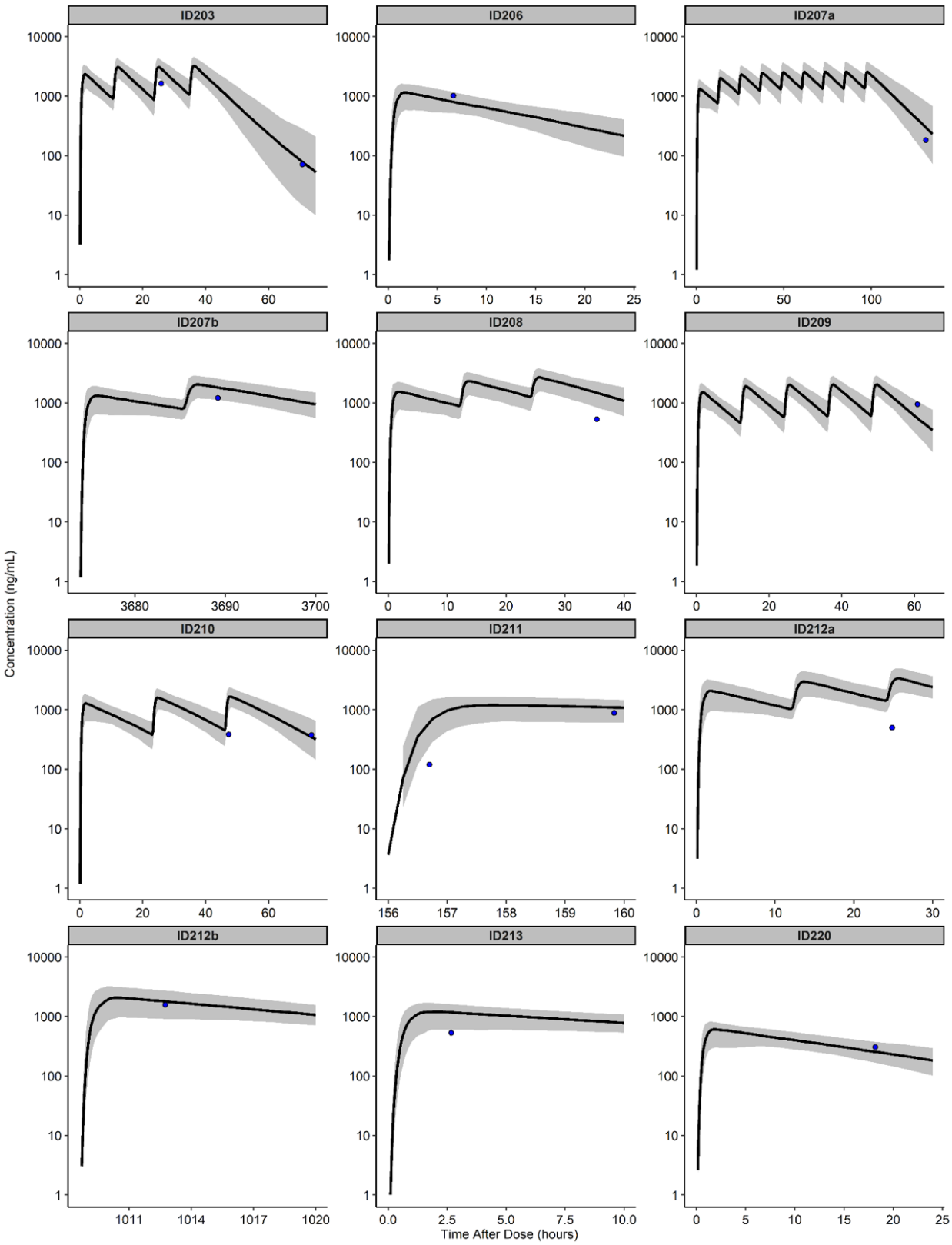
ID203
ID206
ID207a
ID207b
ID208
ID209
ID210
ID211
ID212a
ID212b
ID213
ID220
Concentration (ng/mL)
Time After Dose (hours)

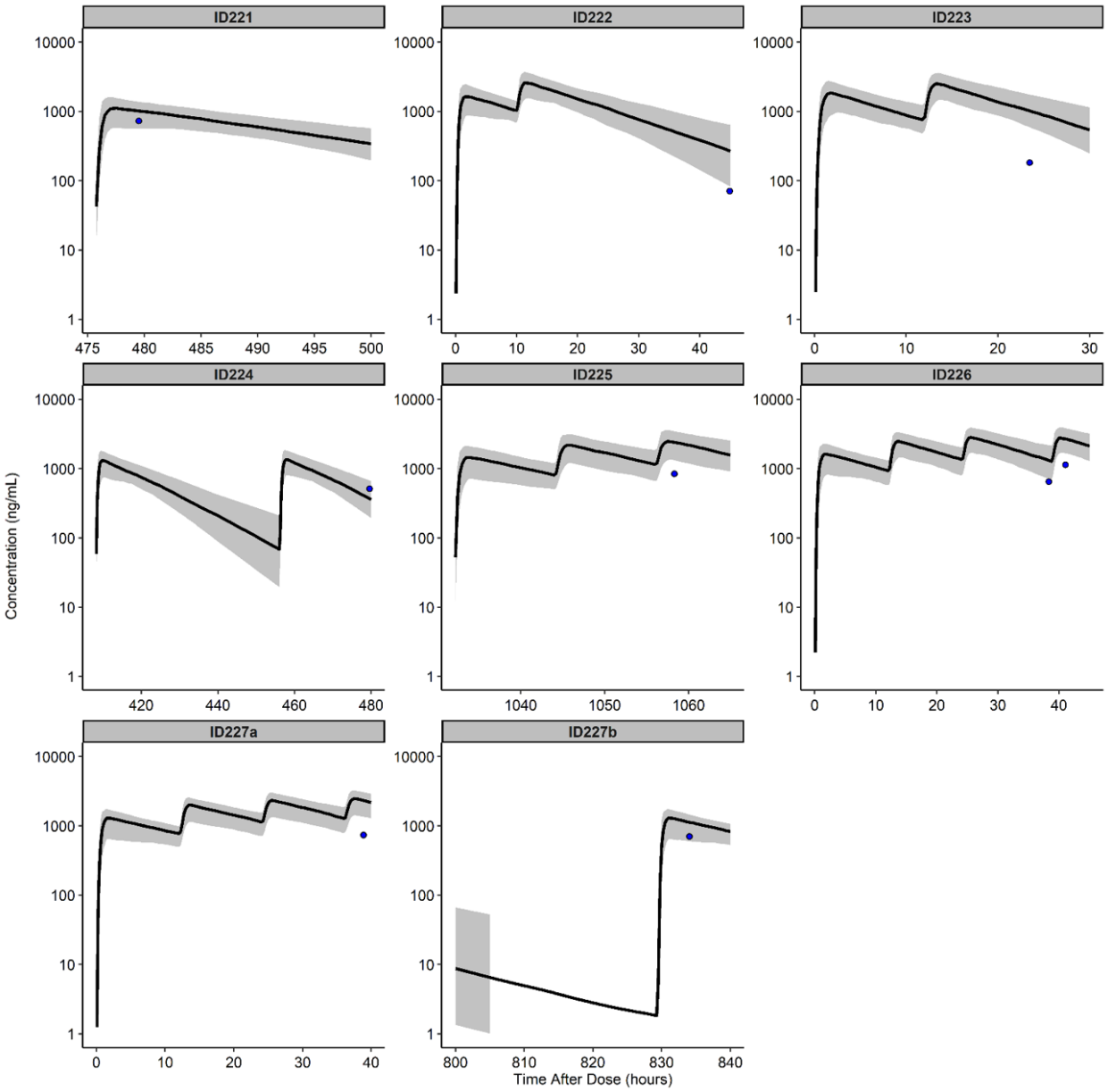

Supplementary Figure 11. Population simulations (n=250) of plasma trimethoprim concentration using "individualized populations" for each observed pediatric subject with obesity that are matched to that particular subject's demographics and dosing regimen. The shaded regions are the 90% model prediction interval, which are overlaid with points representing observed plasma concentrations from the POP01 and External Data Study.

POP01, Pharmacokinetics of Understudied Drugs Administered to Children Per Standard of Care (ClinicalTrials.gov #NCT01431326) Study

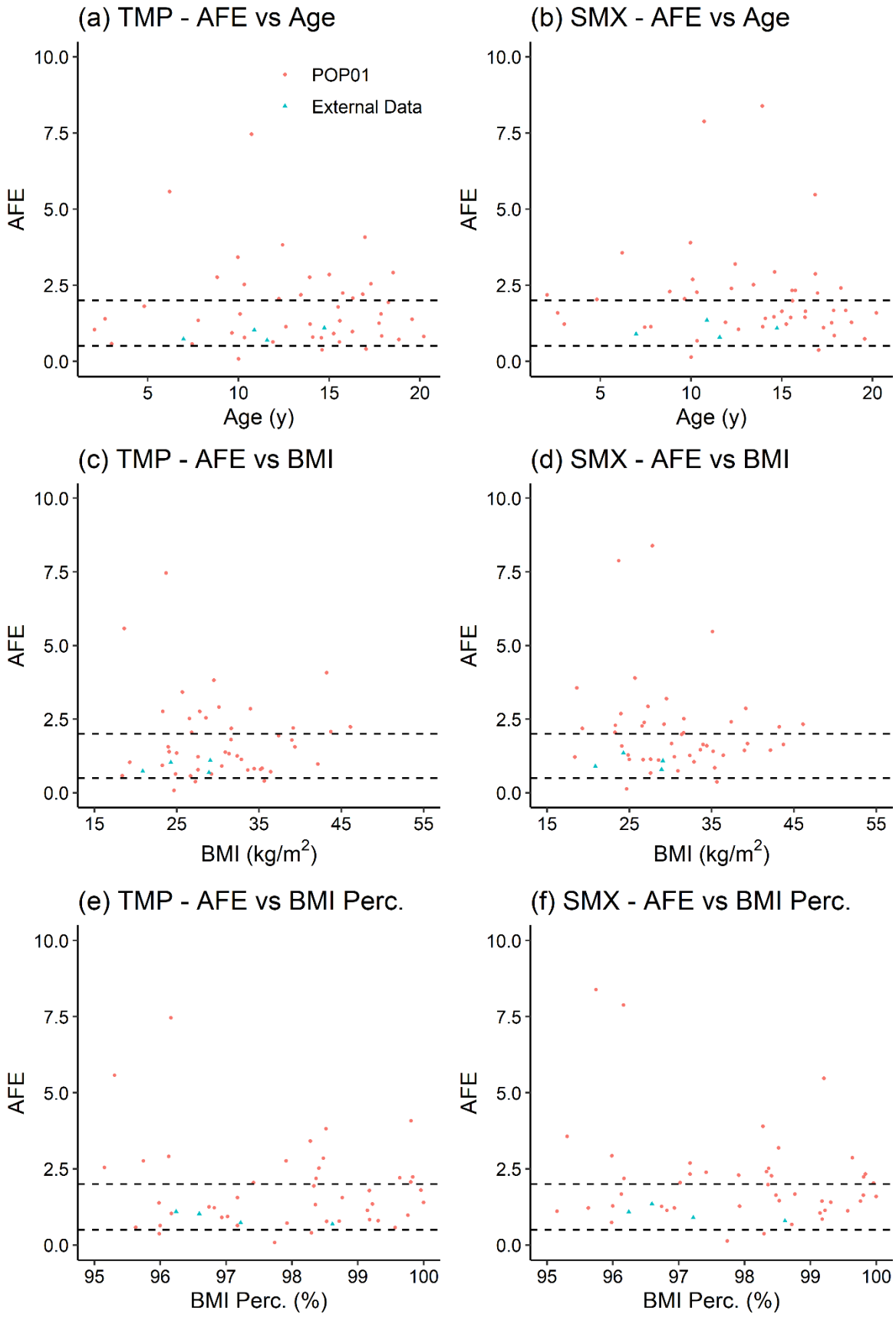
(a) TMP - AFE vs Age
(b) SMX - AFE vs Age
(c) TMP - AFE vs BMI
(d) SMX - AFE vs BMI
(e) TMP - AFE vs BMI Perc.
(f) SMX - AFE vs BMI Perc.
POP01
External Data
AFE
Age (y)
BMI (kg/m2)
BMI Perc. (%)
10.0
7.5
5.0
2.5
0.0
5
10
15
20
25
35
45
55
95
96
97
98
99
100

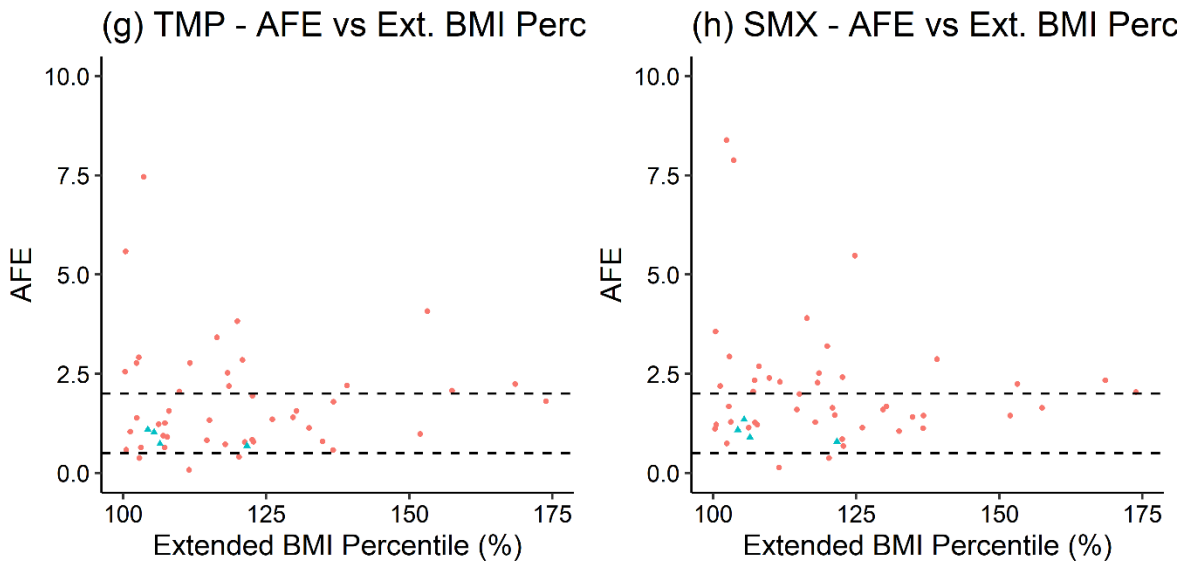

Supplementary Figure 12. AFE for pediatric subjects with obesity who received trimethoprim (a, c, e, and g) and sulfamethoxazole (b, d, f, and h) plotted versus age and body size. Dashed lines represent 2-fold error for reference. AFE was calculated using median simulated concentration. Ext. BMI percentile is calculated as BMI divided by the 95th BMI percentile for a subject's age and sex, where children with an extended BMI percentile ≥ 100% are considered obese.

AFE, average fold error; BMI, body mass index; Perc., percentile; Ext., extended; POP01, Pharmacokinetics of Understudied Drugs Administered to Children Per Standard of Care (ClinicalTrials.gov #NCT01431326) Study; SMX, sulfamethoxazole; TMP, trimethoprim

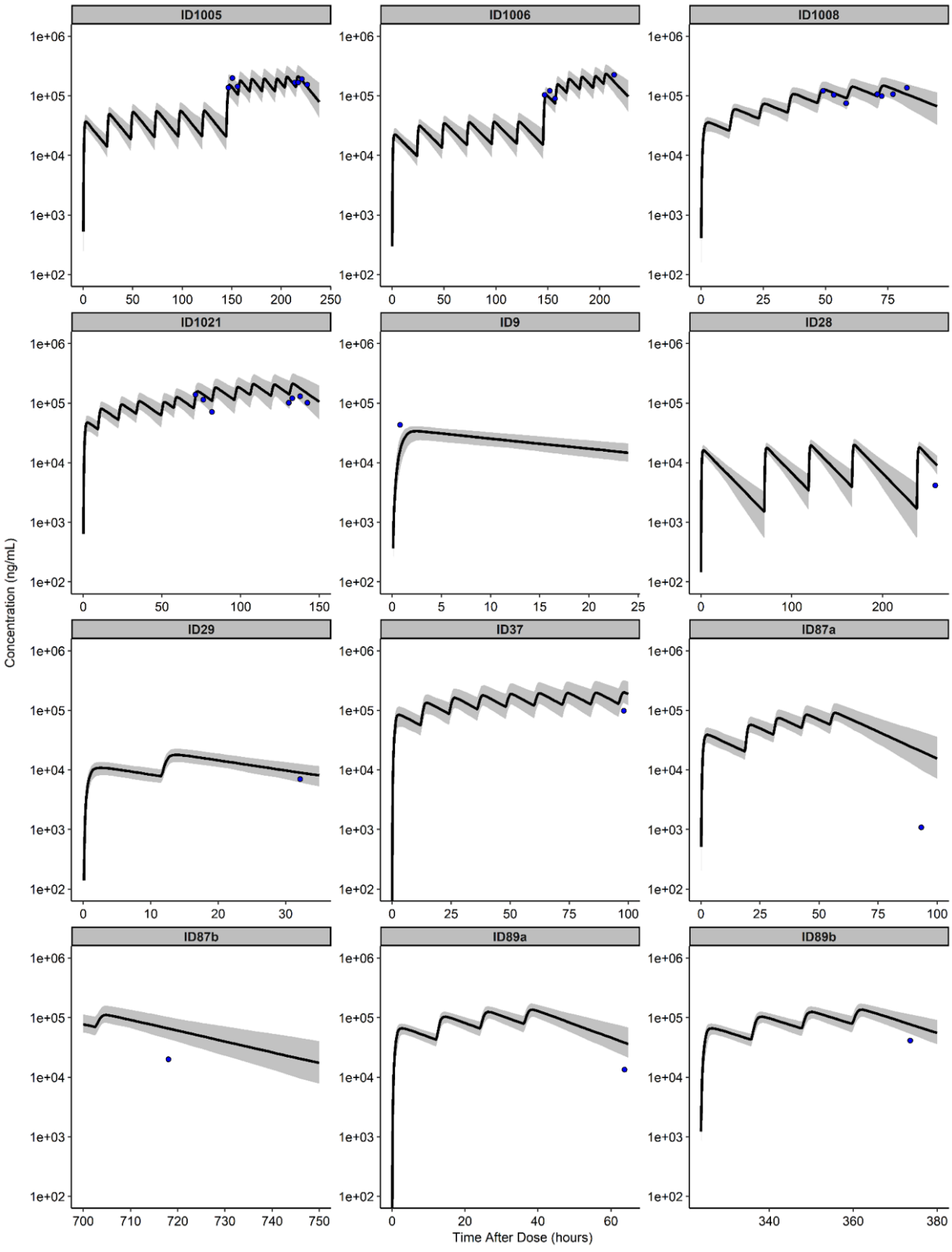
ID1005
ID1006
ID1008
ID1021
ID9
ID28
ID29
ID37
ID87a
ID87b
ID89a
ID89b
Concentration (ng/mL)
Time After Dose (hours)

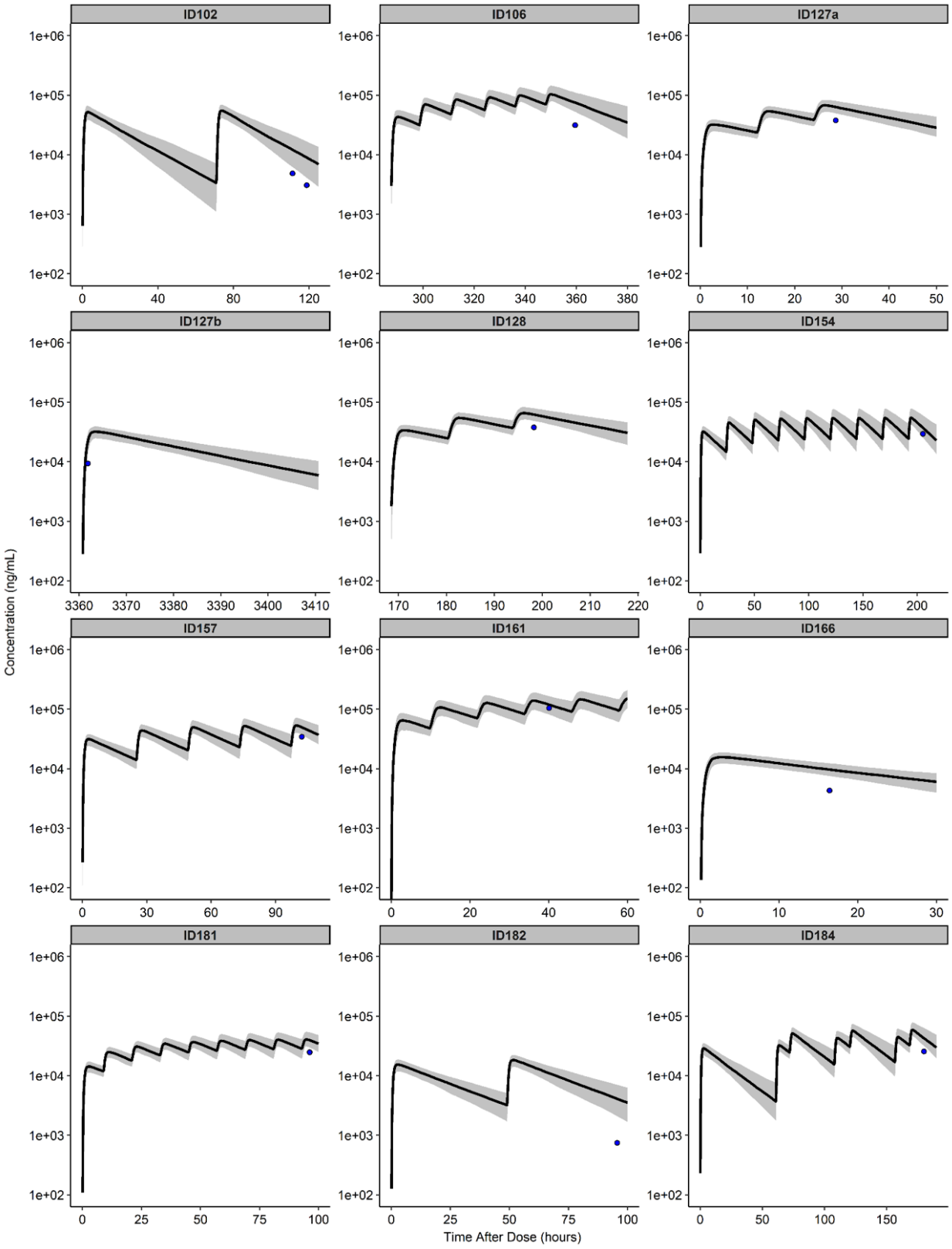
ID102
ID106
ID127a
ID127b
ID128
ID154
ID157
ID161
ID166
ID181
ID182
ID184
Concentration (ng/mL)
Time After Dose (hours)

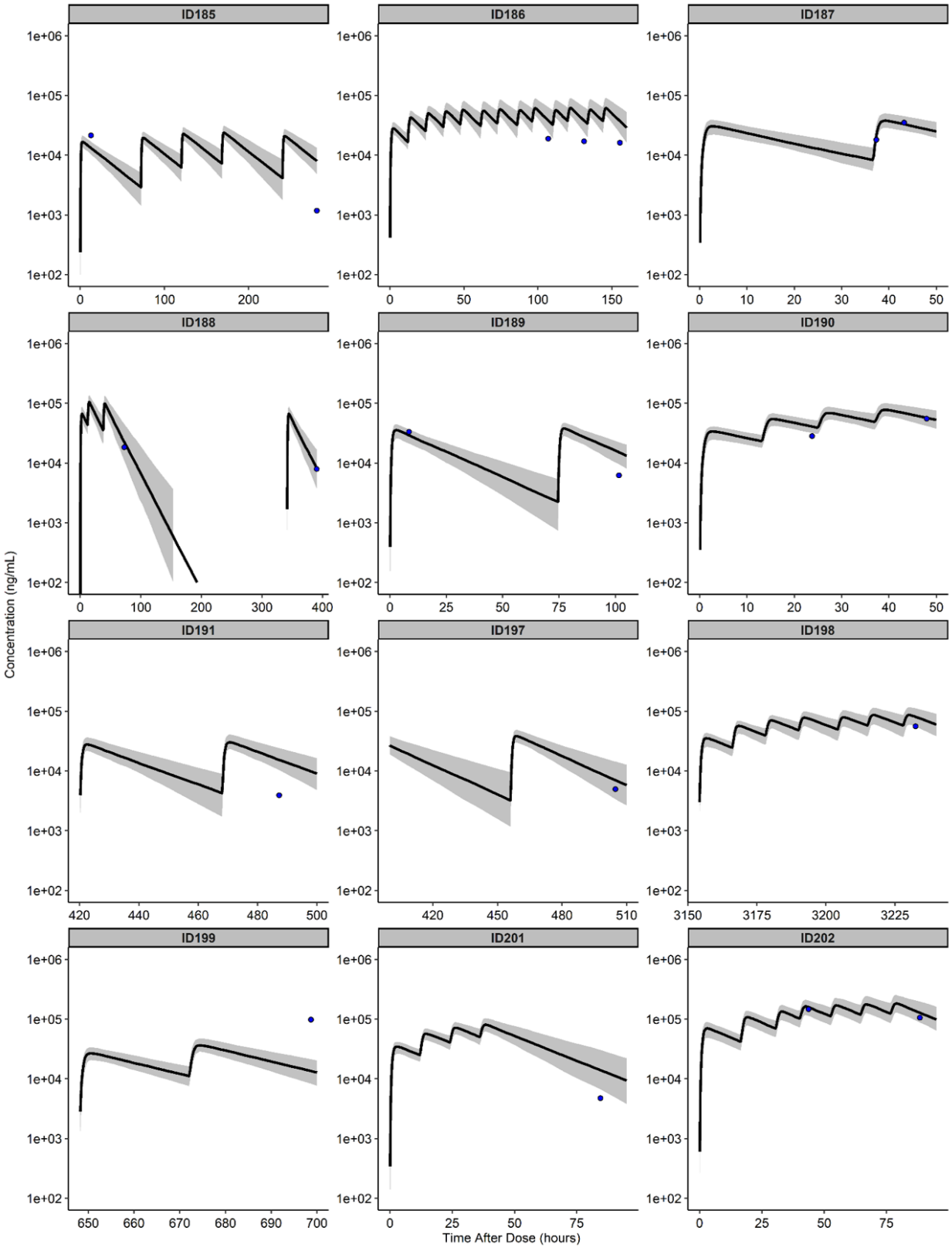
ID185
ID186
ID187
ID188
ID189
ID190
ID191
ID197
ID198
ID199
ID201
ID202
Concentration (ng/mL)
Time After Dose (hours)

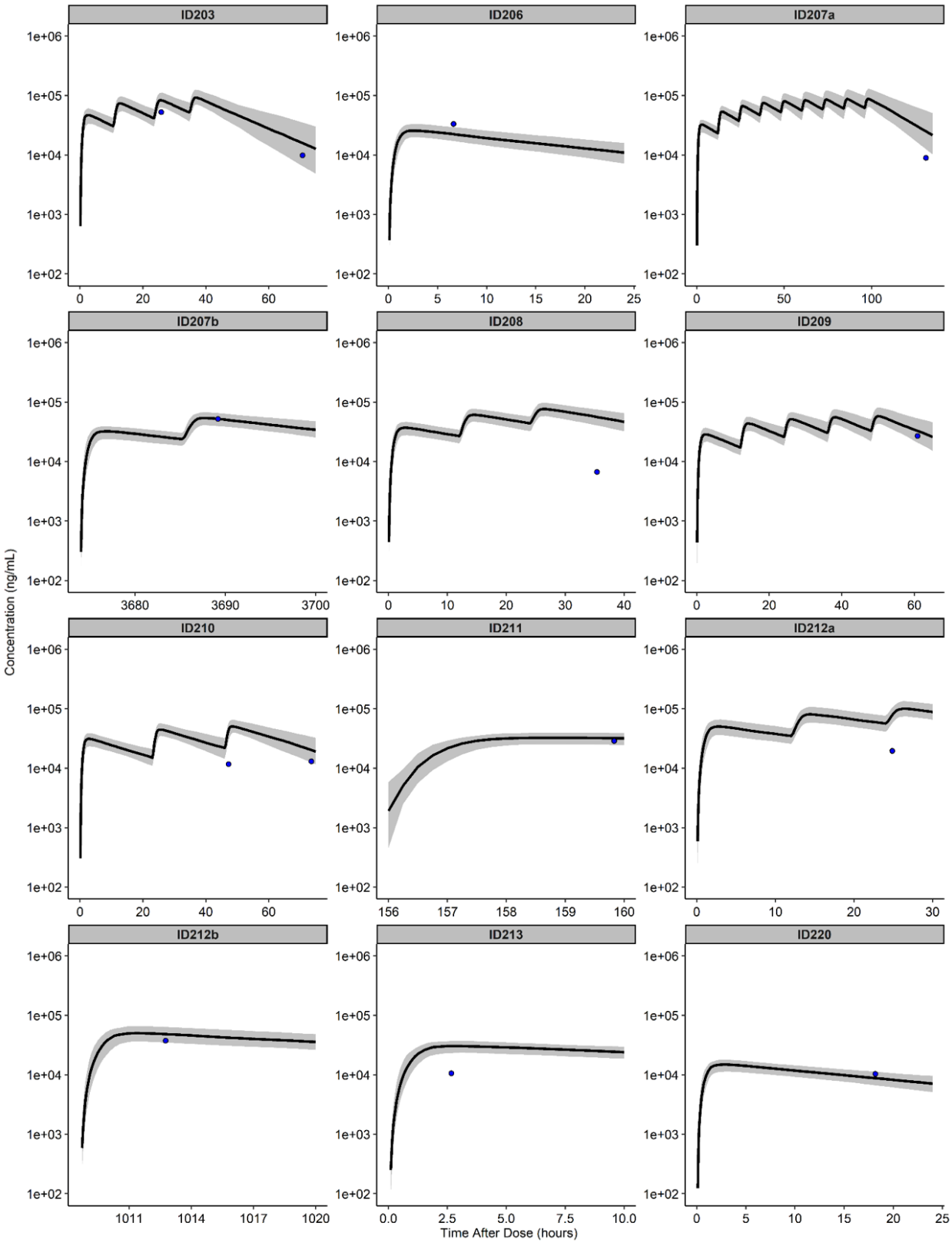
ID203
ID206
ID207a
ID207b
ID208
ID209
ID210
ID211
ID212a
ID212b
ID213
ID220
Concentration (ng/mL)
Time After Dose (hours)

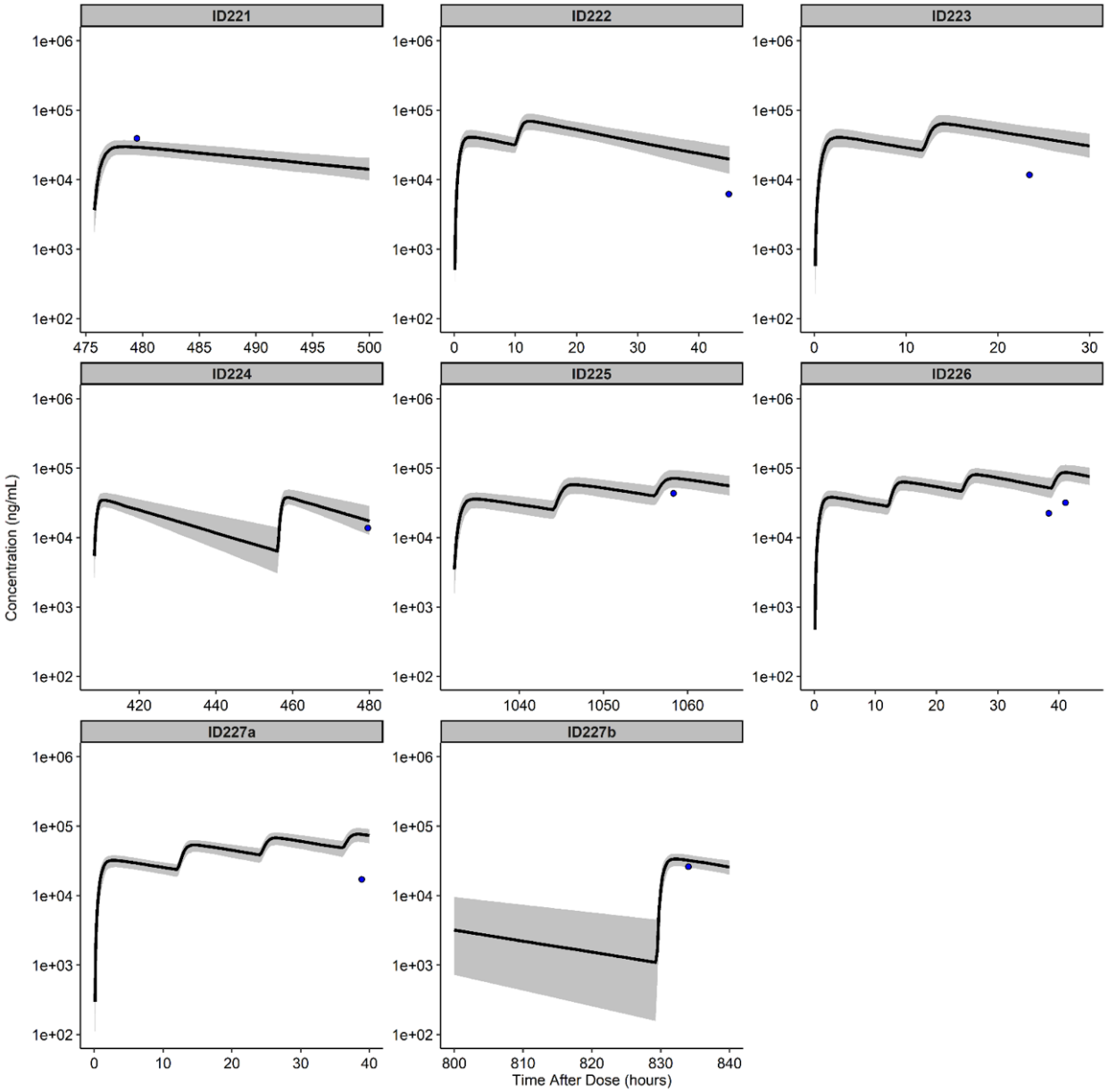

Supplementary Figure 13. Population simulations (n=250) of plasma sulfamethoxazole concentration using "individualized populations" for each observed pediatric subject with obesity that are matched to that particular subject's demographics and dosing regimen. The shaded regions are the 90% model prediction interval, which are overlaid with points representing observed plasma concentrations from the POP01 and External Data Study.

POP01, Pharmacokinetics of Understudied Drugs Administered to Children Per Standard of Care (ClinicalTrials.gov #NCT01431326) Study

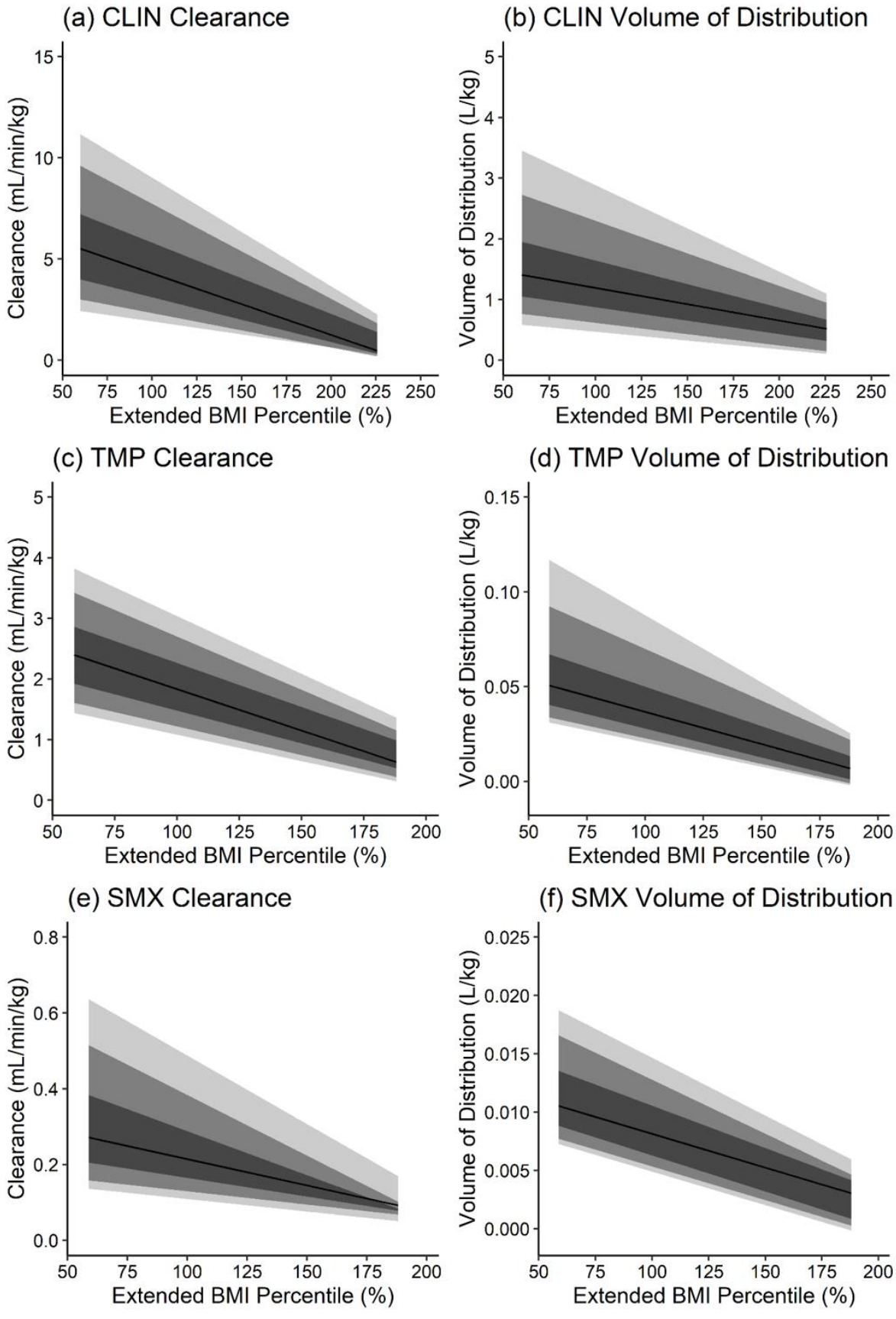
(a) CLIN Clearance
Clearance (mL/min/kg)
Extended BMI Percentile (%)
(b) CLIN Volume of Distribution
Volume of Distribution (L/kg)
Extended BMI Percentile (%)
(c) TMP Clearance
Clearance (mL/min/kg)
Extended BMI Percentile (%)
(d) TMP Volume of Distribution
Volume of Distribution (L/kg)
Extended BMI Percentile (%)
(e) SMX Clearance
Clearance (mL/min/kg)
Extended BMI Percentile (%)
(f) SMX Volume of Distribution
Volume of Distribution (L/kg)
Extended BMI Percentile (%)

Supplementary Figure 14. Changes in simulated weight-normalized clearance (a, c, e) and weight-normalized volume of distribution (b, d, f) for clindamycin (a, b), trimethoprim (c, d), and sulfamethoxazole (e, f) with increasing body size, or extended BMI percentile. Clearance and volume of distribution were calculated from virtual children aged 6 – 12 years with and without obesity. Extended BMI percentile is calculated as BMI divided by the 95th BMI percentile for a subject's age and sex, where children with an extended BMI percentile ≥ 100% are considered obese. Virtual children received single doses of 600 mg IV infusion (30 min) clindamycin, 160 mg PO trimethoprim, and 800 mg PO sulfamethoxazole. The shaded regions denote the 90% (95th and 5th percentiles), 80% (90th and 10th percentiles), and 50% (75th and 25th percentiles) prediction intervals from lightest to darkest color intensity, respectively. The black line denotes the median. Note that variability in PK parameters appears decreased at the upper extremity of extended BMI percentile due to a lower number of virtual subjects in this range.

BMI, body mass index; CLIN, clindamycin; IV, intravenous; PO, oral dose; SMX, sulfamethoxazole; TMP, trimethoprim

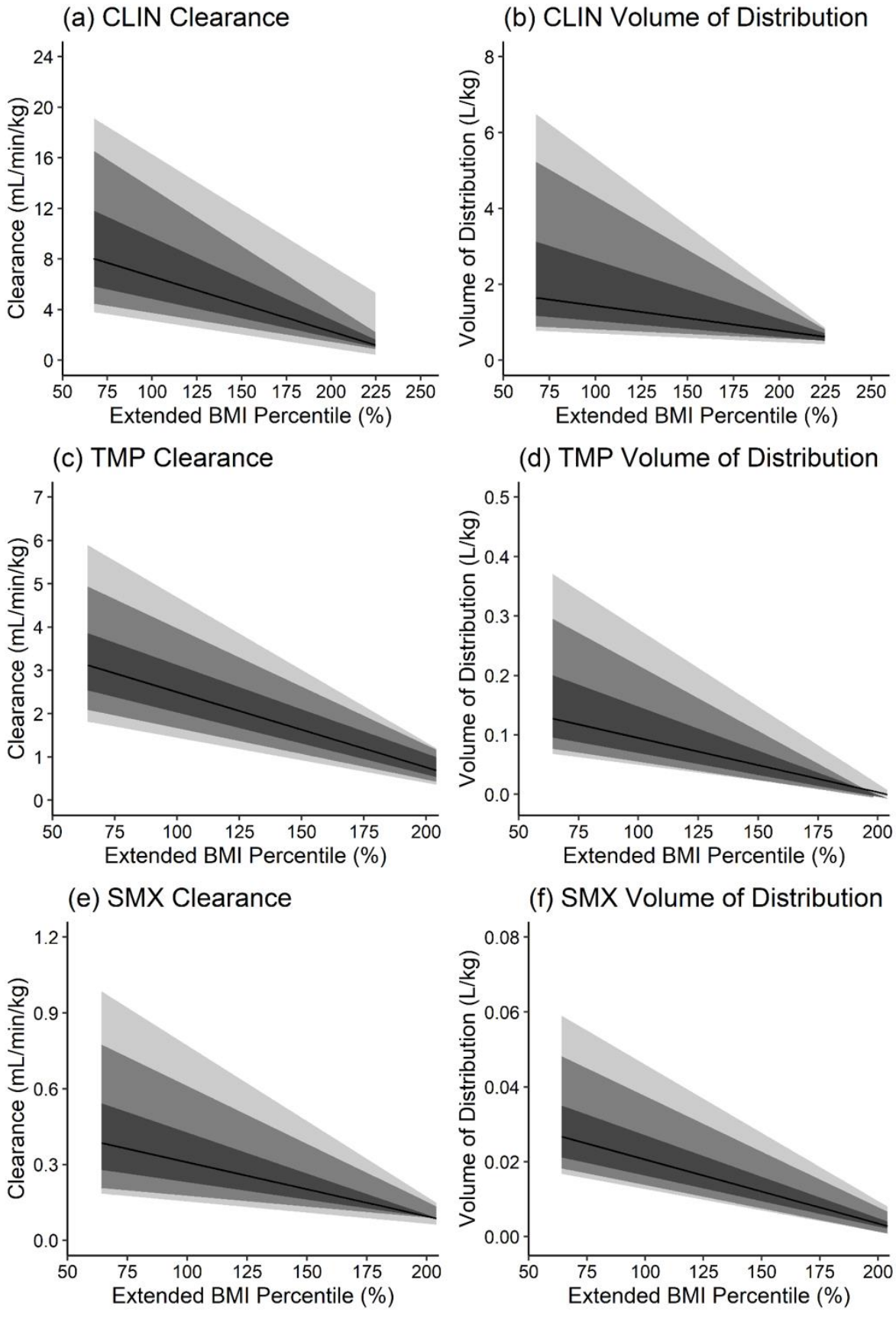
(a) CLIN Clearance
Clearance (mL/min/kg)
Extended BMI Percentile (%)
(b) CLIN Volume of Distribution
Volume of Distribution (L/kg)
Extended BMI Percentile (%)
(c) TMP Clearance
Clearance (mL/min/kg)
Extended BMI Percentile (%)
(d) TMP Volume of Distribution
Volume of Distribution (L/kg)
Extended BMI Percentile (%)
(e) SMX Clearance
Clearance (mL/min/kg)
Extended BMI Percentile (%)
(f) SMX Volume of Distribution
Volume of Distribution (L/kg)
Extended BMI Percentile (%)

Supplementary Figure 15. Changes in simulated weight-normalized clearance (a, c, e) and weight-normalized volume of distribution (b, d, f) for clindamycin (a, b), trimethoprim (c, d), and sulfamethoxazole (e, f) with increasing body size, or extended BMI percentile. Clearance and volume of distribution were calculated from virtual children aged 2 – 6 years with and without obesity. Extended BMI percentile is calculated as BMI divided by the 95th BMI percentile for a subject's age and sex, where children with an extended BMI percentile ≥ 100% are considered obese. Virtual children received single doses of 600 mg IV infusion (30 min) clindamycin, 160 mg PO trimethoprim, and 800 mg PO sulfamethoxazole. The shaded regions denote the 90% (95th and 5th percentiles), 80% (90th and 10th percentiles), and 50% (75th and 25th percentiles) prediction intervals from lightest to darkest color intensity, respectively. The black line denotes the median. Note that variability in PK parameters appears decreased at the upper extremity of extended BMI percentile due to a lower number of virtual subjects in this range.

BMI, body mass index; CLIN, clindamycin; IV, intravenous; PO, oral dose; SMX, sulfamethoxazole; TMP, trimethoprim

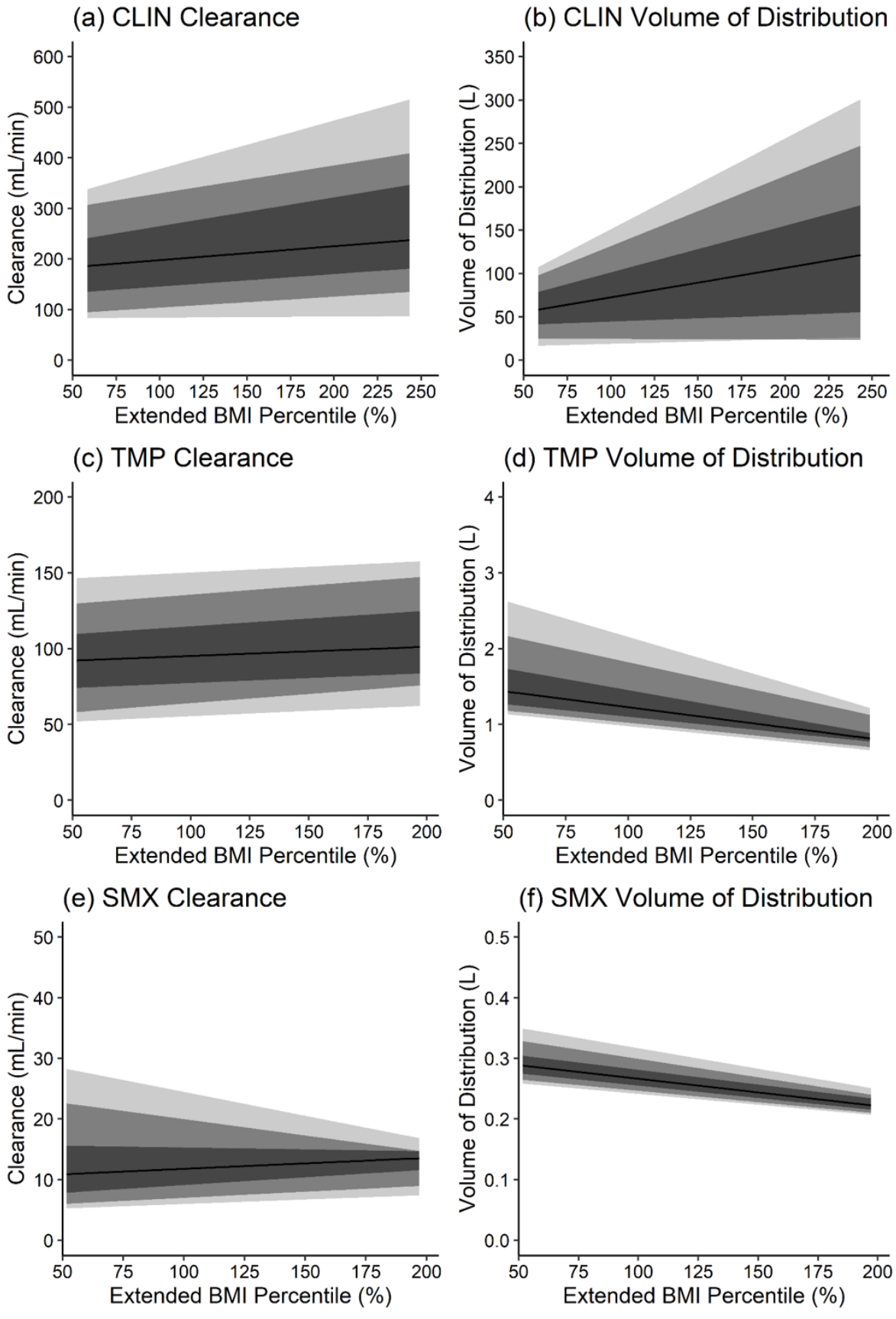
(a) CLIN Clearance
Clearance (mL/min)
0
100
200
300
400
500
600
50 75 100 125 150 175 200 225 250
Extended BMI Percentile (%)
(b) CLIN Volume of Distribution
Volume of Distribution (L)
0
50
100
150
200
250
300
350
50 75 100 125 150 175 200 225 250
Extended BMI Percentile (%)
(c) TMP Clearance
Clearance (mL/min)
0
50
100
150
200
50 75 100 125 150 175 200
Extended BMI Percentile (%)
(d) TMP Volume of Distribution
Volume of Distribution (L)
0
1
2
3
4
50 75 100 125 150 175 200
Extended BMI Percentile (%)
(e) SMX Clearance
Clearance (mL/min)
0
10
20
30
40
50
50 75 100 125 150 175 200
Extended BMI Percentile (%)
(f) SMX Volume of Distribution
Volume of Distribution (L)
0.0
0.1
0.2
0.3
0.4
0.5
50 75 100 125 150 175 200
Extended BMI Percentile (%)

Supplementary Figure 16. Changes in simulated absolute clearance (a, c, e) and volume of distribution (b, d, f) for clindamycin (a, b), trimethoprim (c, d), and sulfamethoxazole (e, f) with increasing body size, or extended BMI percentile. Clearance and volume of distribution were calculated from virtual children aged 12 – 18 years with and without obesity. Extended BMI percentile is calculated as BMI divided by the 95th BMI percentile for a subject's age and sex, where children with an extended BMI percentile ≥ 100% are considered obese. Virtual children received single doses of 600 mg IV infusion (30 min) clindamycin, 160 mg PO trimethoprim, and 800 mg PO sulfamethoxazole. The shaded regions denote the 90% (95th and 5th percentiles), 80% (90th and 10th percentiles), and 50% (75th and 25th percentiles) prediction intervals from lightest to darkest color intensity, respectively. The black line denotes the median. Note that variability in PK parameters appears decreased at the upper extremity of extended BMI percentile due to a lower number of virtual subjects in this range.

BMI, body mass index; CLIN, clindamycin; IV, intravenous; PO, oral dose; SMX, sulfamethoxazole; TMP, trimethoprim

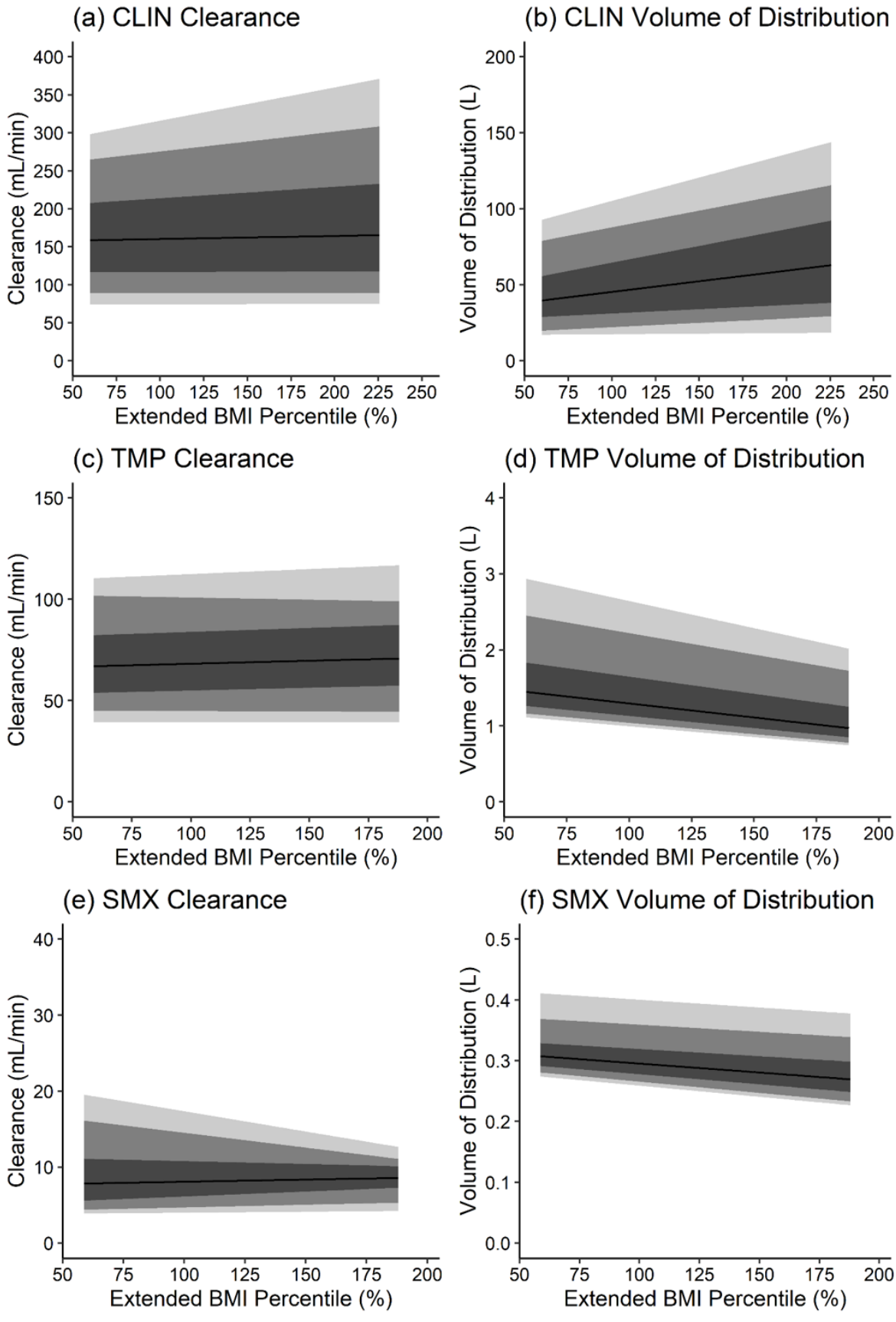
(a) CLIN Clearance
Clearance (mL/min)
0
50
100
150
200
250
300
350
400
50 75 100 125 150 175 200 225 250
Extended BMI Percentile (%)
(b) CLIN Volume of Distribution
Volume of Distribution (L)
0
50
100
150
200
50 75 100 125 150 175 200 225 250
Extended BMI Percentile (%)
(c) TMP Clearance
Clearance (mL/min)
0
50
100
150
50 75 100 125 150 175 200
Extended BMI Percentile (%)
(d) TMP Volume of Distribution
Volume of Distribution (L)
0
1
2
3
4
50 75 100 125 150 175 200
Extended BMI Percentile (%)
(e) SMX Clearance
Clearance (mL/min)
0
10
20
30
40
50 75 100 125 150 175 200
Extended BMI Percentile (%)
(f) SMX Volume of Distribution
Volume of Distribution (L)
0.0
0.1
0.2
0.3
0.4
0.5
50 75 100 125 150 175 200
Extended BMI Percentile (%)

Supplementary Figure 17. Changes in simulated absolute clearance (a, c, e) and volume of distribution (b, d, f) for clindamycin (a, b), trimethoprim (c, d), and sulfamethoxazole (e, f) with increasing body size, or extended BMI percentile. Clearance and volume of distribution were calculated from virtual children aged 6 – 12 years with and without obesity. Extended BMI percentile is calculated as BMI divided by the 95th BMI percentile for a subject's age and sex, where children with an extended BMI percentile ≥ 100% are considered obese. Virtual children received single doses of 600 mg IV infusion (30 min) clindamycin, 160 mg PO trimethoprim, and 800 mg PO sulfamethoxazole. The shaded regions denote the 90% (95th and 5th percentiles), 80% (90th and 10th percentiles), and 50% (75th and 25th percentiles) prediction intervals from lightest to darkest color intensity, respectively. The black line denotes the median. Note that variability in PK parameters appears decreased at the upper extremity of extended BMI percentile due to a lower number of virtual subjects in this range.

BMI, body mass index; CLIN, clindamycin; IV, intravenous; PO, oral dose; SMX, sulfamethoxazole; TMP, trimethoprim

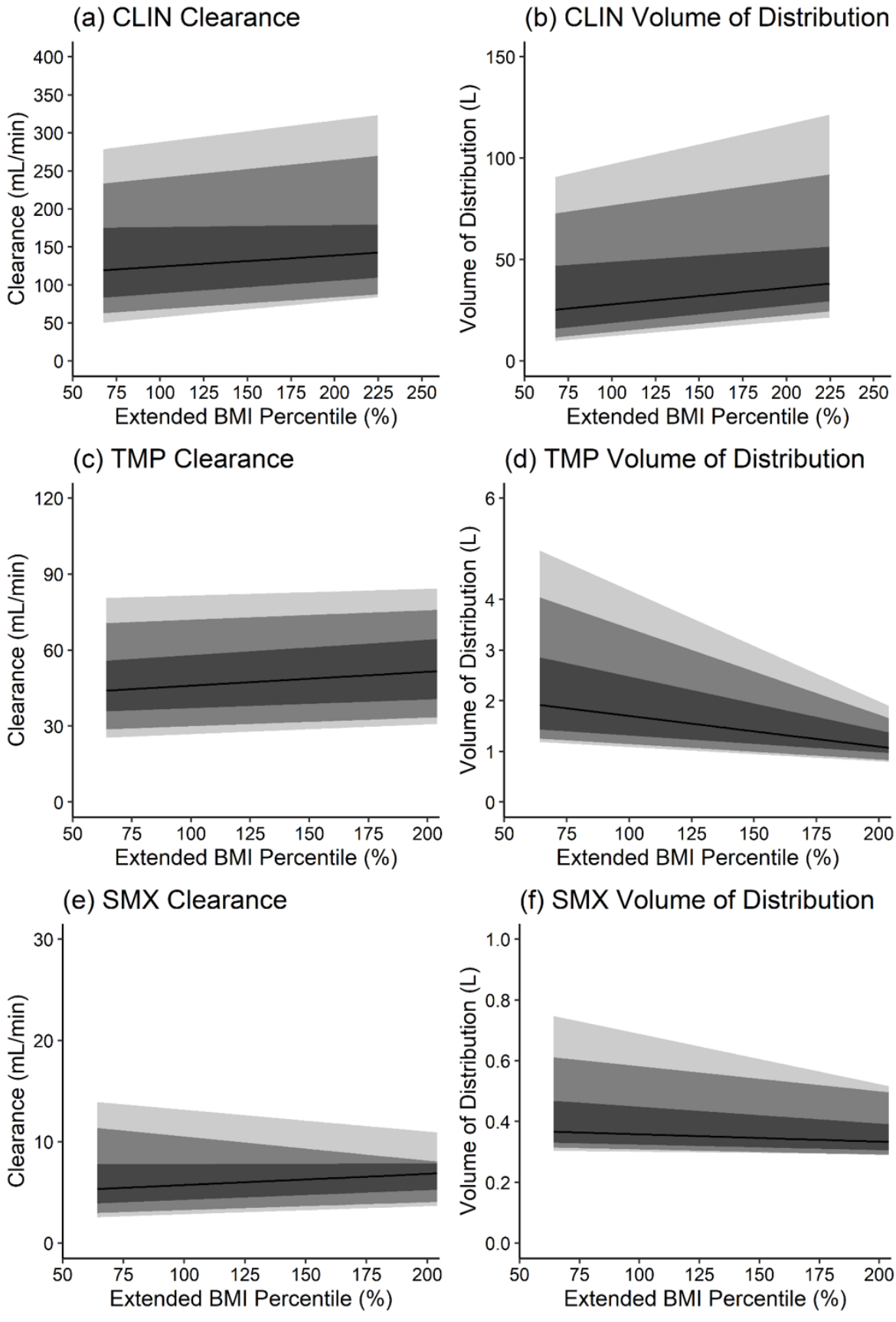
(a) CLIN Clearance
Clearance (mL/min)
0
50
100
150
200
250
300
350
400
50 75 100 125 150 175 200 225 250
Extended BMI Percentile (%)
(b) CLIN Volume of Distribution
Volume of Distribution (L)
0
50
100
150
50 75 100 125 150 175 200 225 250
Extended BMI Percentile (%)
(c) TMP Clearance
Clearance (mL/min)
0
30
60
90
120
50 75 100 125 150 175 200
Extended BMI Percentile (%)
(d) TMP Volume of Distribution
Volume of Distribution (L)
0
1
2
3
4
6
50 75 100 125 150 175 200
Extended BMI Percentile (%)
(e) SMX Clearance
Clearance (mL/min)
0
10
20
30
50 75 100 125 150 175 200
Extended BMI Percentile (%)
(f) SMX Volume of Distribution
Volume of Distribution (L)
0.0
0.2
0.4
0.6
0.8
1.0
50 75 100 125 150 175 200
Extended BMI Percentile (%)

Supplementary Figure 18. Changes in simulated absolute clearance (a, c, e) and volume of distribution (b, d, f) for clindamycin (a, b), trimethoprim (c, d), and sulfamethoxazole (e, f) with increasing body size, or extended BMI percentile. Clearance and volume of distribution were calculated from virtual children aged 2 – 6 years with and without obesity. Extended BMI percentile is calculated as BMI divided by the 95th BMI percentile for a subject's age and sex, where children with an extended BMI percentile ≥ 100% are considered obese. Virtual children received single doses of 600 mg IV infusion (30 min) clindamycin, 160 mg PO trimethoprim, and 800 mg PO sulfamethoxazole. The shaded regions denote the 90% (95th and 5th percentiles), 80% (90th and 10th percentiles), and 50% (75th and 25th percentiles) prediction intervals from lightest to darkest color intensity, respectively. The black line denotes the median. Note that variability in PK parameters appears decreased at the upper extremity of extended BMI percentile due to a lower number of virtual subjects in this range.

BMI, body mass index; CLIN, clindamycin; IV, intravenous; PO, oral dose; SMX, sulfamethoxazole; TMP, trimethoprim

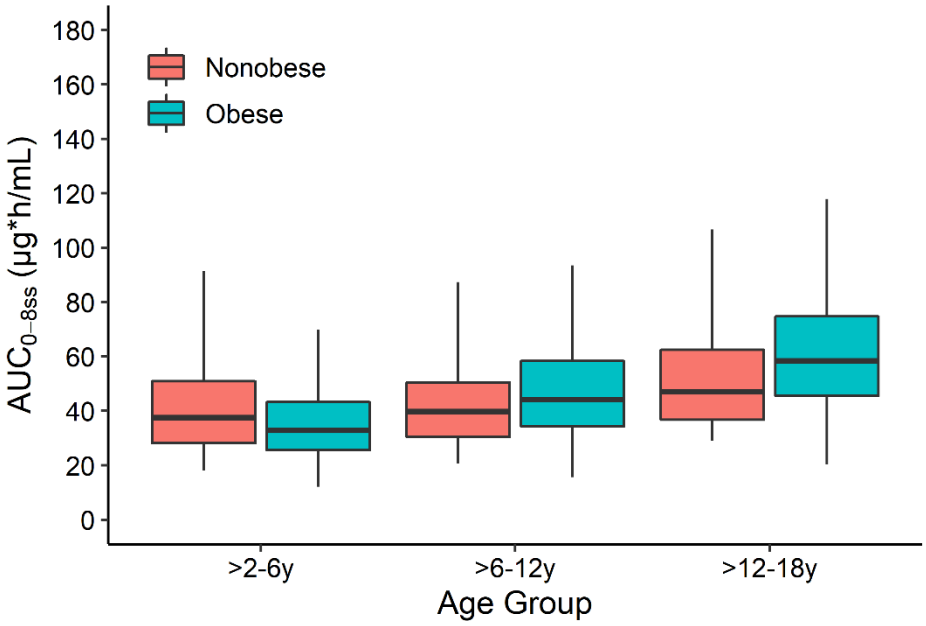

Supplementary Figure 19. Boxplots of simulated clindamycin $AUC_{0\text{-}8,ss}$ in virtual children with and without obesity (n = 1,000) following population simulations. All virtual children received either recommended dosing of 12 mg/kg for children >2-6 years or 10 mg/kg for children >6-18 years. Simulated exposure in virtual children without obesity was previously published [13]. Boxes represent the median and IQR, and whiskers extend to the minimum and maximum values.

$AUC_{0\text{-}8,ss}$, steady-state area under the concentration time curve from 0 to 8 hours; IQR, interquartile range

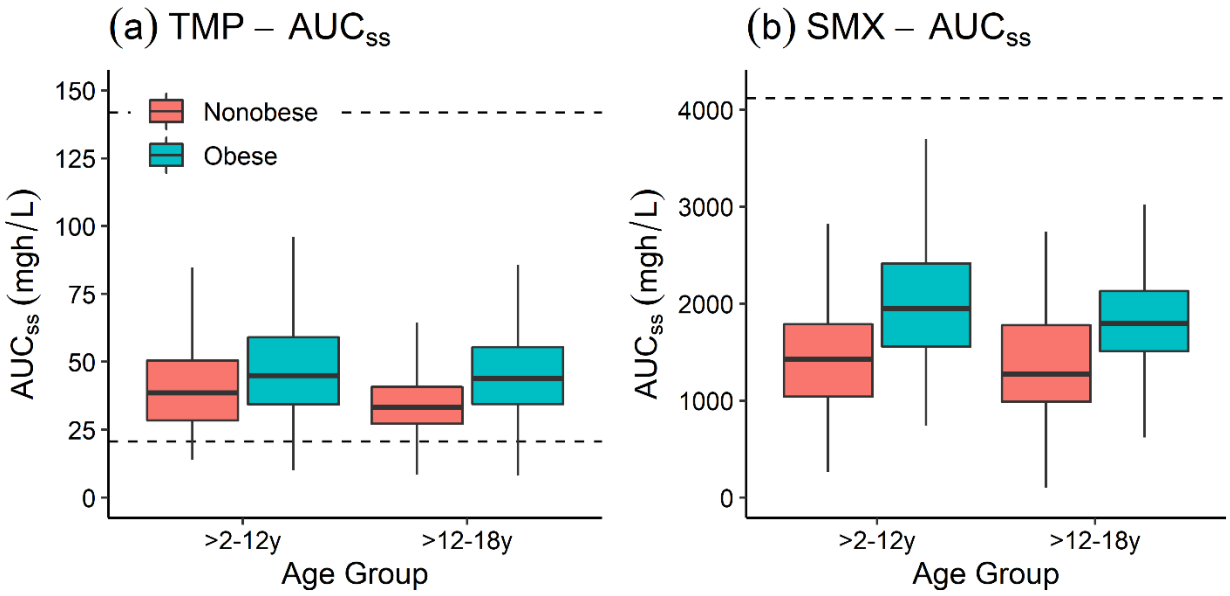

Supplementary Figure 20. Boxplots of simulated trimethoprim and sulfamethoxazole AUC_{ss} in virtual children with (n = 1,000) and without obesity following population simulations. All virtual children received recommended dosing of 6 and 30 mg/kg for children >2-12 years and 4 and 20 mg/kg for children >12-18 years for trimethoprim and sulfamethoxazole, respectively. Simulated exposure in virtual children without obesity was previously published [14]. Boxes represent the median and IQR, and whiskers extend to the minimum and maximum values. The solid line represents the target AUC_{ss} efficacy threshold for trimethoprim, and the dashed lines represent the toxicity AUC_{ss} threshold for both trimethoprim and sulfamethoxazole.

AUC_{ss}, steady-state area under the concentration time curve from 0 to 8 hours; IQR, interquartile range; SMX, sulfamethoxazole; TMP, trimethoprim

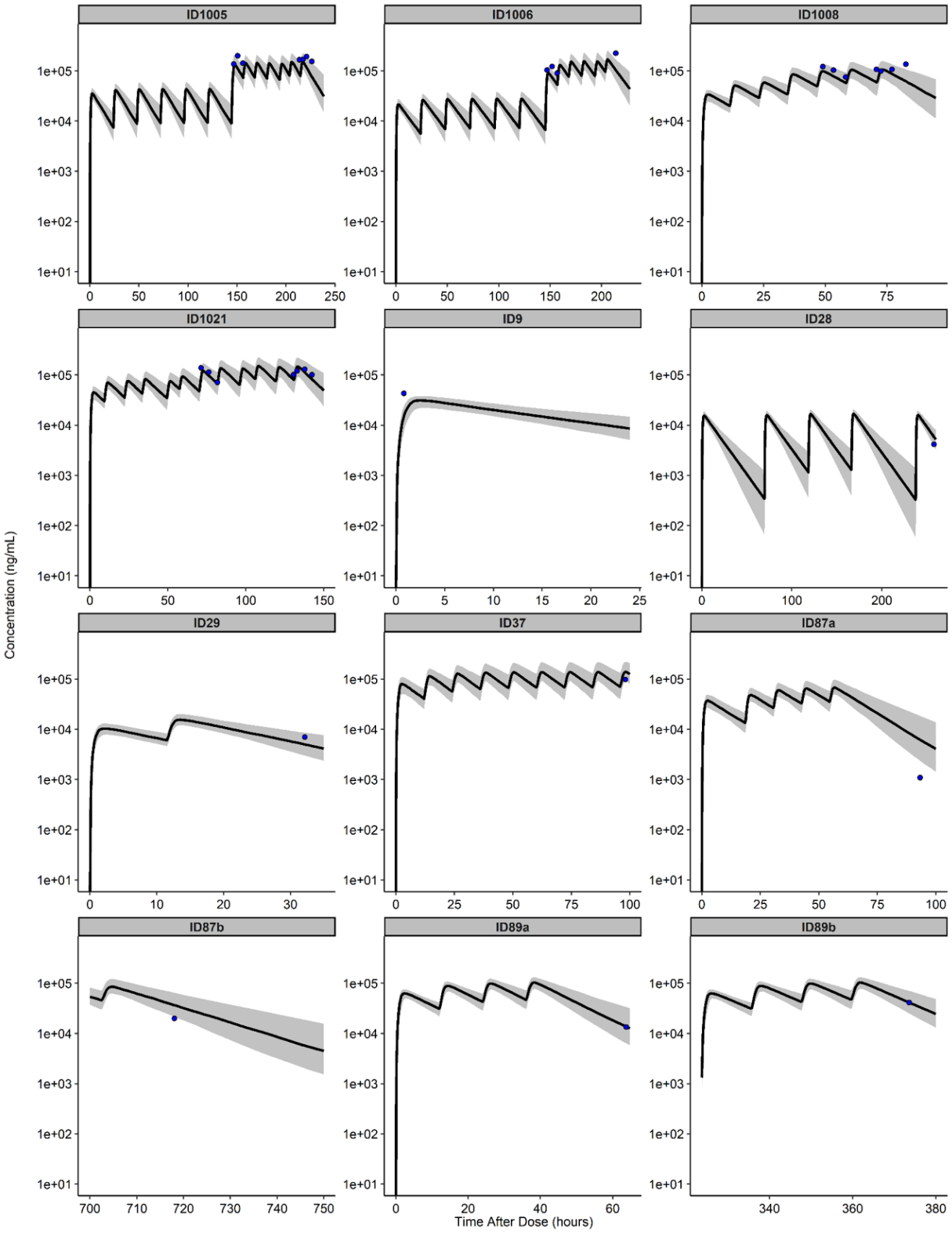
ID1005
ID1006
ID1008
ID1021
ID9
ID28
ID29
ID37
ID87a
ID87b
ID89a
ID89b
Concentration (ng/mL)
Time After Dose (hours)

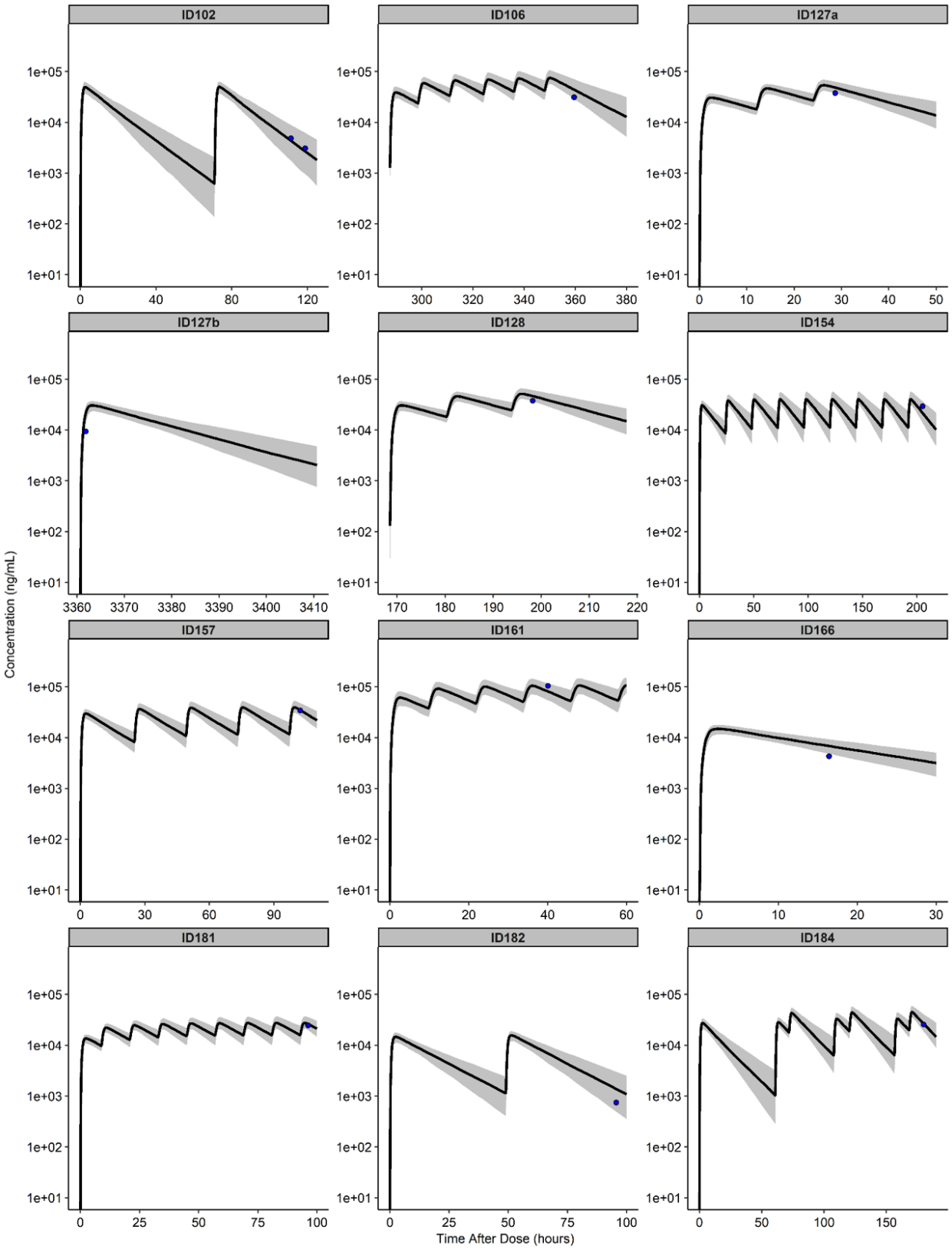
ID102
ID106
ID127a
ID127b
ID128
ID154
ID157
ID161
ID166
ID181
ID182
ID184
Concentration (ng/mL)
Time After Dose (hours)

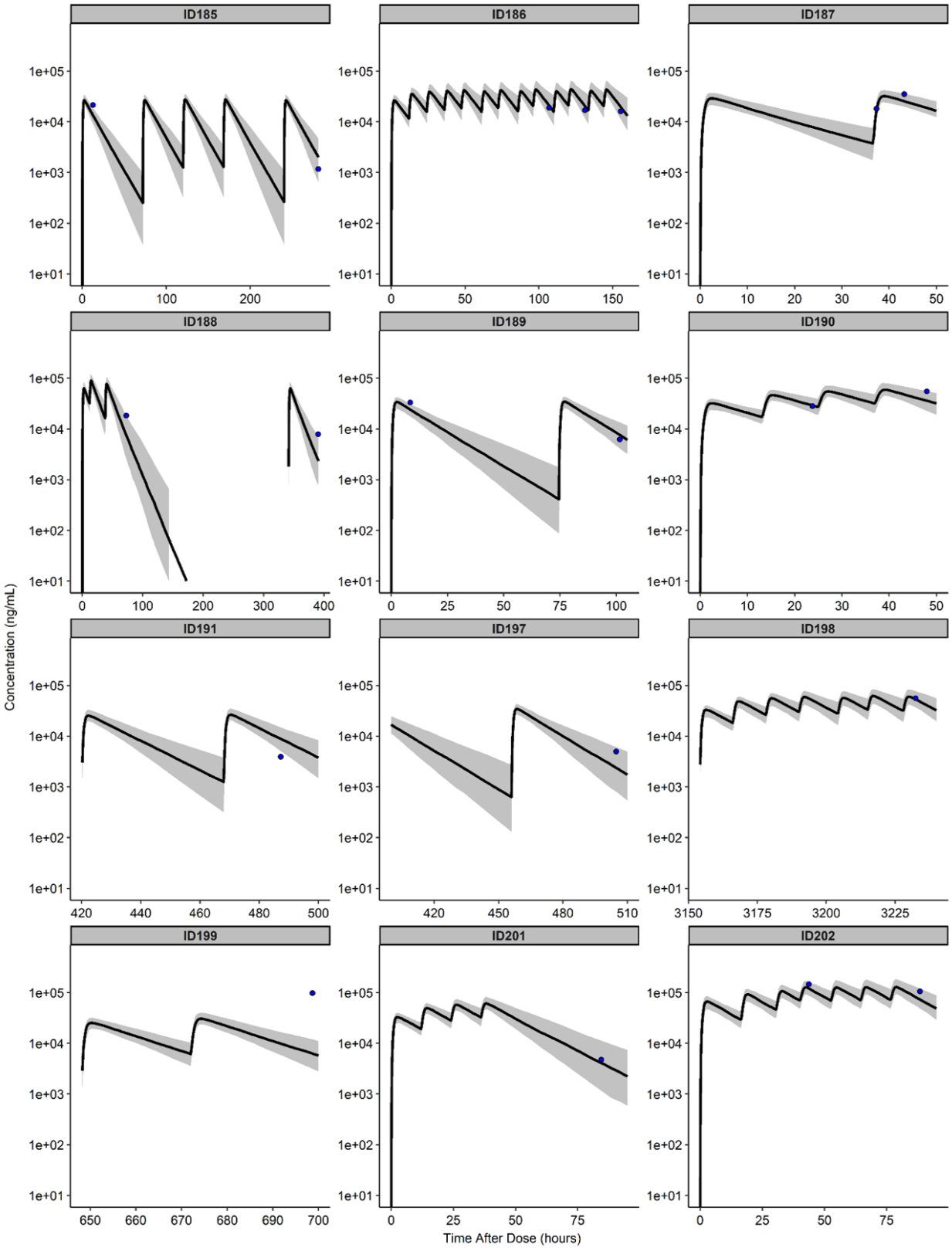
ID185
ID186
ID187
ID188
ID189
ID190
ID191
ID197
ID198
ID199
ID201
ID202
Concentration (ng/mL)
Time After Dose (hours)

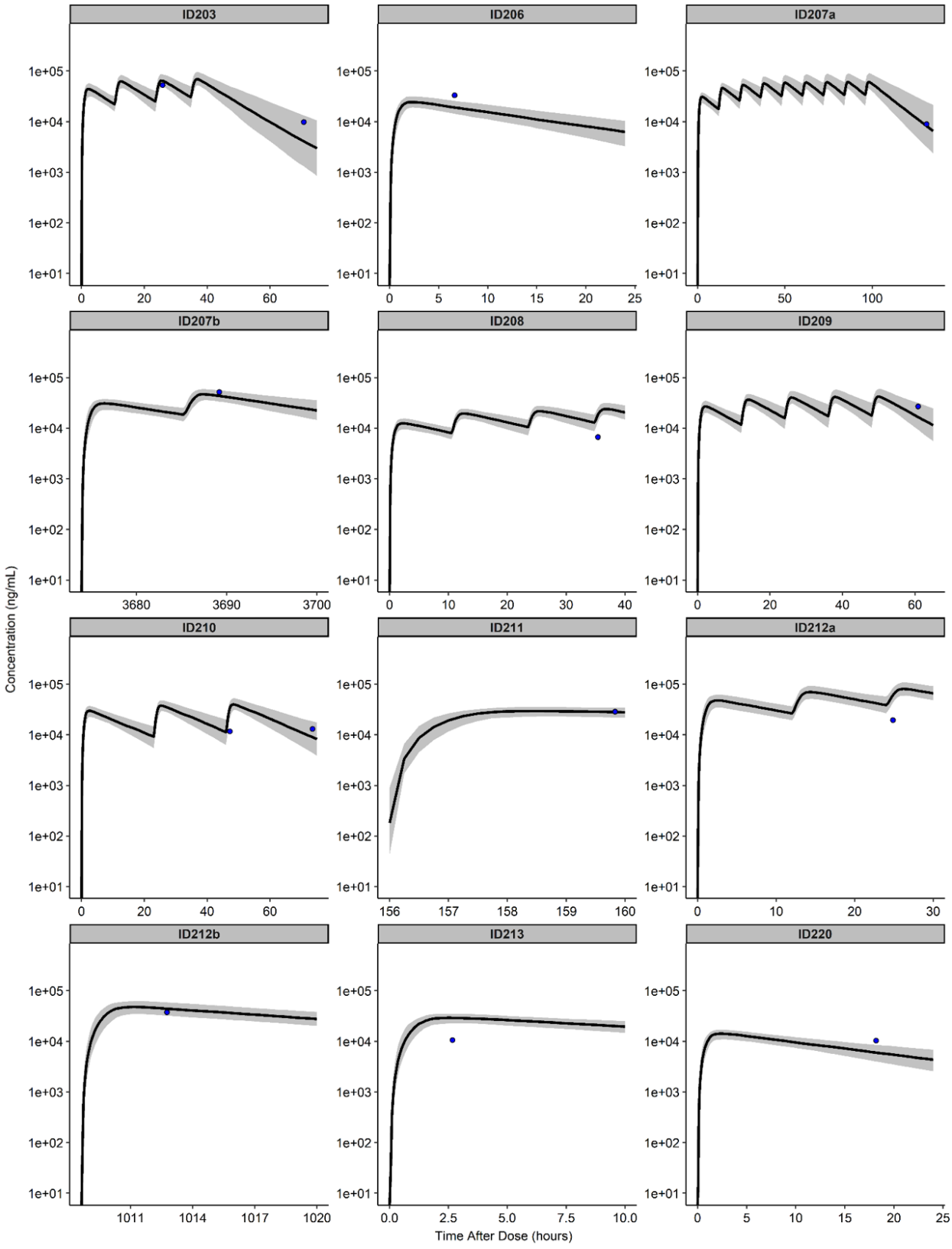
ID203
ID206
ID207a
ID207b
ID208
ID209
ID210
ID211
ID212a
ID212b
ID213
ID220
Concentration (ng/mL)
Time After Dose (hours)

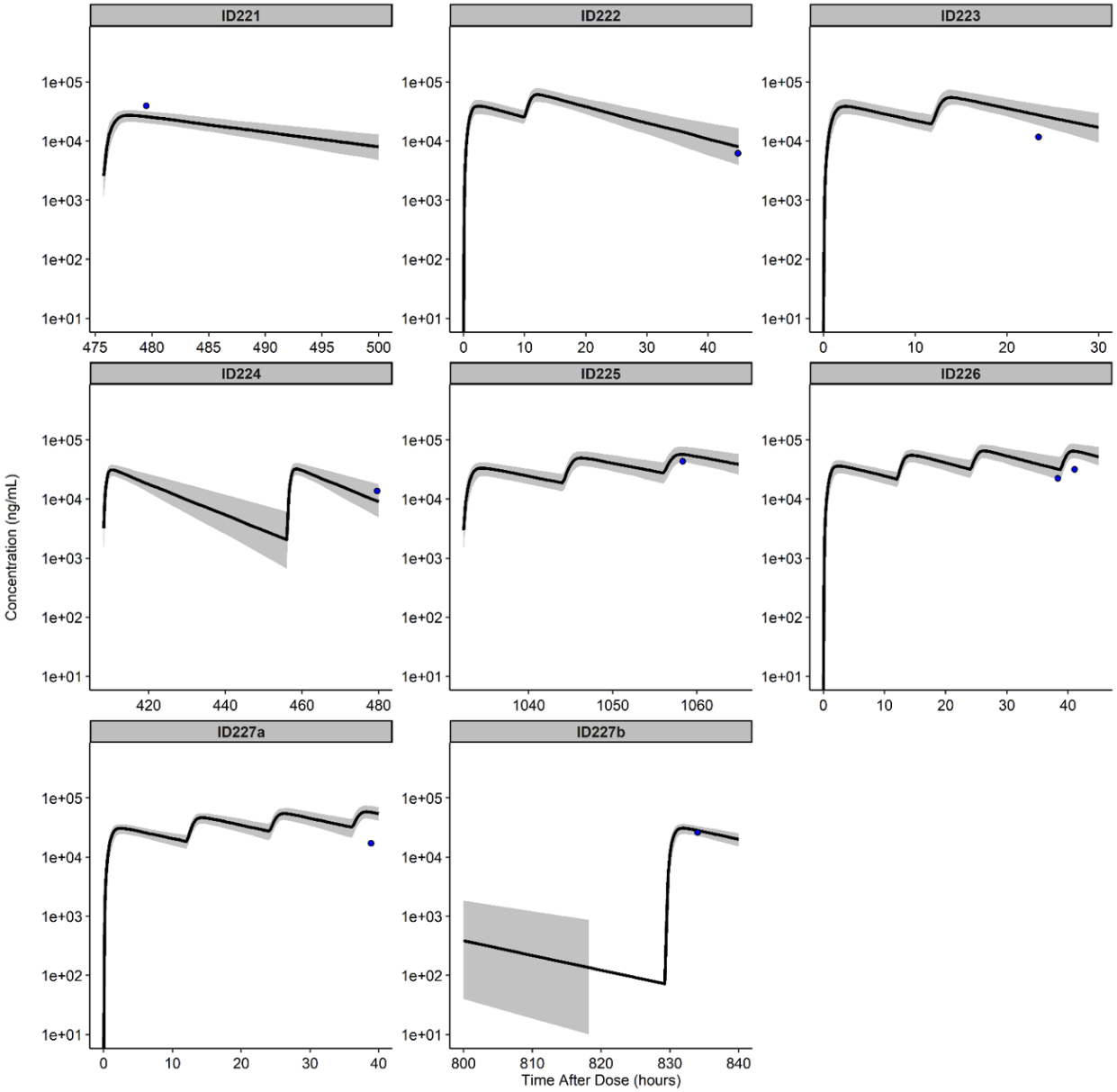

Supplementary Figure 21. Population simulations (n=250) of plasma sulfamethoxazole concentration using "individualized populations" for each observed pediatric subject with obesity that are matched to that particular subject's demographics and dosing regimen, after increasing NAT2 clearance five-fold for obesity. The shaded regions are the 90% model prediction interval, which are overlaid with points representing observed plasma concentrations from the POP01 and External Data Study.

NAT2, N-acetyl transferase 2; POP01, Pharmacokinetics of Understudied Drugs Administered to Children Per Standard of Care (ClinicalTrials.gov #NCT01431326) Study

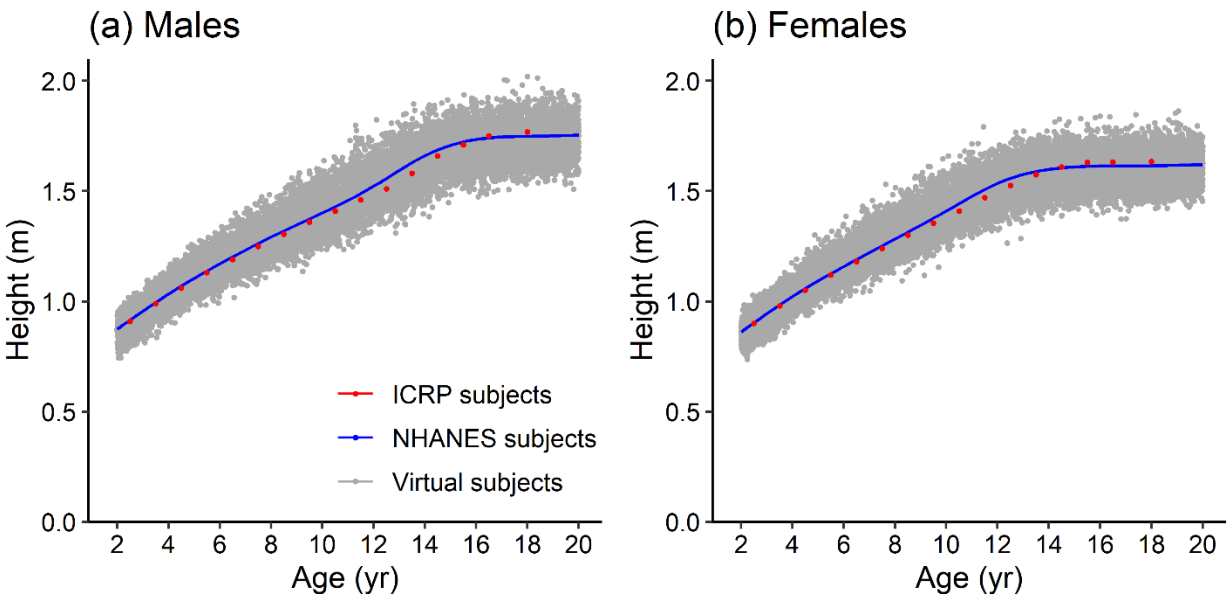

Supplementary Figure 22. Height versus age for male (a) and female (b) children. Simulated Asian, Black, Mexican, and White American virtual children with obesity are represented by the gray points. The central tendency of the data for all NHANES subjects is represented by the blue line, which is the Loess line as calculated by the generalized additive model. Average reported ICRP values for each age bin are represented by the red points.

ICRP, International Commission on Radiological Protection; NHANES, National Health and Nutrition Examination Survey

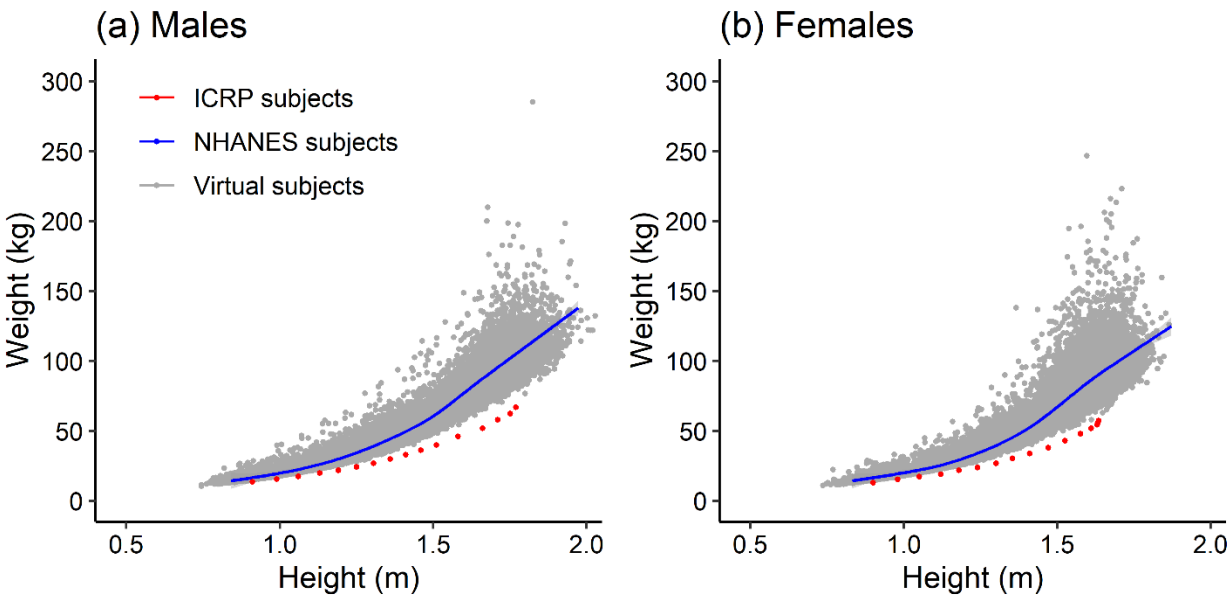

Supplementary Figure 23. Weight versus height for male (a), and female (b) children. Simulated Asian, Black, Mexican, and White American virtual children with obesity are represented by the gray points. The central tendency of the data for NHANES subjects with obesity is represented by the blue lines, which are the Loess line as calculated by the generalized additive model. Average reported ICRP values, developed from observed children without obesity, for each age bin are represented by the red points.

ICRP, International Commission on Radiological Protection; NHANES, National Health and Nutrition Examination Survey

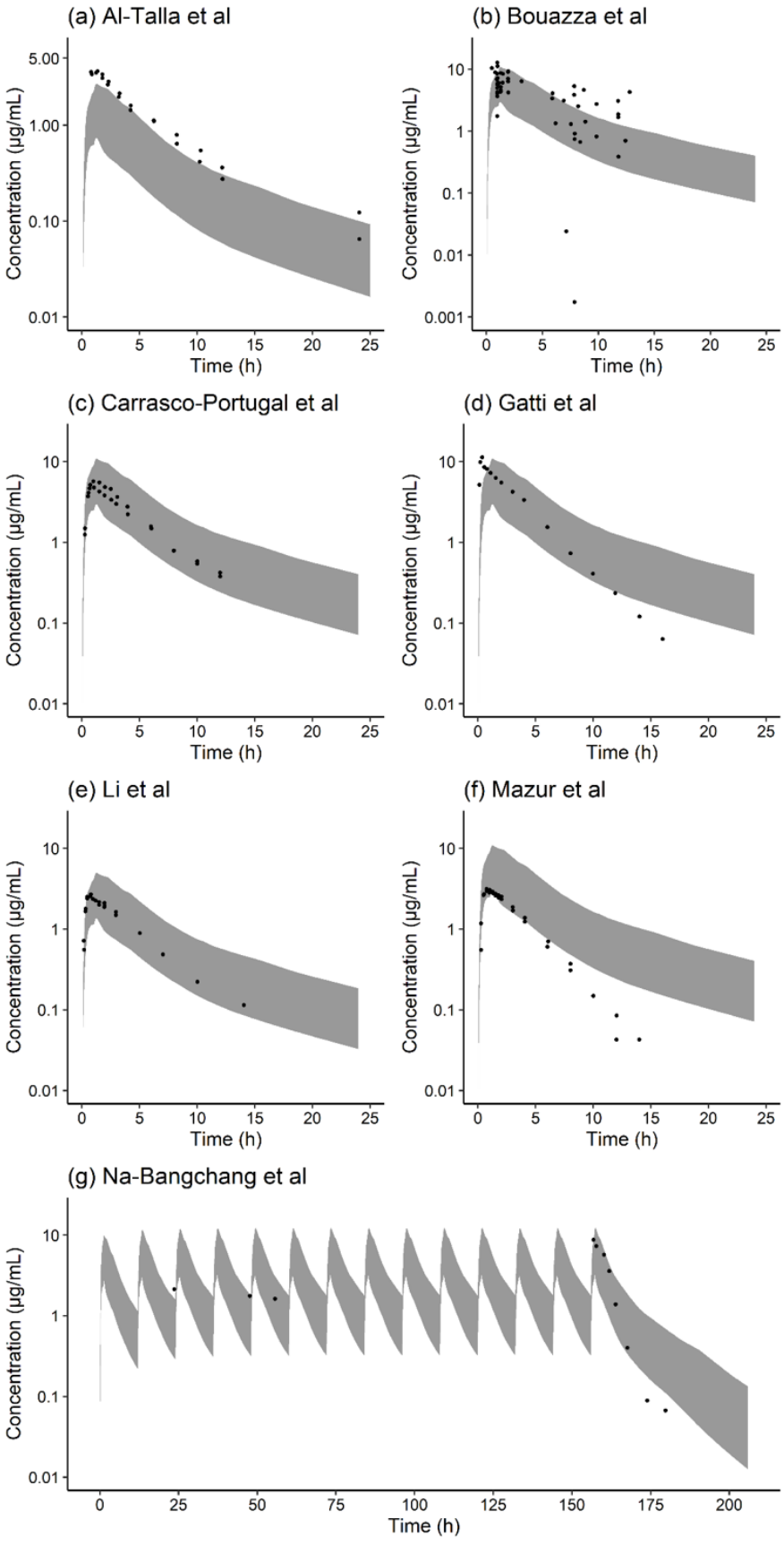
(a) Al-Talla et al
(b) Bouazza et al
(c) Carrasco-Portugal et al
(d) Gatti et al
(e) Li et al
(f) Mazur et al
(g) Na-Bangchang et al
Concentration (µg/mL)
Time (h)

Supplementary Figure 24. Population simulations (n=100) of plasma clindamycin concentrations digitized from healthy adult volunteers receiving orally administered clindamycin. Shaded regions represent the 90% model prediction interval, and points are digitized observed plasma concentrations [15-21]. Simulated dosing included 150 mg (a), 600 mg (b, c, d, f), and 300 mg (e) single oral doses and 600 mg multiple oral dosing every 12 hours (g).

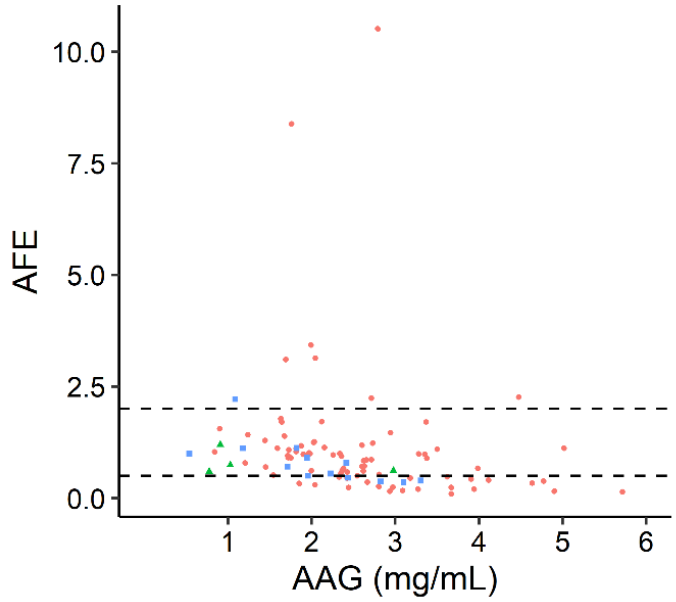

Supplementary Figure 25. AFE for pediatric subjects with obesity who received clindamycin plotted versus AAG without adjusting fraction unbound based on observed AAG concentration. Dashed lines represent 2-fold error for reference. AFE was calculated using median simulated concentration.

AAG, α1-acid glycoprotein; AFE, average fold error; BMI, body mass index

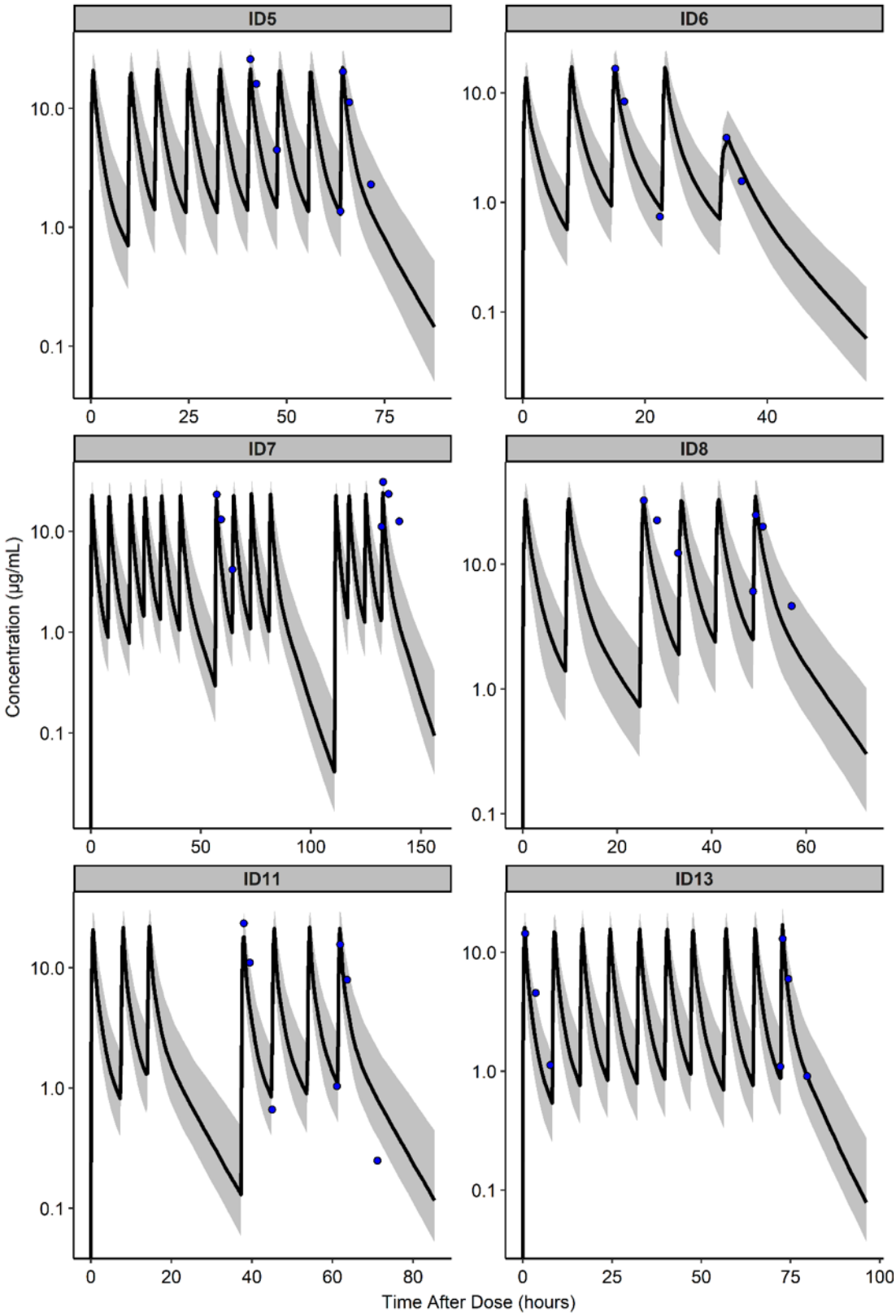
ID5
ID6
ID7
ID8
ID11
ID13
Concentration (µg/mL)
Time After Dose (hours)

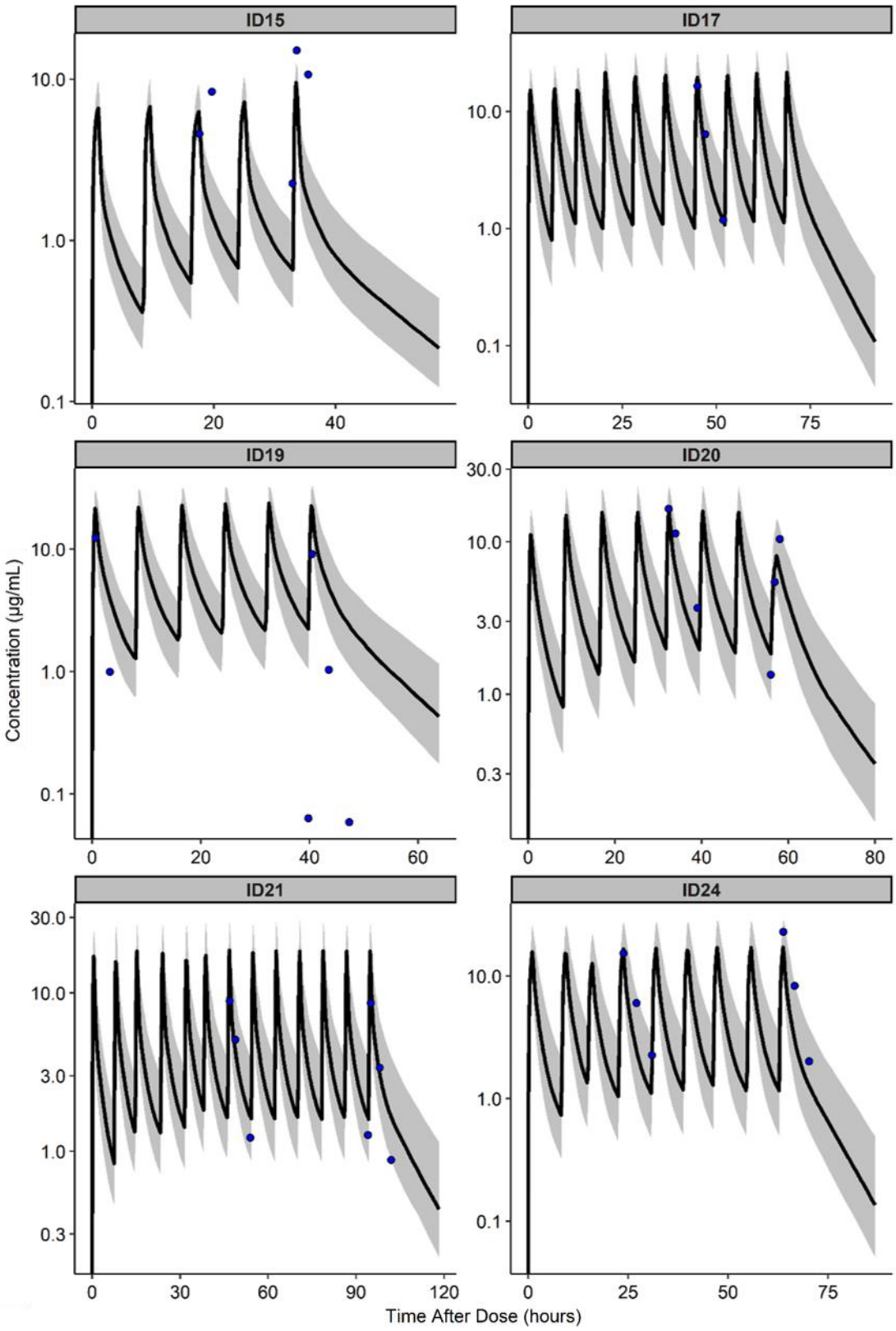
ID15
ID17
ID19
ID20
ID21
ID24
Concentration (µg/mL)
Time After Dose (hours)

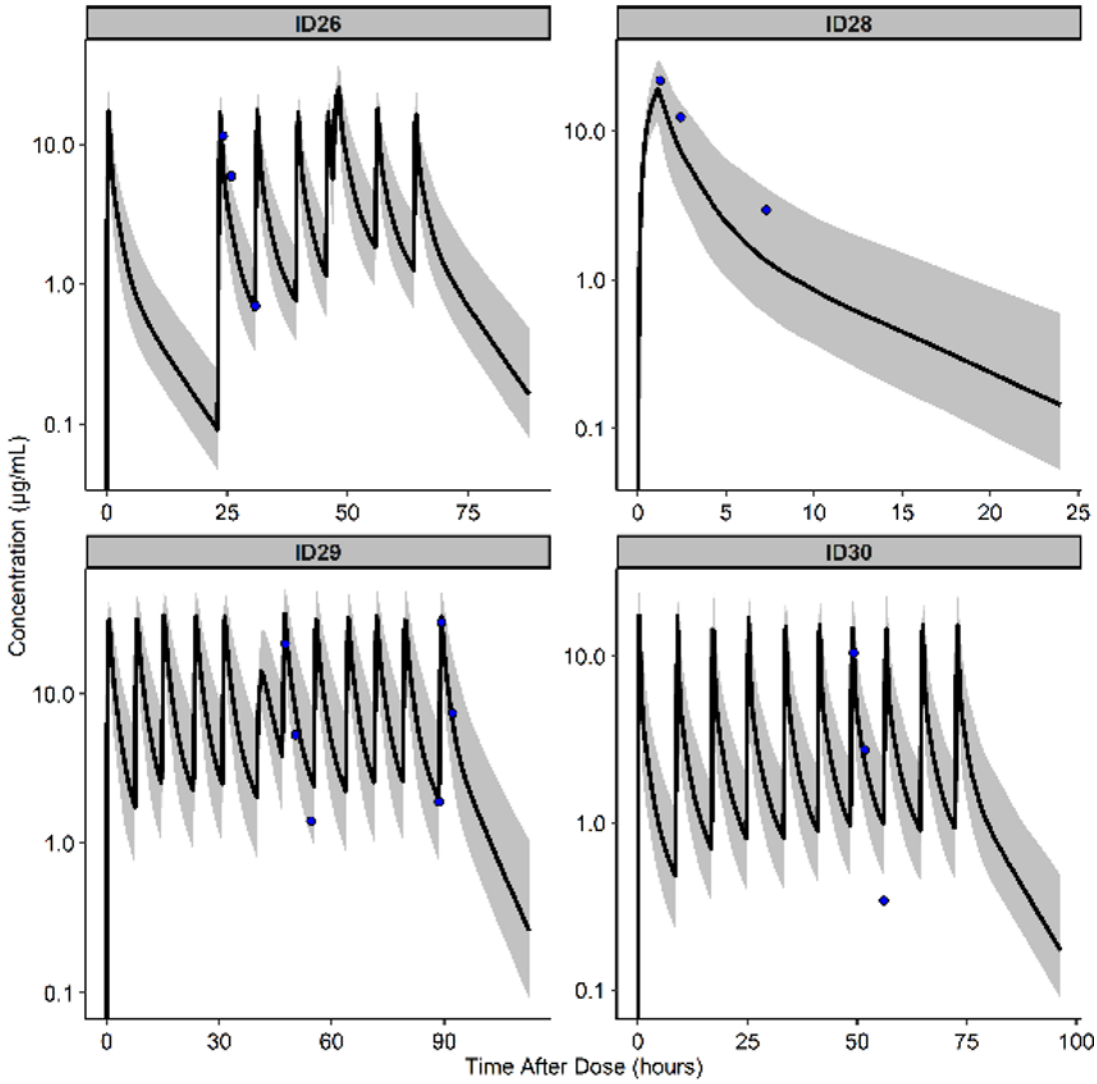

Supplementary Figure 26. Population simulations (n=250) of plasma clindamycin concentration after adjusting fraction unbound using reported AAG concentrations using "individualized populations" for each observed pediatric subject without obesity that are matched to that particular subject's demographics and dosing regimen. The shaded regions are the 90% model prediction interval, which are overlaid with points representing observed plasma concentrations from the External Data Study.

AAG, α1-acid glycoprotein

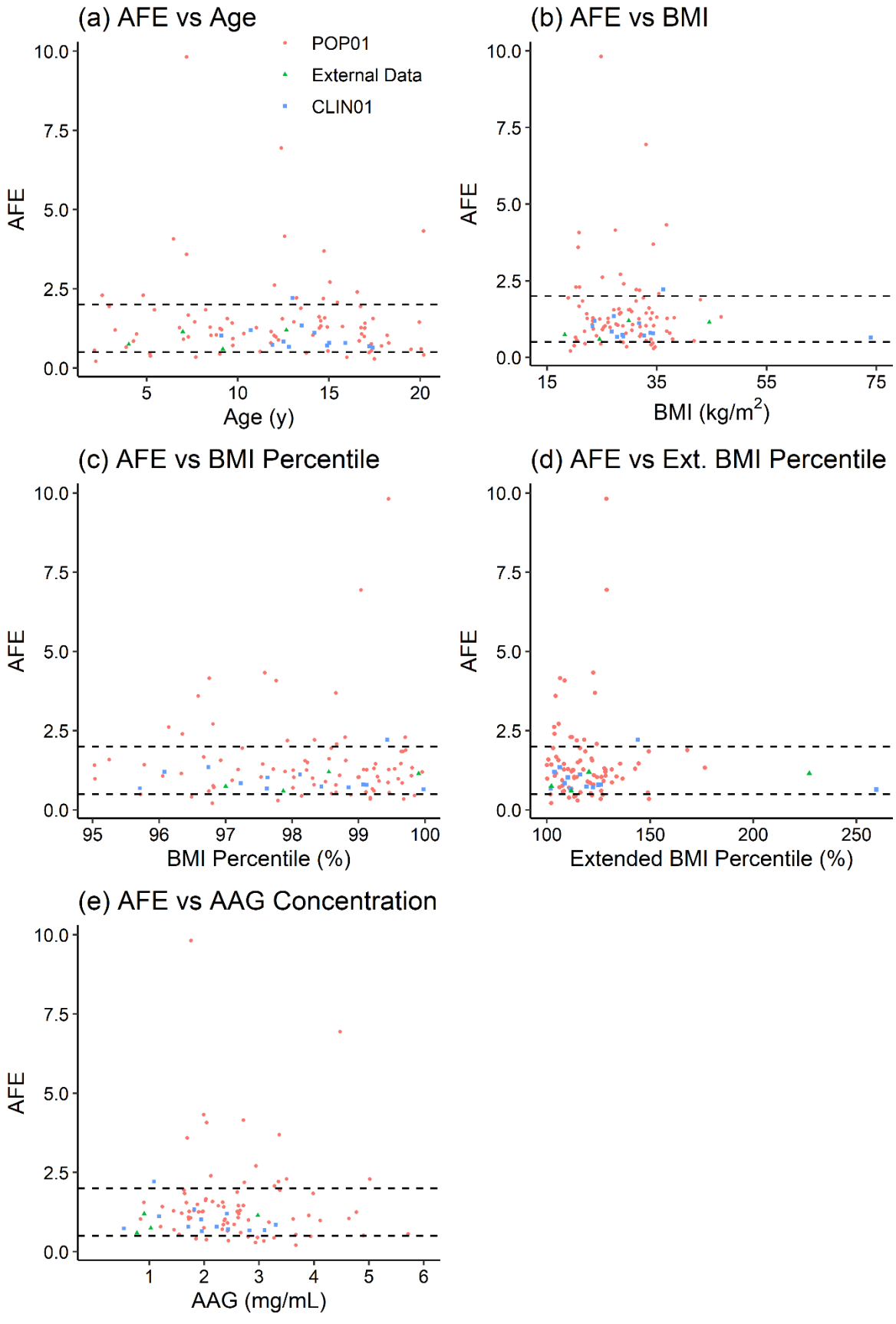
(a) AFE vs Age
POP01
External Data
CLIN01
AFE
Age (y)
(b) AFE vs BMI
BMI (kg/m2)
(c) AFE vs BMI Percentile
BMI Percentile (%)
(d) AFE vs Ext. BMI Percentile
Extended BMI Percentile (%)
(e) AFE vs AAG Concentration
AAG (mg/mL)

Supplementary Figure 27. AFE for pediatric subjects with obesity who received clindamycin plotted versus age, body size, and AAG after adjusting fraction unbound based on observed AAG concentration. Dashed lines represent 2-fold error for reference. AFE was calculated using median simulated concentration. Note that one subject (aged 7 years with a BMI of 22.9, BMI percentile of 98.3%, and AAG concentration of 2.8 mg/mL) with an outlying AFE of 21.0 was removed for better visualization. Ext. BMI percentile is calculated as BMI divided by the 95th BMI percentile for a subject's age and sex, where children with an extended BMI percentile ≥ 100% are considered obese.

AAG, α1-acid glycoprotein; AFE, average fold error; BMI, body mass index; CLIN01, Safety and Pharmacokinetics of Clindamycin in Pediatric Subjects with BMI ≥ 85th Percentile (ClinicalTrials.gov #NCT01744730) Study; Ext., extended; POP01, Pharmacokinetics of Understudied Drugs Administered to Children Per Standard of Care (ClinicalTrials.gov #NCT01431326) Study

4 SUPPLEMENTARY TABLES

Supplementary Table 1. Summary of clinical studies used for pediatric PBPK modeling.

CLINDAMYCIN	
POP01 Study	Originally described in Gonzalez et al [22]
	Nonobese PBPK modeling published in Hornik et al [13]
	Obese PBPK modeling presented here
External Data Study	Originally published here
	Nonobese PBPK modeling presented here
	Obese PBPK modeling presented here
CLIN01 Study	Originally described in Smith et al [23]
	Obese PBPK modeling presented here
TRIMETHOPRIM / SULFAMETHOXAZOLE	
POP01 Study	Originally described in Autmizguine et al [9]
	Nonobese PBPK modeling published in Thompson et al [13]
	Obese PBPK modeling presented here
External Data Study	Originally described in Wu et al [24]
	Nonobese PBPK modeling presented here
	Obese PBPK modeling presented here

CLIN01, Safety and Pharmacokinetics of Clindamycin in Pediatric Subjects with BMI ≥ 85th Percentile (ClinicalTrials.gov #NCT01744730) Study; PBPK, physiologically-based pharmacokinetic; POP01, Pharmacokinetics of Understudied Drugs Administered to Children Per Standard of Care (ClinicalTrials.gov #NCT01431326) Study

Supplementary Table 2. Population demographics for pediatric subjects without obesity who received clindamycin from the External Data Study used to evaluate the pediatric PBPK model.

Demographics[a]	External Data Study (*n=16*)
n, samples	88
Age, years	7.2 (3.6, 16.0)
Age group	
2 ≤ and < 6 years	6 (37.5%)
6 ≤ and < 12 years	6 (37.5%)
12 ≤ and < 21 years	4 (25.0%)
Weight, kg	25.1 (14.7, 63.2)
Height, cm	126.0 (96.5, 176.0) [1[b]]
BMI, kg/m^2	16.6 (14.2, 22.4) [1[b]]
BMI percentile, %	60.4 (18.5, 85.9) [1[b]]
Extended BMI percentile, %	86.6 (68.1, 92.4) [1[b]]
Male	8 (50.0%)
Race	
White	13 (81.3%)
Black or African American	2 (12.5%)
Asian	0 (0%)
Native Hawaiian/Pacific Islander	0 (0%)
Unknown/Not reported	1 (6.3%)
Ethnicity	
Hispanic/Latino	0 (0%)
Not Hispanic/Latino	0 (0%)
Unknown/Not reported	16 (100.0%)
AAG, mg/mL	1.75 (0.29, 3.19)
Albumin, g/dL	3.30 (3.20, 4.00) [11]
SCR, mg/dL	0.40 (0.23, 0.63)
AST, U/L	[16]
ALT, U/L	[16]

[a]Demographics recorded at the time of the first study dose were used to calculate descriptive statistics. Values are medians (range) [missing] for continuous variables and counts (%) for categorical variables. Extended BMI percentile is calculated as BMI divided by the 95th BMI percentile for a subject's age and sex, where children with an extended BMI percentile ≥ 100% are considered obese.

[b]One subject did not have a height recorded, so BMI, BMI percentile, and extended BMI percentile could not be calculated. This subject was included in the nonobese cohort since her weight was approximately 50th percentile for age.

AAG, α1-acid glycoprotein; ALT, alanine transaminase; AST, aspartate aminotransferase; BMI, body mass index; SCR, serum creatinine

Supplementary Table 3. Population demographics for pediatric subjects with obesity who received clindamycin from the POP01, CLIN01, and External Data Study and combined dataset.

Demographics[a]	**POP01 (*n=84*)**	**CLIN01 (*n=13*)**	**External Data Study (*n=4*)**	**Combined (*n=101*)**
n, samples	107	53	28	188
Age, years	12.3 (2.1, 20.2)	13.5 (9.1, 17.4)	8.1 (4.0, 12.7)	12.5 (2.1, 20.2)
Age group				
2 ≤ and < 6 years	12 (14.3%)	0 (0%)	1 (25.0%)	13 (12.9%)
6 ≤ and < 12 years	27 (32.1%)	3 (23.1%)	2 (50.0%)	32 (31.7%)
12 ≤ and < 21 years	45 (53.6%)	10 (76.9%)	1 (25.0%)	56 (55.4%)
Weight, kg	63.9 (12.8, 139.8)	76.4 (49.5, 224.0)	51.1 (16.8, 72.7)	66.6 (12.8, 224.0)
Height, cm	147.5 (81.0, 193.0)	155.0 (134.4, 188.0)	123.2 (96.0, 156.0)	152.0 (81.0, 193.0)
BMI, kg/m^2	28.8 (18.9, 46.7)	28.9 (23.3, 74.0)	27.2 (18.2, 44.6)	28.9 (18.2, 74.0)
BMI percentile, %	98.5 (95.0, 100.0)	98.1 (95.7, 100.0)	98.2 (97.0, 99.9)	98.4 (95.0, 100.0)
Extended BMI percentile, %	115.6 (100.0, 176.6)	116.1 (101.9, 259.6)	116.1 (102.2, 227.2)	116.1 (100.0, 259.6)
Male	41 (48.8%)	12 (92.3%)	2 (50.0%)	55 (54.5%)
Race				
White	63 (75.0%)	11 (84.6%)	4 (100.0%)	78 (77.2%)
Black or African American	12 (14.3%)	1 (7.7%)	0 (0%)	13 (12.9%)
Asian	1 (1.2%)	0 (0%)	0 (0%)	1 (1.0%)
Native Hawaiian/Pacific Islander	1 (1.2%)	0 (0%)	0 (0%)	1 (1.0%)
Unknown/Not reported	7 (8.3%)	1 (7.7%)	0 (0%)	8 (7.9%)
Ethnicity				
Hispanic/Latino	31 (36.9%)	1 (7.7%)	0 (0%)	32 (31.7%)
Not Hispanic/Latino	53 (63.1%)	11 (84.6%)	0 (0%)	64 (63.4%)
Unknown/Not reported	0 (0%)	1 (7.7%)	4 (100.0%)	5 (5.0%)
AAG, mg/mL	2.43 (0.84, 5.72) [4]	2.04 (0.54, 3.31)	0.97 (0.78, 2.98)	2.37 (0.54, 5.72) [4]
Albumin, g/dL	3.22 (1.90, 4.40) [59]	3.70 (2.60, 4.43)	2.85 (2.70, 3.00) [2]	3.45 (1.90, 4.43) [63]

SCR, mg/dL	0.60 (0.20, 1.60) [46]	0.58 (0.31, 1.54)	0.47 (0.27, 0.62)	0.60 (0.20, 1.60) [50]
AST, U/L	36 (15, 165) [69]	23 (8, 151)	[4]	30 (8, 165) [73]
ALT, U/L	36 (9, 165) [69]	28 (10, 114)	[4]	32 (9, 165) [73]

[a]Demographics recorded at the time of the first study dose were used to calculate descriptive statistics. Values are medians (range) [missing] for continuous variables and counts (%) for categorical variables. Extended BMI percentile is calculated as BMI divided by the 95th BMI percentile for a subject's age and sex, where children with an extended BMI percentile ≥ 100% are considered obese.

AAG, α1-acid glycoprotein; ALT, alanine transaminase; AST, aspartate aminotransferase; BMI, body mass index; CLIN01, Safety and Pharmacokinetics of Clindamycin in Pediatric Subjects with BMI ≥ 85th Percentile (ClinicalTrials.gov #NCT01744730) Study; POP01, Pharmacokinetics of Understudied Drugs Administered to Children Per Standard of Care (ClinicalTrials.gov #NCT01431326) Study; SCR, serum creatinine

Supplementary Table 4. Population demographics for pediatric subjects without obesity who received trimethoprim/sulfamethoxazole from the External Data Study to evaluate the pediatric PBPK model.

Demographics[a]	External Data Study (*n=8*)
n, samples (TMP; SMX)	50; 50
Age, years	7.1 (2.8, 13.4)
Age group	
2 ≤ and < 6 years	4 (50%)
6 ≤ and < 12 years	1 (12.5%)
12 ≤ and < 21 years	3 (37.5%)
Weight, kg	25.3 (11.1, 53.1)
Height, cm	122.1 (80.0, 157.0)
BMI, kg/m^2	16.6 (13.9, 21.5)
BMI percentile, %	56.0 (4.7, 82.3)
Extended BMI percentile, %	81.6 (58.0, 94.0)
Male	6 (75.0%)
Race	
White	7 (87.5%)
Black or African American	0 (0%)
Asian	0 (0%)
American Indian/Alaskan Native	0 (0%)
Native Hawaiian/Pacific Islander	1 (12.5%)
Multiple races	0 (0%)
Unknown/Not reported	0 (0%)
Ethnicity	
Hispanic/Latino	0 (0%)
Not Hispanic/Latino	0 (0%)
Unknown/Not reported	4 (100%)
Albumin, g/dL	3.75 (3.27, 4.10) [5]
SCR, mg/dL	0.37 (0.25, 0.57)

[a]Demographics recorded at the time of the first study dose were used to calculate descriptive statistics. Values are medians (range) [missing] for continuous variables and counts (%) for categorical variables. Extended BMI percentile is calculated as BMI divided by the 95^{th} BMI percentile for a subject's age and sex, where children with an extended BMI percentile ≥ 100% are considered obese.

BMI, body mass index; SCR, serum creatinine; SMX, sulfamethoxazole; TMP, trimethoprim

Supplementary Table 5. Population demographics for pediatric subjects with obesity who received trimethoprim/sulfamethoxazole from the POP01 and External Data Study and combined dataset.

Demographics[a]	POP01 (*n=46*)	External Data Study (*n=4*)	Combined (*n=50*)
n, samples (TMP; SMX)	62; 64	25; 25	87; 89
Age, years	14.3 (2.1, 20.2)	11.2 (7.0, 14.7)	14.0 (2.1, 20.2)
Age group			
2 ≤ and < 6 years	4 (8.7%)	0 (0%)	4 (8.0%)
6 ≤ and < 12 years	12 (26.1%)	3 (75.0%)	15 (30.0%)
12 ≤ and < 21 years	30 (65.2%_	1 (25.0%)	31 (62.0%)
Weight, kg	70.3 (12.6, 147.9)	53.6 (32.2, 65.4)	68.1 (12.6, 147.9)
Height, cm	156.1 (80.2, 190.0)	141.9 (124.2, 150.0)	155.0 (80.2, 190.0)
BMI, kg/m^2	30.3 (18.4, 46.1)	26.6 (20.9, 29.1)	29.4 (18.4, 46.1)
BMI percentile, %	98.3 (83.0, 100.0)	96.9 (96.2, 98.6)	98.1 (83.0, 100.0)
Extended BMI percentile, %	118.1 (100.3, 173.9)	105.9 (104.3, 121.6)	117.1 (100.3, 173.9)
Male	33 (71.7%)	2 (50.0%)	35 (70.0%)
Race			
White	31 (67.4%)	4 (100.0%)	35 (70.0%)
Black or African American	8 (17.4%)	0 (0%)	8 (16.0%)
Asian	1 (2.2%)	0 (0%)	1 (2.0%)
American Indian/Alaskan Native	1 (2.2%)	0 (0%)	1 (2.0%)
Native Hawaiian/Pacific Islander	2 (4.3%)	0 (0%)	2 (4.0%)
Multiple races	2 (4.3%)	0 (0%)	2 (4.0%)
Unknown/Not reported	1 (2.2%)	0 (0%)	1 (2.0%)
Ethnicity			
Hispanic/Latino	5 (10.9%)	0 (0%)	5 (10.0%)
Not Hispanic/Latino	40 (87.0%)	0 (0%)	40 (80.0%)
Unknown/Not reported	1 (2.2%)	4 (100%)	5 (10.0%)
SCR, mg/dL	0.60 (0.20, 4.50) [7]	0.50 (0.40, 0.57)	0.60 (0.20, 4.50) [7]

[a]Demographics recorded at the time of the first study dose were used to calculate descriptive statistics. Values are medians (range) [missing] for continuous variables and counts (%) for categorical variables. Extended BMI percentile is calculated as BMI divided by the 95th BMI percentile for a subject's age and sex, where children with an extended BMI percentile ≥ 100% are considered obese.

BMI, body mass index; POP01, Pharmacokinetics of Understudied Drugs Administered to Children Per Standard of Care (ClinicalTrials.gov #NCT01431326) Study; SCR, serum creatinine; SMX, sulfamethoxazole; TMP, trimethoprim

Supplementary Table 6. Parameters used in clindamycin PBPK model development.

Parameter	Clindamycin phosphate	Clindamycin	Source
PHYSICOCHEMICAL PROPERTIES			
Molecular weight, g/mol	504.96	424.98	Hornik et al [13]
Effective molecular weight, g/mol	482.96	402.98	Hornik et al [13]
pKa value	6.78	7.55	Hornik et al [13]
Compound type	base	base	Hornik et al [13]
Lipophilicity	0.95	2.16	Hornik et al [13]
Protein binding partner	AAG	AAG	Hornik et al [13]
Fraction unbound	0.22	0.06	Hornik et al [13]
Solubility, mg/L	3,220	30.6	Hornik et al [13]
Solubility reference pH	7.0	7.0	Hornik et al [13]
Solubility gain per charge	1,000	1,000	Hornik et al [13]
Blood to plasma ratio	0.62	0.61	Calculated value[a]
ABSORPTION			
Dissolution function	---	Weibull	Optimized
Dissolution time, min	---	71.69	Optimized
Dissolution shape	---	0.92	Optimized
Lag time, h	---	0	Optimized
Specific intestinal permeability, cm/min	$1.19e^{-7}$	$6.73e^{-3}$	Calculated value[b] / Optimized
Specific organ permeability, cm/min	$2.02e^{-5}$	$9.71e^{-4}$	Calculated value[c]
DISTRIBUTION			
Partition coefficients	Rodgers & Rowland	Rodgers & Rowland	Literature [25]
Cellular permeabilities	PK-Sim® Standard	Charge dependent Schmidt	PK-Sim® algorithm
METABOLISM			
Alkaline phosphatase			
Reference concentration, µmol/L	1.0	---	Hornik et al [13]
CL_{int}, L/min	0.80	---	Hornik et al [13]
CL_{spec}, 1/min[d]	0.51	---	Hornik et al [13]
CYP3A4			
Reference concentration, µmol/L	---	4.32	Hornik et al [13]
CL_{int}, µL/min/pmol CYP	---	0.51	Hornik et al [13]
CYP3A5			
Reference concentration, µmol/L	---	0.04	Hornik et al [13]
CL_{int}, µL/min/pmol CYP	---	7.00	Hornik et al [13]
EXCRETION			
GFR fraction	0.044	1.0	Hornik et al [13]
Renal transporter			
Reference concentration, µmol/L	---	1.0	Hornik et al [13]
V_{max}, µmol/L/min[e]	---	1,829.24	Hornik et al [13]

K_m, μM[e]	---	10,000	Hornik et al [13]

[a] $\left[\left(f_{water_{rbc}} + f_{lipids_{rbc}} * 10^{logP} + f_{proteins_{rbc}} * KProt\right) * f_u * HCT\right] - HCT + 1$; where f_{water_rbc} is the fractional volume content of water in blood cells, f_{lipids_rbc} is the fractional volume content of lipid in blood cells, *logP* is the lipophilicity measure, $f_{proteins\_rbc}$ is the fractional volume content of protein in blood cells, *KProt* is partition coefficient of water to protein, f_u is the fraction unbound, and *HCT* is the hematocrit.

[b] $266 * \left(MW_{eff} * 10^9\right)^{-4.5} * 10^{logP} * 60 * 10^{-1}$; where MW_{eff} is the effective molecular weight and *logP* is the lipophilicity measure.

[c] $\left(\frac{MW_{eff} * 10^9}{336}\right)^{-6} * \frac{10^{logP}}{5} * 10^{-5}$; where MW_{eff} is the effective molecular weight and *logP* is the lipophilicity measure.

[d] CL_{spec} is a PK-Sim® software-specific term that is calculated by $CL_{spec} = \frac{CL_{int}}{V * f_{cell}}$; where *V* is the volume of the liver and f_{cell} is the fraction intracellular in the liver.

[e] Note that these values, as inputted in PK-Sim®, are calculated for liver tissue.

AAG, α1-acid glycoprotein; CL_{int}, intrinsic clearance; CL_{spec}, specific clearance; CYP, cytochrome P450; K_m, concentration of half-maximal metabolism or transport; PBPK, physiologically-based pharmacokinetic; pKa, negative log of the acid dissociation constant; V_{max}, maximal rate of metabolism or transport

Supplementary Table 7. Parameters used in trimethoprim/sulfamethoxazole PBPK model development.

Parameter	Trimethoprim	Sulfamethoxazole	Source
PHYSICOCHEMICAL PROPERTIES			
Molecular weight, g/mol	290.32	253.28	Thompson et al [14]
Effective molecular weight, g/mol	290.32	253.28	Thompson et al [14]
pKa value	7.3	6.0	Thompson et al [14]
Compound type	base	acid	Thompson et al [14]
Lipophilicity	1.36	0.89	Thompson et al [14]
Protein binding partner	albumin	albumin	Thompson et al [14]
Fraction unbound	0.56	0.30	Thompson et al [14]
Solubility, mg/L	500	700	Thompson et al [14]
Solubility reference pH	7.0	7.0	Thompson et al [14]
Solubility gain per charge	1,000	1,000	Thompson et al [14]
Blood to plasma ratio	0.79	0.65	Calculated value[a]
ABSORPTION			
Dissolution function	Weibull	Weibull	Thompson et al [14]
Dissolution time, min	15	20	Thompson et al [14]
Dissolution shape	0.77	0.73	Thompson et al [14]
Lag time, h	0	0	Optimized
Specific intestinal permeability, cm/min	$5.9e^{-6}$	$4.52e^{-5}$	Thompson et al [14]
Specific organ permeability, cm/min	$1.11e^{-3}$	$8.46e^{-4}$	Calculated value[b]
DISTRIBUTION			
Partition coefficients	Rodgers & Rowland	Rodgers & Rowland	Literature [25]
Cellular permeabilities	PK-Sim® Standard	PK-Sim® Standard	PK-Sim® algorithm
METABOLISM			
CYP2C9			
Reference concentration, µmol/L	3.84	3.84	Thompson et al [14]
CL_{int}, mL/min	4.19	5.21	Thompson et al [14]
CL_{spec}, 1/min[c]	0.0027	0.0033	Thompson et al [14]
CYP3A4			
Reference concentration, µmol/L	4.32	---	Thompson et al [14]
CL_{int}, mL/min	4.19	---	Thompson et al [14]
CL_{spec}, 1/min[c]	0.0027	---	Thompson et al [14]
NAT2 *(unadjusted)*			
Reference concentration, µmol/L	---	1.0	Thompson et al [14]
CL_{int}, mL/min	---	5.21	Thompson et al [14]
CL_{spec}, 1/min[c]	---	0.0033	Thompson et al [14]
NAT2 *(adjusted with obesity)*			
Reference concentration, µmol/L	---	1.0	Thompson et al [14]
CL_{int}, mL/min	---	26.05	Chiney et al [26]

CL_{spec}, 1/min	---	0.0165	Chiney et al [26]
EXCRETION			
GFR fraction	1.0	0.117	Thompson et al [14]
Renal transporter			
Reference concentration, µmol/L	1.0	---	Thompson et al [14]
V_{max}, µmol/L/min[d]	1,306.6	---	Thompson et al [14]
K_m, µM[d]	10,000	---	Thompson et al [14]

[a] $\left[\left(f_{water_{rbc}} + f_{lipids_{rbc}} * 10^{logP} + f_{proteins_{rbc}} * KProt\right) * f_u * HCT\right] - HCT + 1$; where f_{water_rbc} is the fractional volume content of water in blood cells, f_{lipids_rbc} is the fractional volume content of lipid in blood cells, *logP* is the lipophilicity measure, $f_{proteins\_rbc}$ is the fractional volume content of protein in blood cells, *KProt* is partition coefficient of water to protein, f_u is the fraction unbound, and *HCT* is the hematocrit.

[b] $\left(\frac{MW_{eff} * 10^9}{336}\right)^{-6} * \frac{10^{logP}}{5} * 10^{-5}$; where MW_{eff} is the effective molecular weight and *logP* is the lipophilicity measure.

[c] CL_{spec} is a PK-Sim® software-specific term that is calculated by $CL_{spec} = \frac{CL_{int}}{V * f_{cell}}$; where *V* is the volume of the liver and f_{cell} is the fraction intracellular in the liver.

[d] Note that these values, as inputted in PK-Sim®, are calculated for liver tissue.

CL_{int}, intrinsic clearance; CL_{spec}, specific clearance; CYP, cytochrome P450; K_m, concentration of half-maximal metabolism or transport; NAT2, N-acetyl transferase 2; PBPK, physiologically-based pharmacokinetic; pKa, negative log of the acid dissociation constant; V_{max}, maximal rate of metabolism or transport

Supplementary Table 8. Population demographics for virtual pediatric subjects with obesity who were used in dosing simulations for clindamycin and trimethoprim/sulfamethoxazole.

Demographics[a]	Clindamycin Simulations	TMP/SMX Simulations
Age, years	9.1 (2.1, 18.0)	12.0 (2.0, 18.0)
Age group		
2 ≤ and < 6 years	1,000 (33.3%)	1,000 (50.0%)[c]
6 ≤ and < 12 years	1,000 (33.3%)	
12 ≤ and < 21 years	1,000 (33.3%)	1,000 (50.0%)
Weight, kg	43.9 (12.1, 174.5)	61.9 (12.8, 174.5)
Height, cm	134.5 (77.1, 200.5)	78.1 (149.9, 200.5)
BMI, kg/m^2	24.5 (17.8, 74.3)	17.8 (27.1, 74.3)
BMI percentile, %	97.8 (95.0, 100.0)	97.6 (95.0, 100.0)
Extended BMI percentile, %	108.7 (100.0, 287.3)	109.1 (100.0, 287.3)
Obesity Stage[b]		
Stage I	2,340 (78.0%)	1,555 (77.8%)
Stage II	491 (16.4%)	332 (16.6%)
Stage III	169 (5.6%)	113 (5.7%)
Male	33 (71.7%)	983 (49.2%)

[a]Values are medians (range) for continuous variables and counts (%) for categorical variables. Extended BMI percentile is calculated as BMI divided by the 95th BMI percentile for a subject's age and sex, where children with an extended BMI percentile ≥ 100% are considered obese.

[b]Obesity stages are defined by extended BMI percentiles of 100-120% (Stage I), 120-140% (Stage II), and >140% (Stage III).

[c]One thousand virtual subjects were generated for each age group for both clindamycin and TMP/SMX PBPK model simulations. For clindamycin, the age groups were >2-6 years, >6-12 years, and <12-18 years. For TMP/SMX, the age groups were >2-12 years and >12-18 years.

BMI, body mass index; SMX, sulfamethoxazole; TMP, trimethoprim

Supplementary Table 9. Summarized results from a comprehensive literature search for reported hematocrit values in children with obesity.

n, subjects	Age (y)	Males	Race	Weight (kg)	BMI (kg/m^2)	Hematocrit (L/L)	Reference
182	11.6 (2.9)	0%	NR	72.1 (22.5)	30.7 (5.8)	0.40 (0.02)	Belo et al [27]
168	11.7 (2.9)	100%	NR	76.2 (27.4)	30.5 (6.4)	0.42 (0.03)	Belo et al [27]
43	11.0 (2.4)	65%	NR	NR	NR[a]	0.38 (0.03)	Cacciari et al [28]
43	16.0 (1.1)	0%	NR	126.2 (22.8)	46.0 (6.0)	0.43 (0.03)	Elhag et al [29]
36	16.0 (1.1)	100%	NR	126.2 (22.8)	46.0 (6.0)	0.39 (0.03)	Elhag et al [29]

Values are mean (standard deviation) unless otherwise noted.

[a]The study reported subjects with obesity, but did not report BMI directly.

BMI, body mass index; NR, not reported

Supplementary Table 10. Summarized results from a comprehensive literature search for reported albumin values in children with obesity.

n, subjects	Age (y)	Males	Race	Weight (kg)	BMI (kg/m^2)	Albumin (g/L)	Reference
230	10.1 (3.0)[a]	57%	Non-Hispanic White	NR	25.4 (23.1, 28.7)[b]	4.9 (4.7, 50.5)[b]	Di Costanzo et al [30]
7	(10, 16)[c]	43%	Non-Hispanic Black	(85, 148)[c]	(34.2, 65.6)[c]	3.6 (3.3, 3.9)[b]	Adelman et al [31]
1[d]	10	0%	Non-Hispanic Black	94	52	3.3	Adelman et al [31]
1[d]	16	0%	Non-Hispanic Black	164	65.5	3.6	Adelman et al [31]
1[d]	14	100%	Non-Hispanic Black	85	38	3.9	Adelman et al [31]
1[d]	15	0%	Non-Hispanic Black	148	51.6	3.7	Adelman et al [31]
1[d]	16	100%	Non-Hispanic Black	141	39	3.6	Adelman et al [31]
1[d]	16	0%	Non-Hispanic Black	105	42.5	3.6	Adelman et al [31]
1[d]	16	100%	Non-Hispanic Black	103	34.3	3.8	Adelman et al [31]
47	11.3 (2.7)	40%	Egyptian	NR	NR[e]	3.5 (0.5)	Ahmed et al [32]
23	10.6 (3.1)	39%	Egyptian	NR	NR[e]	3.9 (0.2)	Ahmed et al [32]
21	(7, 9)[c]	52%	Asian	NR	NR[e]	4.0 (0.2)	Wu et al [33]
42	11.7 (3.1)	52%	NR	41.4 (17.7)	18.4 (3.9)	3.8 (0.4)	White et al [34]
10	16.3 (1.7)	NR[f]	NR	138.8	51.7	4.3 (0.3)	Velhote et al [35]
242	17.1 (1.6)	24%	Non-Hispanic White	NR	50.5 (45.2, 58.3)[b]	4.1 (0.3)	Xiao et al [36]
43	11.0 (2.4)	65%	NR	NR	NR[e]	4.4 (0.3)	Cacciari et al [37]
36	17.5 (0.3)	44%	Non-Hispanic White	NR	37.4 (1.2)	4.3 (0.3)	Cohen et al [38]
36	16.0 (1.1)	100%	NR	126.2 (22.8)	46.0 (6.0)	4.1 (0.4)	Elhag et al [29]
43	16.0 (1.1)	0%	NR	126.2 (22.8)	46.0 (6.0)	4.1 (0.4)	Elhag et al [29]
22	(1, 21)[c]	36%	Non-Hispanic Black	NR	NR[e]	3.9 (0.8)	Abitbol et al [39]
22	(1, 21)[c]	50%)	Non-Hispanic Black	NR	NR[e]	4.0 (0.5)	Abitbol et al [39]
8	12.0 (2.5)	NR[f]	NR	82.8 (23.2)	NR[e]	4.8 (0.2)	Widhalm et al [40]
242	17.1[g]	NR[f]	Non-Hispanic White	NR	50.5 (45.2, 58.3)[b]	4.1 (3.9, 4.4)[b]	Nehus et al [41]
65	11.3 (2.8)	55%	NR	NR	27.3 (4.3)	4.5 (0.3)	Cindik et al [42]
23	13.3 (2.7)	48%	Non-Hispanic Black[g]	NR	NR[e]	4.5 (0.3)	Alkhouri et al [43]
37	14.6 (2.7)	51%	Non-Hispanic White[g]	NR	NR[e]	4.4 (0.3)	Alkhouri et al [43]
8	11.3 (2.7)	38%	NR	NR	26.2 (4.4)	4.7 (0.3)	Del Chierico et al [44]
27	12.0 (2.8)	78%	NR	NR	26.5 (4.4)	4.7 (0.2)	Del Chierico et al [44]

26	12.3 (2.5)	42%	NR	NR	27.4 (6.5)	4.8 (0.2)	Del Chierico et al [44]
19	15.2 (1.5)	89%	NR	NR	35.4 (6.0)	4.7 (0.3)	Hudert et al [45]
17	14.5 (2.2)	59%	NR	NR	36.7 (5.8)	4.6 (0.3)	Hudert et al [45]
13	14.0 (2.4)	85%	NR	NR	33.6 (6.9)	4.7 (0.3)	Hudert et al [45]
18	12.8 (2.0)	72%	NR	NR	32.6 (5.9)	4.6 (0.3)	Hudert et al [45]
60	10.6 (2.7)	33%	NR	71.9 (19.4)	35.1 (4.6)	4.4 (0.4)	Amin et al [46]
60	10.1 (3.5)	40%	NR	64.0 (13.8)	34.6 (7.8)	4.5 (0.4)	Amin et al [46]
37	7.7 (3.3)	46%	NR	NR	NR[e]	4.3 (0.2)	El-Karaksy et al [47]
39	7.7 (3.3)	54%	Egyptian	NR	NR[e]	4.3 (0.2)	El-Karaksy et al [47]
34	14.1 (11.0, 16.7)[b]	41%	Egyptian	78.0 (56.2, 123.9)[b]	NR[e]	3.7[h]	Gade et al [48]
36	14.4 (11.1, 17.7) [b]	58%	NR	56.0 (33.2, 75.8)[b]	NR[e]	3.8[h]	Gade et al [48]

Values are mean (standard deviation) unless otherwise noted.

[a]Reported as median (standard deviation).

[b]Reported as median (range).

[c]Reported as (range).

[d]Reported individual-level data.

[e]The study reported subjects with obesity, but did not report BMI directly.

[f]Includes both male and females subjects with an unreported ratio.

[g]Reported as the majority.

[h]Reported as mean.

BMI, body mass index; NR, not reported

Supplementary Table 11. Summarized results from a comprehensive literature search for reported AAG values in children with obesity.

n, subjects	Age (y)	Males	Race	Weight (kg)	BMI (kg/m^2)	AAG (g/L)	Reference
48	(3, 6)[a]	NR[b]	Hispanic	NR	NR[c]	1.05 (0.9, 1.3)[d,e]	Gibson et al [49]
876	14.9 (13.9, 16.0)[d]	46%	NR	57.3 (50.5, 64.9)[d]	NR[c]	0.8 (0.6, 1.1)[d]	Ferrari et al [50]

Values are mean (standard deviation) unless otherwise noted.

[a]Reported as range.

[b]Includes both male and females subjects with an unreported ratio.

[c]The study reported subjects with obesity, but did not report BMI directly.

[d]Reported as median (range).

[e]Reported in molar units and converted to mass units using a molecular weight of 42 kDa.

AAG, α1-acid glycoprotein; BMI, body mass index; NR, not reported

Supplementary Table 12. Organ volume scaling factors for virtual children with obesity.

Organ	Mean Scaling Factor[a]	Standard Deviation[a]
Brain	104%	0.3%
Bone	106%	0.5%
Gonads	114%	2.6%
Heart[b]	---	---
Kidneys	115%	2.6%
Large Intestine	114%	2.6%
Liver	115%	2.3%
Lungs	114%	2.6%
Muscle	115%	2.2%
Pancreas	114%	2.6%
Small Intestine	114%	2.6%
Spleen	125%	8.8%
Stomach	114%	2.6%

[a]Scaling factor mean and standard deviation were determined from organ volumes of adults with obesity and normal weight adults reported in Hwaung et al [51]. While scaling factors were derived from adults, they were assumed to be similar in children and validated with pediatric data when available (**Supplementary Table 13; Figure 2**)

[b]No significant increase in size with obesity reported.

Supplementary Table 13. Summarized results from a comprehensive literature search for kidney and liver sizes in children with and without obesity.

n, subjects	Age (y)	Measurement	Nonobese (mm)[a]	Obese (mm)[a]	Obese/Nonobese (%)	Reference
KIDNEY						
22	2-4y	Right kidney length	6.7	7.5	112	Konus et al [52]
26	4-6y		7.4	8.3	112	
32	6-8y		8.0	9.1	114	
27	8-10y		8.0	8.9	111	
15	10-12y		8.9	10.0	112	
22	12-14y		9.4	10.2	109	
11	14-18y		9.2	10.2	111	
133	2-4y	Right kidney length	6.4	7.7	120	Otiv et al [53]
129	4-6y		6.8	8.0	118	
102	6-8y		7.0	8.0	114	
115	8-10y		7.8	9.1	117	
75	10-12y		8.3	9.8	118	
62	12-14y		8.6	10.2	119	
28	2-3y	Right kidney length	6.8	8.5	125	Coombs et al [54]
24	3-4y		7.3	9.2	126	
15	4-5y		7.6	9.4	124	
21	5-6y		7.7	9.5	123	
18	6-7y		7.8	9.8	126	
26	7-8y		8.1	10.2	126	
28	8-9y		8.4	10.6	126	
39	9-10y		8.7	11.0	126	
37	10-11y		9.0	11.2	124	
43	11-12y		9.2	11.4	124	
36	12-13y		9.6	11.6	121	
38	13-14y		10.0	11.8	118	
15	14-15y		10.4	11.8	113	

17	15-16y		10.8	12.1	112	
43	2-4y	Right kidney length	6.3	7.4	117	Thapa et al [55]
28	4-6y		7.0	8.0	115	
38	6-8y		7.8	8.5	108	
19	8-10y		8.3	9.5	115	
11	10-12y		8.6	9.7	113	
6397	6y	Combined kidney volume	12.0	16.7	139	Bakker et al [56]
1748	0.5-16y	Kidney volume	14.0[b]	17.0[b]	121	DiZazzo et al [57]
794	0-18y	Right kidney length	10.0	11.8	118	Kim et al [58]
950	>2y	Kidney length	8.1	10.3	127	Mohtasib et al [59]
368	5-18y	Kidney length	NR	NR	110	Parmaksiz et al [60]
204	1-19y	Kidney length	NR	NR	105	Zuzuárregui et al [61]
100	1-19y	Kidney length	NR	NR	106	Soheilipour et al [62]
671	NR	Kidney volume	NR	NR	125	Wang et al [63]
				Median (range)	**118 (105-139)**	
LIVER						
27	2-4y	Liver length	8.6	10.5	122	Konus et al [52]
30	4-6y		10.0	12.4	124	
38	6-8y		10.5	12.3	117	
30	8-10y		10.5	12.8	122	
16	10-12y		11.5	13.6	118	
23	12-14y		11.8	13.6	115	
12	14-18y		12.1	13.9	115	
43	2-4y	Liver length	8.7	10.5	121	Thapa et al [53]
41	4-6y		9.2	10.7	116	
25	6-8y		9.9	11.8	119	
19	10-12y		10.6	12.7	119	
11	12-14y		11.6	13.0	112	
132	2-4y	Liver length	9.0	11.6	130	Dhingra et al [64]
115	4-6y		10.1	14.0	139	
51	6-8y		10.9	12.8	118	
62	8-10y		11.8	14.1	119	

53	10-12y		13.3	15.4	116	
48	2-4y	Liver length	9.9	11.0	111	Da Rocha et al [65]
181	4-6y		10.4	12.6	121	
109	6-8y		10.9	13.3	122	
45	4-6y	Liver length	9.2	10.8	117	Amatya et al [66]
45	10-12y		10.7	12.9	121	
699	0-19y	Liver volume	NR	NR	110	Cervantes et al [67]
				Median (range)	**119 (110-139)**	

[a]Units are cm for organ length measurements cm and cm^3 for organ volume measurements.

[b]Normalized by height, weight, age, and gender.

Supplementary Table 14. Summarized results from a comprehensive literature search for reported cardiac output values in children with obesity.

n, subjects	Age (y)	Males	Race	Weight (kg)	BMI (kg/m^2)	Cardiac Output (L/min)	Reference
61	13.5 (2.7)	46%	Non-Hispanic White	85.7 (20.8)	30.8 (5.3)	4.9 (1.3)	Mangner et al [68]
32	10.2 (3.0)	47%	NR	52.1 (19.1)	NR[a]	4.9 (0.7)	Castro et al [69]
143	10.3 (2.7)	56%	NR	59.0 (23.1)	NR[a]	5.2 (0.8)	Castro et al [69]
39	16.0 (12.0, 17.0)[b]	44%	NR	NR	NR[a]	5.5 (4.0, 6.6)[b]	Wójtowicz et al [70]
45	15.0 (14.0, 16.0 [b]	58%	NR	NR	NR[a]	6.5 (5.0, 7.3)[b]	Wójtowicz et al [70]
65	11.7 (2.9)	NR[c]	NR	66.1 (18.1)	NR[a]	5.1 (1.5)	Özkan et al [71]
36	13.3 (7.9, 17.4)[b]	0%	NR	79.0 (38.0, 132.0)[b]	31.5 (22.3, 43.7)[b]	5.1 (1.2)	Rauch et al [72]
28	12.3 (8.5, 17.6)[b]	100%	NR	77.0 (46.0, 155.0)[b]	29.9 (23.7, 50.0)[b]	5.3 (1.2)	Rauch et al [72]
10	11.7 (0.6)	100%	NR	54.2 (6.7)	23.3 (1.8)	4.4 (1.1)	Schuster et al [73]
8	11.4 (1.0)	100%	NR	74.0 (13.9)	29.0 (2.0)	5.4 (1.7)	Schuster et al [73]
24	11.9 (2.1)	79%	NR	NR	32.4 (5.8)	7.3 (1.9)	Giordano et al [74]
34	9.4 (0.15)[d]	NR[c]	Non-Hispanic White	51.7 (2.2)[d]	NR[a]	5.3 (0.19)[d]	Humphries et al [75]
53	9.4 (0.13)[d]	0%	NR	54.6 (1.9)[d]	NR[a]	5.1 (0.16)[d]	Humphries et al [75]
44	9.6 (0.15)[d]	NR[c]	Non-Hispanic Black	62.7 (2.9)[d]	NR[a]	5.5 (0.24)[d]	Humphries et al [75]
25	9.8 (0.19)[d]	100%	NR	64.9 (4.6)[d]	NR[a]	6.1 (0.32)[d]	Humphries et al [75]
120	12.0 (4.0)	51%	NR	69.0 (25.0)	28.0 (5.0)	6.2 (1.2)	McGavock et al [76]
10	15 (0.4)[d]	0%	NR	83.1 (4.6)[d]	31.1 (1.6)[d]	4.7[e]	Gusso et al [77]

Values are mean (standard deviation) unless otherwise noted.

[a]The study reported subjects with obesity, but did not report BMI directly.

[b]Reported as median (range).

[c]Includes both male and females subjects with an unreported ratio.

[d]Reported as mean (standard error).

[e]Reported as mean.

BMI, body mass index; NR, not reported

Supplementary Table 15. Search terms used in PubMed for the comprehensive literature search for physiological data to inform development of the virtual population of children with obesity.

Search phrase for 'obesity'	
"pediatric obesity"[MeSH] OR "obesity"[MeSH] OR "obesity, abdominal"[MeSH] OR "obesity, morbid"[MeSH] OR "obesity, metabolically benign"[MeSH] OR "fat"[MeSH] OR "adipose"[MeSH]	
***AND* search phrase for 'pediatric'**	
"pediatrics"[MeSH] OR "infant"[MeSH] OR "newborn"[MeSH] OR "pediatric"[Title/Abstract] OR "infant"[Title/Abstract] OR "newborn"[Title/Abstract] OR "neonates"[Title/Abstract] OR "neonate"[Title/Abstract] OR "infants"[Title/Abstract] OR "child"[MeSH] OR "juvenile"[MeSH] NOT "pregnant"[MeSH] OR "children"[Title/Abstract] OR "adolescent"[Title/Abstract] OR "adolescents"[Title/Abstract] OR "Adolescent"[MeSH]	
***AND* each of the physiological terms below[a]**	
"AAG"[MeSH]	"low extraction"[MeSH]
"absorption"[MeSH]	"metabolism"[MeSH]
"adipose"[MeSH]	"microsome"[MeSH]
"age"[MeSH]	"MPPGL"[MeSH]
"albumin"[MeSH]	"mucosal blood flow"[MeSH]
"alpha-1 acid glycoprotein"[MeSH]	"muscle"[MeSH]
"anatomy"[MeSH]	"muscle mass"[MeSH]
"anthropometric"[MeSH]	"ontogeny"[MeSH]
"arterial blood"[MeSH]	"organ growth"[MeSH]
"autopsy"[MeSH]	"organ volume"[MeSH]
"blood"[MeSH]	"organ weight"[MeSH]
"blood circulation"[MeSH]	"oxygen uptake"[MeSH]
"blood flow"[MeSH]	"PAH"[MeSH]
"blood vessels"[MeSH]	"pancreas"[MeSH]
"body weight"[MeSH]	"para-aminohippuric acid"[MeSH]
"bone"[MeSH]	"partition"[MeSH]
"bone mass"[MeSH]	"perfusion"[MeSH]
"brain"[MeSH]	"peripheral fatness"[MeSH]
"CACO-2"[MeSH]	"permeability"[MeSH]
"cardiac output"[MeSH]	"pH"[MeSH]
"central fatness"[MeSH]	"physiology"[MeSH]

“compartment”[MeSH]	“plasma”[MeSH]
“composition”[MeSH]	“plasma proteins”[MeSH]
“creatinine clearance”[MeSH]	“portal vein”[MeSH]
“drug metabolism”[MeSH]	“post-mortal”[MeSH]
“duodenum”[MeSH]	“postmortem”[MeSH]
“ejection fraction”[MeSH]	“pre-portal organs”[MeSH]
“enzyme”[MeSH]	“pressure”[MeSH]
“extracellular”[MeSH]	“protein”[MeSH]
“extracellular water”[MeSH]	“protein binding”[MeSH]
“fat depots”[MeSH]	“red blood cells”[MeSH]
“filtering capacity”[MeSH]	“renal”[MeSH]
“gastrointestinal tract”[MeSH]	“respiration”[MeSH]
“glomerular filtration rate”[MeSH]	“rheological profile”[MeSH]
“glomerulus”[MeSH]	“serum”[MeSH]
“gonads”[MeSH]	“sex”[MeSH]
“growth rate”[MeSH]	“skin”[MeSH]
“gut wall”[MeSH]	“small intestine”[MeSH]
“haematocrit”[MeSH]	“splanchnic blood flow”[MeSH]
“heart”[MeSH]	“spleen”[MeSH]
“heart rate”[MeSH]	“stomach”[MeSH]
“height”[MeSH]	“stroke volume”[MeSH]
“hematocrit”[MeSH]	“subcutaneous”[MeSH]
“hemodynamic”[MeSH]	“surface area”[MeSH]
“hemoglobin”[MeSH]	“tissue volume”[MeSH]
“hepatic”[MeSH]	“tissue weight”[MeSH]
“hepatocellularity”[MeSH]	“total blood volume” [MeSH]
“hepatocyte”[MeSH]	“total body lipid”[MeSH]
“high extraction”[MeSH]	“total body water”[MeSH]
“HPGL”[MeSH]	“transporter”[MeSH]
“hydrodynamics”[MeSH]	“tubular reabsorption”[MeSH]
“ileum”[MeSH]	“tubular secretion”[MeSH]
“interstitial”[MeSH]	“vascular”[MeSH]
“intracellular”[MeSH]	“vasculature”[MeSH]
“jejunum”[MeSH]	“venous blood”[MeSH]
“kidneys”[MeSH]	“ventilation”[MeSH]
“kidney volume”[MeSH]	“ventricular output”[MeSH]
“large intestine”[MeSH]	“villous blood flow”[MeSH]
“lipid”[MeSH]	“water”[MeSH]
“liver”[MeSH]	“well-stirred”[MeSH]
“liver volume”[MeSH]	

[a]Note that separate search was conducted for each of the key physiological terms, and the results were combined.

AAG, α1-acid glycoprotein; CACO-2, HPGL, hepatocytes per gram of liver; MeSH, medical subject headings; MPPGL, microsomal protein per gram of liver; PAH, para-aminohippuric acid

Supplementary Table 16. Population demographics and PBPK model simulation results for adult subjects who received PO doses of clindamycin hydrochloride.

Demographics[a]	Value
Al-Talla et al (2011) [15]	
Patient population	healthy adults
n	24
Age, y	28.8 (7.7) [19-45]
Weight, kg	75.6 (11.0) [58-101]
Male	24 (100%)
PO dose, mg	150
Formulation	capsule
AFE	0.50
Bouazza et al (2012) [16]	
Patient population	healthy adults
n	50
Age, y	58.7 (3.0) [18-93]
Weight, kg	69.9 (2.7) [23-133]
Male	30 (60%)
PO dose, mg	600
Formulation	tablet
AFE	0.75
del Carmen Carrasco-Portugal et al (2008) [17]	
Health status	healthy adults
n	24
Age, y[b]	25.45 (1.66), males 21.46 (0.70), females
Weight, kg[b]	68.77 (3.41), males 59.31 (1.88), females
Male	11 (46%)
PO dose, mg	600
Formulation	capsule
AFE	1.02
Gatti et al (1993) [18]	
Patient population	healthy adults
n	16
Age, y	27.1 (3.9)
Weight, kg	73.0 (12.7)
Male	16 (100%)
PO dose, mg	600
Formulation	capsule
AFE	0.73
Li et al (2008) [19]	
Patient population	healthy adults
n	24

Age, y	23.67 (2.16)
Weight, kg	64.33 (4.57)
Male	24 (100%)
PO dose, mg	300
Formulation	capsule
AFE	0.85
Mazur et al (1999) [20]	
Patient population	healthy adults
n	20
Age, y	29.0 [22-39]
Weight, kg	80.0 [66-90]
Male	20 (100%)
PO dose, mg	600
Formulation	tablet & capsule
AFE	2.23
Na-Bangchang et al (2007) [21]	
Patient population	Adults with acute uncomplicated *Plasmodium falciparum* malaria
n	18
Age, y[c]	29 [18-48]
Weight, kg[c]	56 [40-75]
Male	13 (72%)
PO dose, mg	600 (multidose)
Formulation	capsule
AFE	0.87

[a]Age and weight presented as mean (standard deviation) [range] when available. Male presented as n (%).

[b]Standard error of the mean

[c]Geometric mean

AFE, average fold error; PBPK, physiologically-based pharmacokinetic; PO, oral

5 REFERENCES

1. Kuczmarski RJ, Ogden CL, Guo SS, Grummer-Strawn LM, Flegal KM, Mei Z, et al. 2000 CDC growth charts for the United States: Methods and development. National Center for Health Statistics. Vital Heal. Stat. 2000.
2. Correia-Costa L, Schaefer F, Afonso AC, Bustorff M, Guimarães JT, Guerra A, et al. Normalization of glomerular filtration rate in obese children. Pediatr Nephrol. 2016;31:1321–8.
3. Zappitelli M, Parvex P, Joseph L, Paradis G, Grey V, Lau S, et al. Derivation and validation of cystatin C-based prediction equations for GFR in children. Am J Kidney Dis. 2006;48:221–30.
4. Schwartz GJ, Muñoz A, Schneider MF, Mak RH, Kaskel F, Warady BA, et al. New equations to estimate GFR in children with CKD. J Am Soc Nephrol. 2009;20:629–37.
5. Peters AM, Snelling HLR, Glass DM, Bird NJ. Estimation of lean body mass in children. Br J Anaesth. 2011;106(5):719-23.
6. Al-Sallami HS, Goulding A, Grant A, Taylor R, Holford N, Duffull SB. Prediction of fat-free mass in children. Clin Pharmacokinet. 2015;54:1169–78.
7. Haycock GB, Schwartz GJ, Wisotsky DH. Geometric method for measuring body surface area: A height-weight formula validated in infants, children, and adults. J Ped. 1978;93(1):62-6.
8. Schaeffer F, Georgi M, Zieger A, Schärer K. Usefulness of bioelectric impedance and skinfold measurements in predicting fat-free mass derived from total body potassium in children. Ped Res. 1994;35(5):617-24.
9. Autmizguine J, Melloni C, Hornik CP, Dallefeld S, Harper B, Yogev R, et al. Population pharmacokinetics of trimethoprim-sulfamethoxazole in infants and children. Antimicrob Agents Chemother. 2018;62:1–19.
10. Madsen K, Nielson H, Tingleff O. Methods for Non-Linear Least Squares Problems. Tech. Univ. Denamrk. 2004.
11. McNamara PJ, Alcorn J. Protein binding predictions in infants. AAPS PharmSci. 2002;4:E4.
12. Blain PG, Mucklow JC, Rawlins MD, Roberts DF, Routledge PA, Shand DG. Determinants of plasma α1-acid glycoprotein (AAG) concentrations in health. Br J Pharmacol. 1985;20:500–2.
13. Hornik CP, Wu H, Edginton AN, Watt K, Cohen-Wolkowiez M, Gonzalez D. Development of a pediatric physiologically-based pharmacokinetic model of clindamycin using opportunistic pharmacokinetic data. Clin Pharmacokinet. 2017;56:1343–53.
14. Thompson EJ, Wu H, Maharaj A, Edginton AN, Balevic SJ, Cobbaert M, et al. Physiologically based pharmacokinetic modeling for trimethoprim and sulfamethoxazole in children. Clin Pharmacokinet. 2019;58:887–98.
15. Al-Talla ZA, Akrawi SH, Emwas AHM. Solid state NMR and bioequivalence comparison of the pharmacokinetic parameters of two formulations of clindamycin. Int J Clin Pharmacol Ther. 2011;49:469-76.
16. Bouazza N, Pestre V, Jullien V, Curis E, Urien S, Salmon D, Tréluer JM. Population pharmacokinetics of clindamycin orally and intravenously administered in patients with osteomyelitis. Br J Clin Pharmacol. 2012;74:971-7.

17. del Carmen Carrasco-Portugal M, Luján M, Flores-Murrieta J. Evaluation of gender in the oral pharmacokinetics of clindamycin in humans. Biopharm Drug Disp. 2008;29:427-30.
18. Gatti G, Flaherty J, Bubp J, White J, Borin M, Gambertoglio J. Comparative study of bioavailabilities and pharmacokinetics of clindamycin in healthy volunteers and patients with AIDS. Antimicrob Agents Chemother. 1993;37:1137-43.
19. Li J, Wang N, Zhang ZJ, Tian Y, Tang W, Chen Y. Pharmacokinetics and bioequivalence study of clindamycin hydrochloride formulations after single-dose administration in healthy Chinese male volunteers. Drug Research. 2008;58:358-62.
20. Mazur D, Schug BS, Evers G, Larsimont V, Fieger-Büschges H, Gimbel W, Keilback-Bermann, Blume HH. Bioavailability and selected pharmacokinetic parameters of clindamycin hydrochloride after administration of a new 600 mg tablet formulation. Int J Clin Pharmacol Ther. 1999;37:386-92.
21. Na-Bangchang K, Ruengweerayut R, Karbwang J, Chauemung A, Hutchinson D. Pharmacokinetics and pharmacodynamics of fosmidomycin monotherapy and combination therapy with clindamycin in the treatment of multidrug resistant falciparum malaria. Malaria J. 2007;6:1-10.
22. Gonzalez D, Melloni C, Yogev R, Poindexter BB, Mendley SR, Delmore P, et al. Use of opportunistic clinical data and a population pharmacokinetic model to support dosing of clindamycin for premature infants to adolescents. Clin Pharmacol Ther. 2014;96:429-37.
23. Smith MJ, Gonzalez D, Goldman JL, Yogev R, Sullivan JE, Reed MD, et al. Pharmacokinetics of clindamycin in obese and nonobese children. Antimicrob Agents Chemother. 2017;61:1-12.
24. Wu YSS, Cohen-Wolkowiez M, Hornik CP, Gerhart JG, Autmizguine J, Cobbaert M, et al. External evaluation of two pediatric population pharmacokinetics models of oral trimethoprim and sulfamethoxazole. Antimicrob Agents Chemother. 2021. [Published online ahead of print.]
25. Rodgers T, Rowland M. Physiologically based pharmacokinetic modelling 2: Predicting the tissue distribution of acids, very weak bases, neutrals and zwitterions. Int J Drug Dev Res. 2006;95:1238-57.
26. Chiney MS, Schwarzenberg SJ, Johnson LA. Altered xanthine oxidase and N-acetyltransferase activity in obese children. Br J Clin Pharmacol. 2011;72:109-15.
27. Belo L, Nascimento H, Kohlova M, Bronze-da-Rocha E, Fernandes J, Costa E, et al. Body fat percentage is a major determinant of total bilirubin indpendently of UGT1A1*28 polymorphism in young obese. PLoS One. 2014;9(6):e98467.
28. Cacciari E, Balsamo A, Palareti G, Cassio A, Argento R, Poggi M, et al. Haemorheologic and fibrinolytic evaluation in obese children and adolescents. Eur J Pediatr. 1988;147(4):381-4.
29. Elhag W, El Ansari W, Abdulrazzaq S, Abdullah A, Elsherif M, Elgenaied I. Evolution of 29 anthropometric, nutritional, and cardiometabolic parameters among morbidly obese adolescents 2 years post sleeve gastrectomy. Obes Surg. 2018;28(2)474-82.
30. Di Costanzo A, Pacifico L, Chiesa C, Massimo Perla F, Ceci F, Angeloni A, et al. Genetic and metabolic predictors of hepatic fat content in a cohort of Italian children with obesity. Pediatr Res. 2019;85(5):671-7.
31. Adelman RD, Restaino IG, Alon US, Blowey DL. Protinuria and focal segmental glomerulosclerosis in severely obese adolescents. J Pediatr. 2001;138(4):481-5.

32. Ahmed AM, Ghany MA, Hakeem GLA, Kamal A, Khattab R, Abdalla A, et al. Assessment of vitamin D status in a group of Egyptian children with non alcoholic fatty liver disease (multicenter study). Nutr Metab (Lond). 2016;13:53.
33. Wu Y, Yue B, Liu J. Lipopolysaccharide-induced cytokine expression pattern in peripheral blood mononuclear cells in childhood obesity. Mol Med Rep. 2016;14(6)5281-7.
34. White M, Davies P, Murphy A. Correlation between nutrition assessment data and percent body fat via plethysmography in pediatric oncology patients. J Parenter Enteral Nutr. 2011;35(6):715-22.
35. Velhote MCP, Damiani D. Bariatric surgery in adolescents: Preliminary 1-year results with a novel technique (Santoro III). Obes Surg. 2010;20(12):1710-5.
36. Xiao N, Jenkins TM, Nehus E, Inge TH, Michalsky MP, Harmon CM, et al. Kidney function in severely obese adolsecnets undergoing bariatric surgery. Obesity (Silver Spring). 2014;22(11):2319-25.
37. Cacciari E, Balsamo A, Palareti G, Cassio A, Argento R, Poggi M, et al. Haemorheologic and fibrinolytic evaluation in obese children and adolescents. Eur J Pediatr. 1988;147(4):381-4.
38. Cohen JI, Maayan L, Convit A. Preliminary evidence for obesity-associated insulin resistance in adolescents without elevations of inflammatory cytokines. Diabetol Metab Syndr. 2012;4(1)26.
39. Abitbol CL, Chandar J, Rodríguez MM, Berho M, Seeherunvong W, Freundlich M, et al. Obesity and preterm birth: Additive risks in the progression of kidney disease in children. Pediatr Nephrol. 2009;24(7)1363-70.
40. Widhalm KM, Zwiauer KF. Metabolic effects of a very low calorie diet in obese children and adolescents with special reference to nitrogen balance. J Am Coll Nutr. 1987;6(6)467-74.
41. Nehus EJ, Khoury JC, Inge TH, Xiao N, Jenkins TM, Moxey-Mims MM, et al. Kidney outcomes three years after bariatric surgery in severely obese adolescents. Kidney Int. 2017;91(2)451-8.
42. Cindik N, Baskin E, Agras PI, Kinik ST, Turan M, Saatci U. Effect of obesity on inflammatory markers and renal functions. Acta Paediatr. 2005;94(12):1732-7.
43. Alkhouri N, Cikach F, Eng K, Moses J, Patel N, Yan C, et al. Analysis of breath volatile organic compounds as a noninvasive tool to diagnose nonalcoholic fatty liver disease in children. Eur J Gastroenterol Hepatol. 2014;26(1)82-7.
44. Del Chierico F, Nobili V, Vernocchi P, Russo A, De Stefanis C, Gnani D, et al. Gut microbiota profiling of pediatric nonalcoholic fatty liver disease and obese patients unveiled by an integrated meta-omics-based approach. Hepatology. 2017;65(2)451-64.
45. Hudert CA, Tzschätzsch H, Guo J, Rudolph B, Bläker H, Loddenkemper C, et al. US time-harmonic elastography: Detection of liver fibrosis in adolescents with extreme obesity with nonalcoholic fatty liver disease. Radiology. 2018;288(1):99-106.
46. Amin S, El Amrousy D, Elrifaey S, Gamal R, Hodeib H. Serum osteocalcin levels in children with nonalcoholic fatty liver disease. J Pediatr Gastroenterol Nutr. 2018;66(1):117-21.
47. El-Karaksy HM, El-Koofy NM, Anwar GM, El-Mougy FM, El-Hennawy A, Fahmy ME. Predictors of non-alcoholic fatty liver disease in obese and overweight Egyptian children: Single center study. Saudi J Gastroenterol. 2011;17(1):40-6.

48. Gade C, Dalhoff K, Petersen TS, Riis T, Schmeltz C, Chabanova E, et al. Higher chlorzoxazone clearance in obese children compared with nonobese peers. Br J Pharmacol. 2018;84(8):1738-47.
49. Gibson RS, Bailey KB, Williams S, Houghton L, Costa-Ribeiro HC, Mattos AP, et al. Tissue iron deficiency and adiposity-related inflammation in disadvantaged preschoolers from NE Brazil. Eur J Clin Nutr. 2014;68(8)887-91.
50. Ferrari M, Cuenca-García M, Valtueña J, Moreno LA, Censi L, González-Gross M, et al. Inflammation profile in overweight/obese adolescents in Europe: An analysis in relation to iron status. Eur J Clin Nutr. 2015;69(2):247-55.
51. Hwaung P, Bosy-Westphal A, Muller MJ, Geisler C, Heo M, Thomas DM, et al. Obesity tissue: Composition, energy expenditure, and energy content in adult humans. Obesity (Silver Spring). 2019;27(9):1472-81.
52. Konuş OL, Ozdemir A, Akkaya A, Erbaş G, Celik H, Işik S. Normal liver, spleen, and kidney dimensions in neonates, infants, and children, Evaluation with sonography. AJR Am J Roentgenol. 1998;171:1693-8.
53. Otiv A, Mehta K, Ali U, Nadkarni M. Sonographic measurement of renal size in normal Indian children. Indian Pediatr. 2012;49:533-6.
54. Coombs PR, Lavender I, Leung MYZ, Woods JC, Paul E, Webb N, et al. Normal sonographic renal length measurements in an Australian pediatric population. Pediatr Radiol. 2019;49:1754-61.
55. Thapa NB, Shah S, Pradhan A, Rijal K, Pradhan A, Basnet S. Sonographic assessment of the normal dimensions of liver, spleen, and kidney in healthy children at tertiary care hospital. Kathmandu Univ Med J. 2016;13:286-91.
56. Bakkar H, Kooijman MN, van der Heijden AJ, Hofman A, Franco OH, Taal HR, et al. Kidney size and function in a multi-ethnic population-based cohort of school-age children. Pediatr Nephrol. 2014;29:1589-98.
57. Di Zazzo G, Stringini G, Matteucci MC, Muraca M, Malena S, Emma F. Serum creatinine levels are significantly influenced by renal size in the normal pediatric population. Clin J Am Soc Nephrol. 2011;6(1):107-13.
58. Kim JH, Kim MJ, Lim SH, Kim J, Lee MJ. Length and volume of morphologically normal kidneys in Korean children: Ultrasound measurement and estimation using body size. Korean J Imaging. 2013;14(4):677-82.
59. Mohtasib RS, Alshamiri KM, Jobeir AA, Saidi FMA, Masawi AM, Alabdulaziz LS, et al. Sonographic measurements for kidney length in normal Saudi children: Correlation with other body parameters. Ann Saudi Med. 2019;39(3):143-54.
60. Parmaksiz G, Kekeç ŞD, Cengiz ND, Noyan A. The relationship between body mass index and renal length in obese children. Pediatr Nephrol. 2020;35(5):901-5.
61. Zuzuárregui JRP, Mallios R, Murphy J. The effect of obesity on kidney length in a health pediatric population. Pediatr Nephrol. 2009;24:2023-7.
62. Soheilipour F, Jesmi F, Rahimzadeh N, Pishgahroudsari M, Almassinokian F, Mazaherinezhad. Configuring a better estimation of kidney size in obese children and adolescents. Iran J Pediatr. 2016;26(2):e4700.

63. Wang H, Quintana FG, Cervantes FJ, Faz M. Analysis of the relationship among kidney volume, obesity, and blood pressure in Mexican-American children. J Ped Nephrol. 2019;7(3):1-7.
64. Dhingra B. Normal values of liver and spleen size by ultrasonography in Indian children. Indian Pediatr. 2010;47:475-6.
65. da Rocha SMS, Ferrer APS, de Olveira IRS, et al. Determinação do tamanho do figado de crianças normais, entre 0 e 7 anos, por ulrassonografia. Radiol Bras. 2009;42:7-13.
66. Amatya P, Shah D, Gupta N, Bhatta NK. Clinical and ultrasonographic measurement of liver size in normal children. Indian J Pediatr. 2014;81:441-5.
67. Cervantes FJ, Faz M, Quintana FG, Wang H. Measurement of liver size by ultrasound unveils large livers in overweight children. Diabetes Obes Int J. 2019;4(4):000210.
68. Mangner N, Scheuermann K, Winzer E, Wagner I, Hoellriegel R, Sandri M, et al. Childhood obesity: Impact on cardiac geometry and function. JACC Cardiovasc Imaging. 2014;7(12):1198-205.
69. Castro JM, García-Espinosa V, Curcio S, Arana M, Chiesa P, Giachetto G, et al. Childhood obesity associates haemodynamic and vascular changes that result in increased central aortic pressure with augmented incident and reflected wave components, without changes in peripheral amplification. Int J Vasc Med. 2016;2016:3129304.
70. Wójtowicz J, Lempicka A, Łuczyński W, Szczepański W, Zomerfeld A, Semeran K, et al. Central aortic pressure, arterial stiffness and echocardiographic parameters of children with overweight/obesity and arterial hypertension. Adv Clin Exp Med. 2017;26(9)1399-404.
71. Özkan EA, Khosroshahi HE, Kiliç M, Geçit UA, Domur E. Obesity-related cardiovascular behavior in children. Eur Rev Pharmacol Sci. 2016;20(8):1559-65.
72. Rauch R, Welisch E, Lansdell N, Burrill E, Jones J, Robinson T, et al. Non-invasive measurement of cardiac output in obese children and adolescents: Comparison of electrical cardiometry and transthoracic Doppler echocardiography. J Clin Monit Comput. 2013;27(2):187-93.
73. Schuster I, Karpoff L, Perez-Martin A, Oudot C, Startun A, Rubini M, et al. Cardiac function during exercise in obese prepubertal boys: Effect of degree of obesity. Obesity (Silver Spring). 2009;17(10)1878-83.
74. Giordano U, Ciampalini P, Turchetta A, Santilli IA, Calzolari F, Crinò A, et al. Cardiovascular hemodynamics: Relationships with insulin resistance in obese children. Pediatr Cardiol. 2003;24(6)548-52.
75. Humphries MC, Gutin B, Barbeau P, Vemulapalli S, Allison J, Owens S. Relations of adiposity and effects of training on the left ventricle in obese youths. Med Sci Sports Exerc. 2002;34(9):1428-35.
76. McGavock JM, Torrance B, McGuire KA, Wozny P, Lewanczuk RZ. The relationship between weight gain and blood pressure in children and adolescents. Am J Hypertens. 2007;20(10):1038-44.
77. Gusso S, Hofman P, Lalande S, Cutfield W, Robinson E, Baldi JC. Impaired stroke volume and aerobic capacity in female adolescents with type 1 and type 2 diabetes mellitus. Diabetologia. 2008;51(7):1317-20.